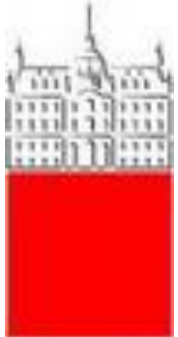


Particle Identification

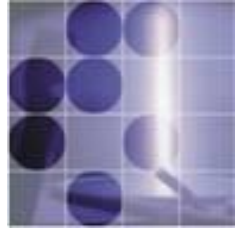
Peter Križan

University of Ljubljana and J. Stefan Institute



University
of Ljubljana

“Jožef Stefan”
Institute



Contents

Why particle identification?

Ring Imaging CHerenkov counters

- New concepts, photon detectors, radiators

Time-of-flight measurement

dE/dx

Transition radiation detectors

Muon and K_L detection

→ write-up in a review paper: JINST 4:P11017,2009.

Introduction: Why Particle ID?

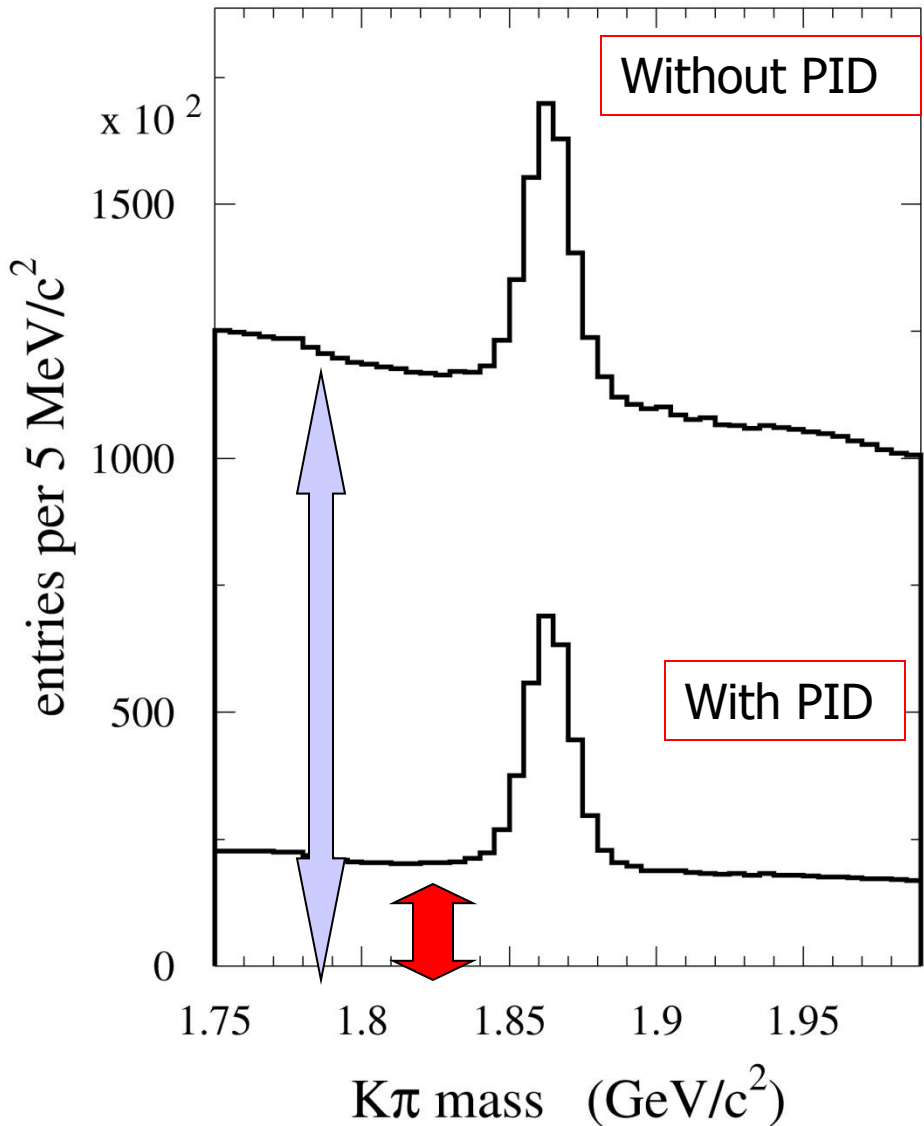
Particle identification is an important aspect of particle, nuclear and astroparticle physics experiments.

Some physical quantities in particle physics are only accessible with sophisticated particle identification (B-physics, CP violation, rare decays, search for exotic hadronic states).

Nuclear physics: final state identification in quark-gluon plasma searches, separation between isotopes

Astrophysics/astroparticle physics: identification of cosmic rays – separation between nuclei (isotopes), charged particles vs high energy photons

Why particle ID?



Example 1: B factory

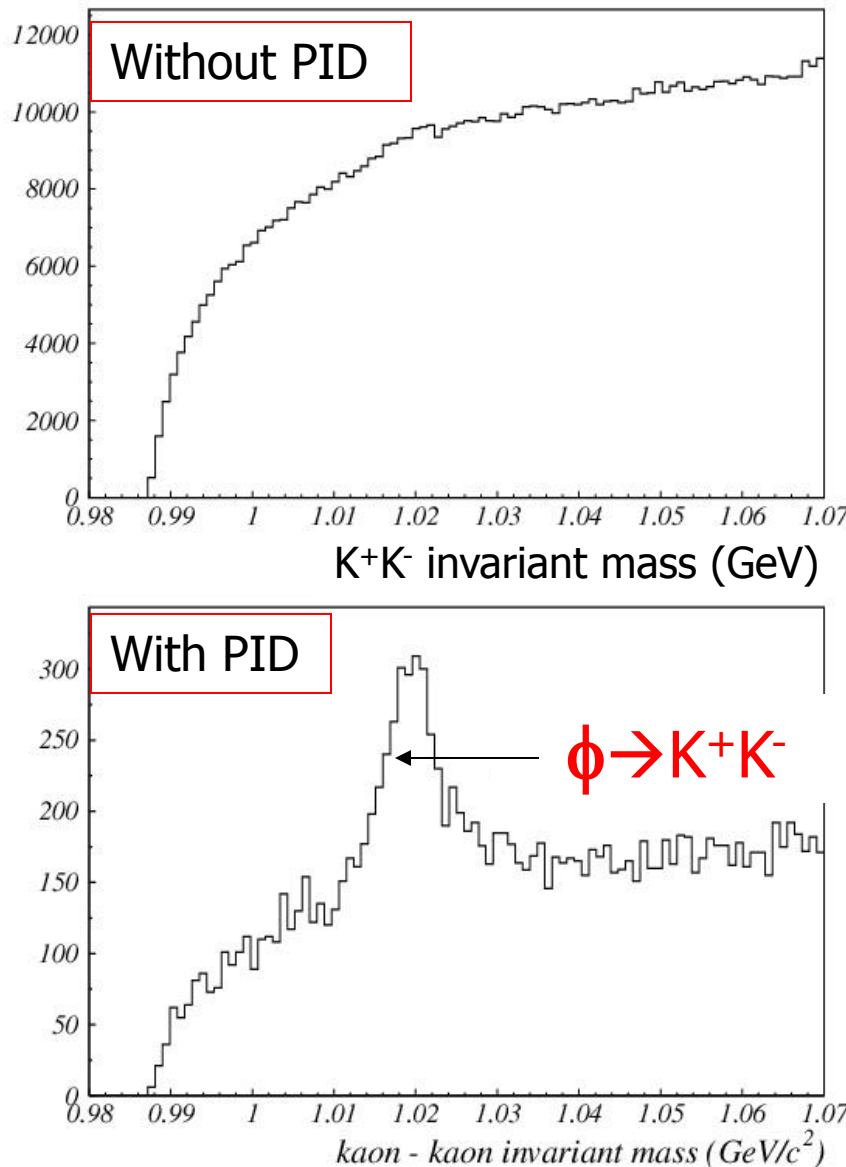
Particle identification reduces the fraction of wrong $K\pi$ combinations (combinatorial background) by $\sim 5x$

Searching for a D meson decay to $K\pi$:
From measured kaon and pion tracks calculate the invariant mass of the system ($i = K, \pi$):

$$Mc^2 = \sqrt{(\sum E_i)^2 - (\sum \vec{p}_i)^2 c^2}$$

The candidates for the $D \rightarrow K\pi$ decay show up as a peak in the distribution on a background of false combinations ("combinatorial").

Why particle ID?

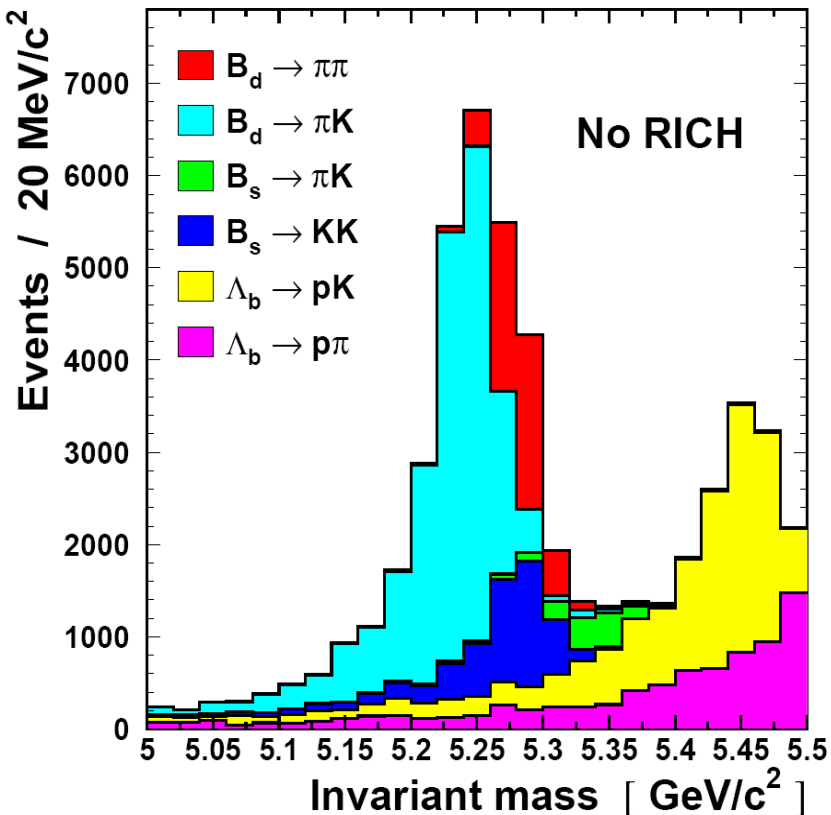


Example 2: HERA-B

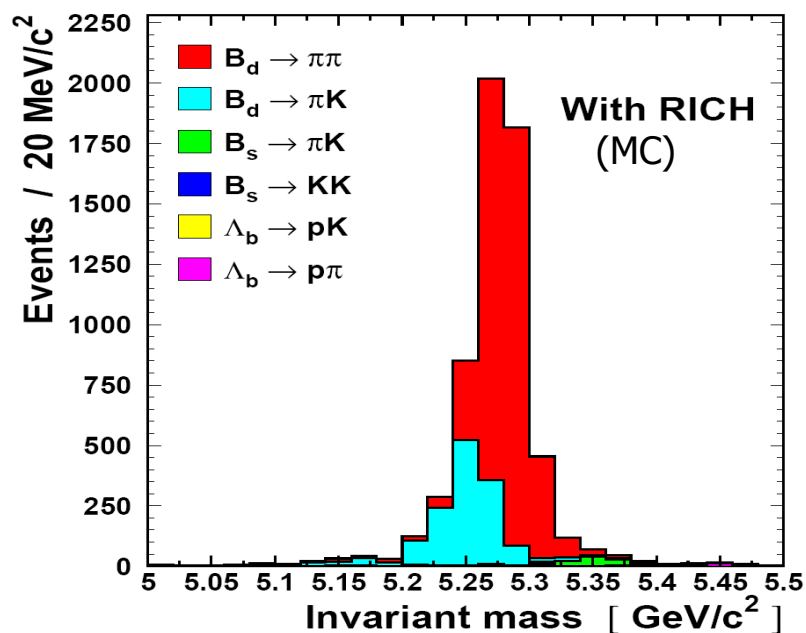
K^+K^- invariant mass.

The inclusive $\phi \rightarrow K^+K^-$ decay only becomes visible after particle identification is taken into account.

Why particle ID?



Example 3: LHCb



Need to distinguish $B_d \rightarrow \pi\pi$ from other similar topology 2-body decays and to distinguish B from anti-B using K tag.

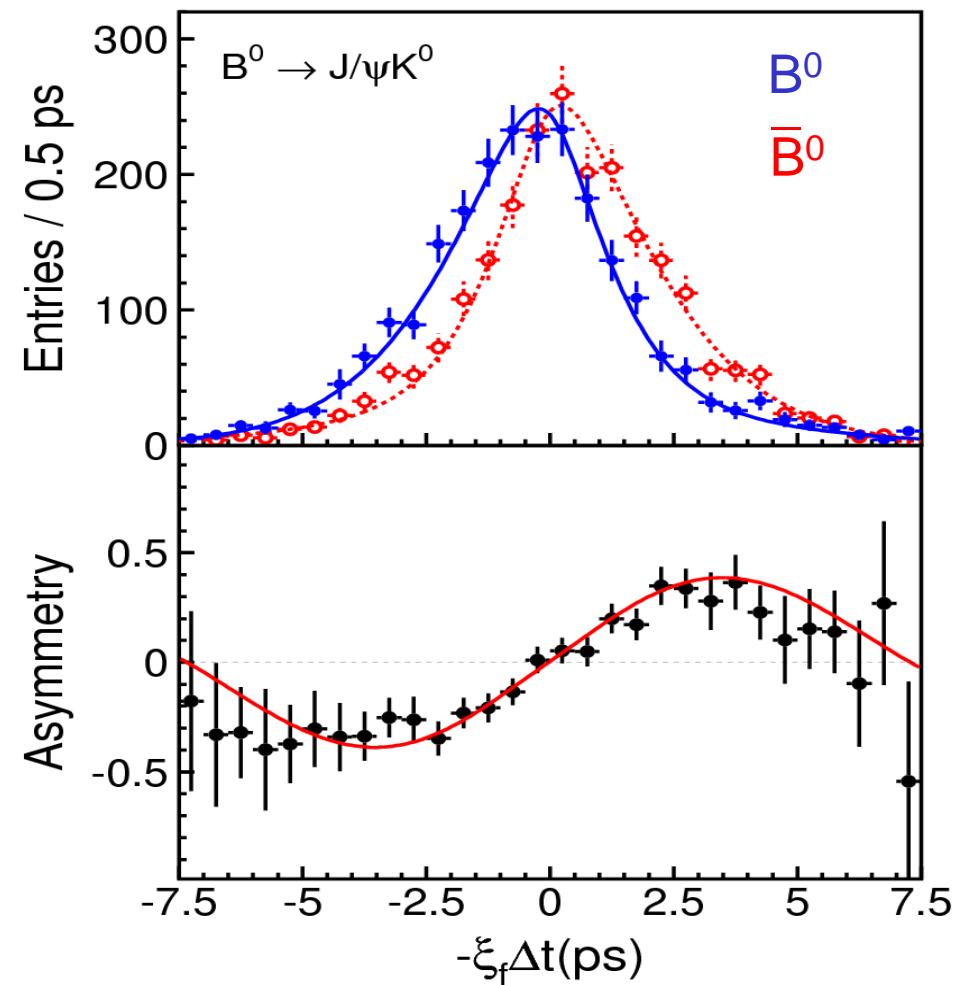
Why particle ID?

PID is also needed in:

- General purpose LHC experiments: final states with electrons and muons
- Searches for exotic states of matter (quark-gluon plasma)
- Spectroscopy and searches for exotic hadronic states
- Studies of fragmentation functions

Why particle ID?

Particle identification at B factories (Belle and BaBar):
was essential for the observation of CP violation in the B meson system.

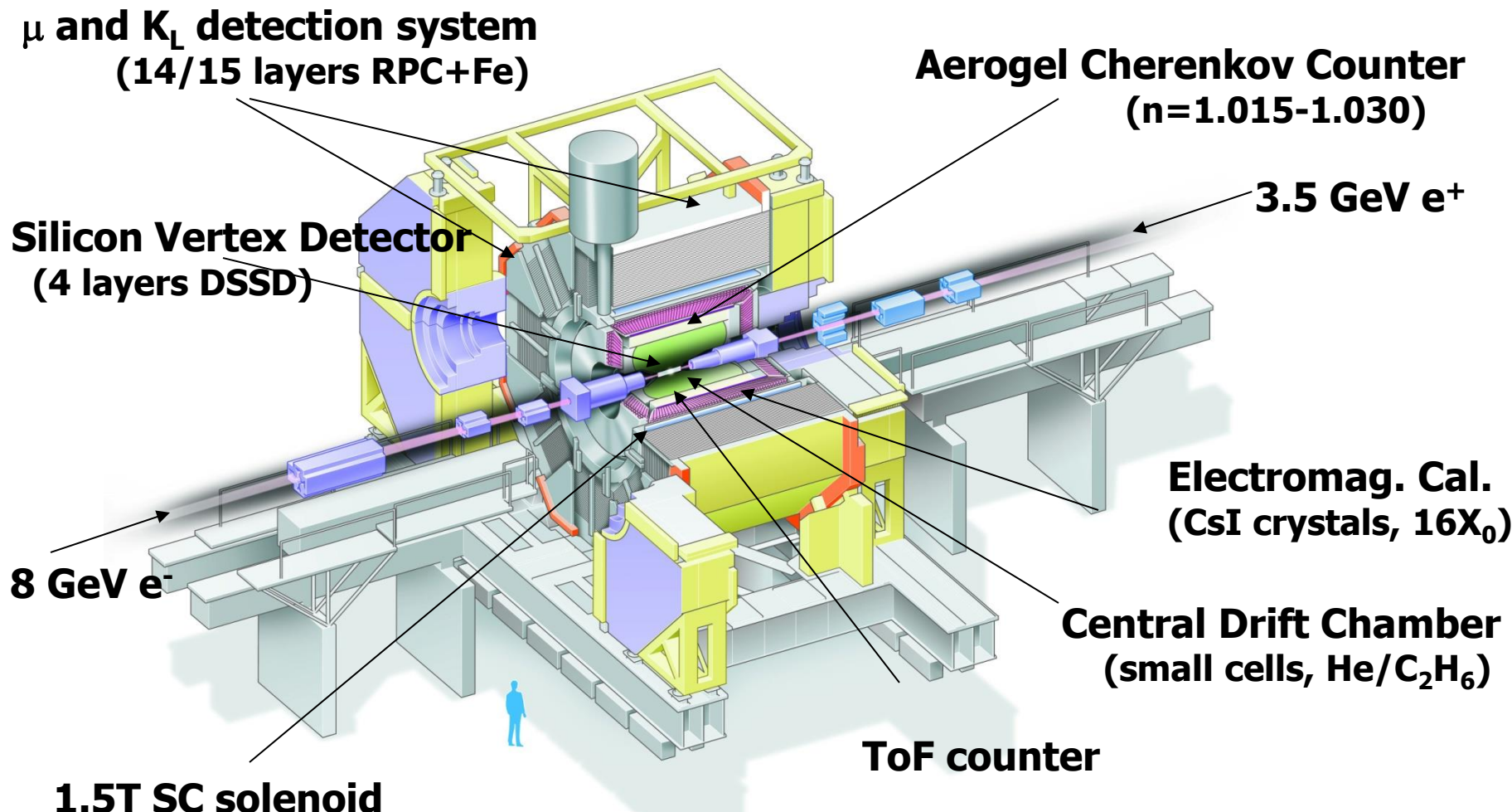


B^0 and its anti-particle decay differently to the same final state $J/\psi K^0$

Flavour of the B: from decay products of the other B:
charge of the kaon, electron, muon

→ particle ID is compulsory

Example: Belle



Particle identification systems in Belle



**μ and K_L detection system
(14/15 layers RPC+Fe)**

**Silicon Vertex Detector
(4 layers DSSD)**

8 GeV e^-

1.5T SC solenoid

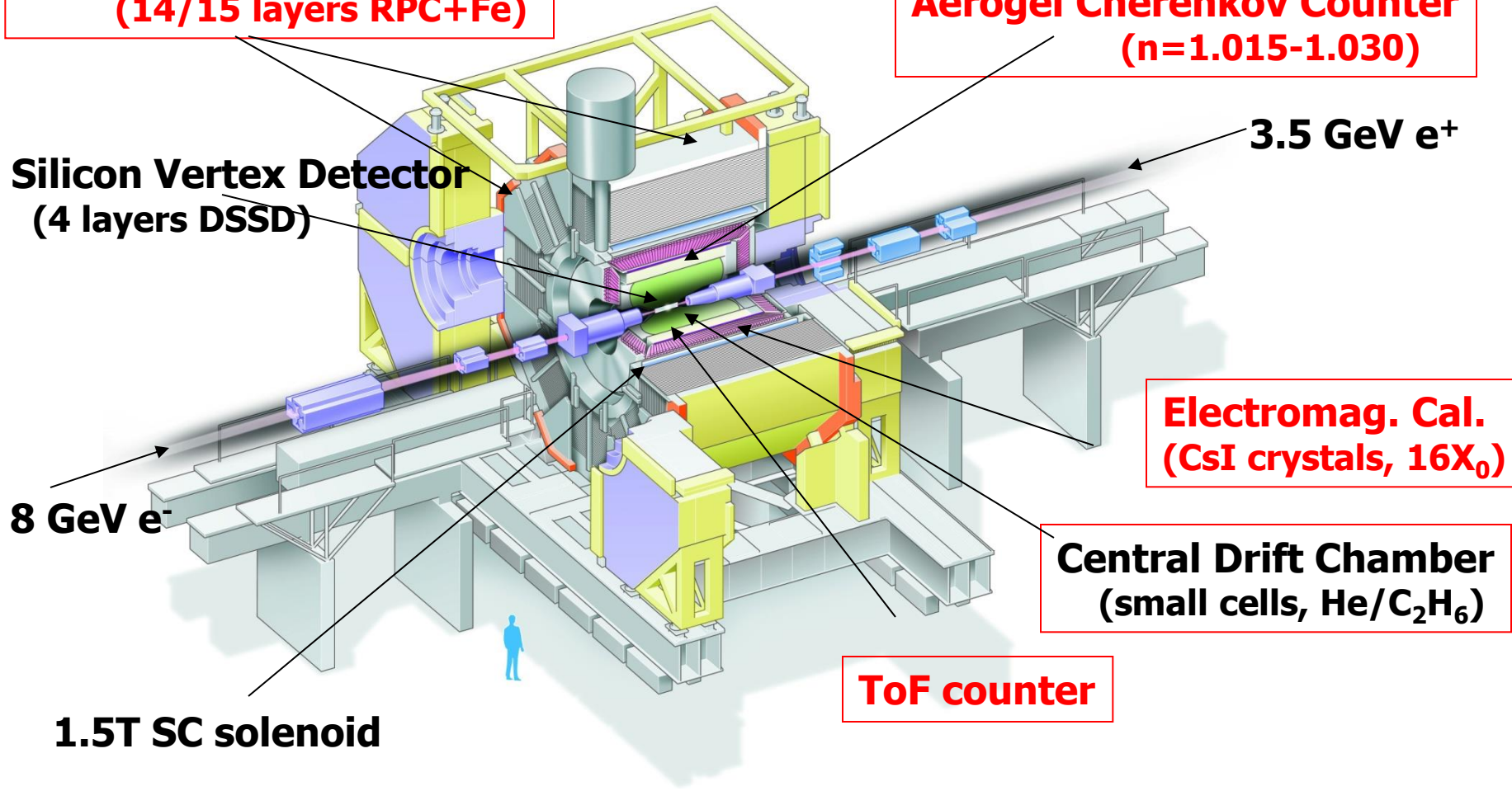
**Aerogel Cherenkov Counter
($n=1.015-1.030$)**

3.5 GeV e^+

**Electromag. Cal.
(CsI crystals, $16X_0$)**

**Central Drift Chamber
(small cells, He/C₂H₆)**

ToF counter



Identification of charged particles

Particles are identified by their **mass** or by the **way they interact**.

Determination of **mass**: from the relation between momentum and velocity, $p=\gamma mv$ (p is known - radius of curvature in magnetic field)

→ Measure velocity by:

- time of flight
- ionisation losses dE/dx
- Cherenkov photon angle (and/or yield)
- transition radiation

Mainly used for the identification of hadrons.

Identification through **interaction**: electrons and muons

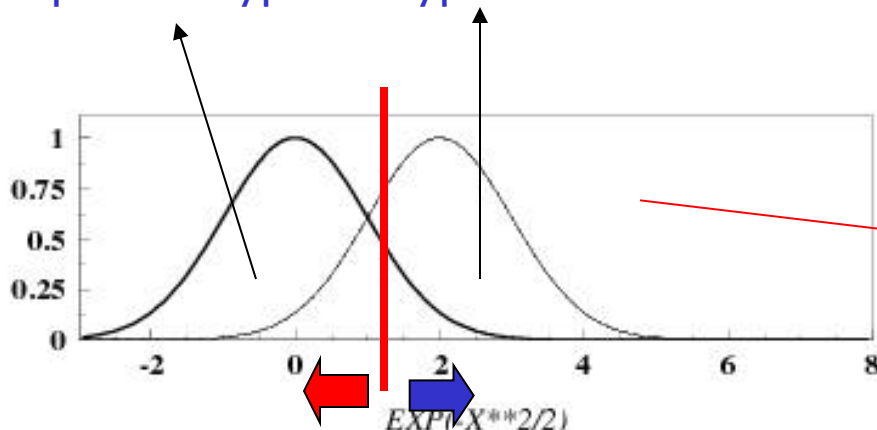
→ calorimeters, muon systems

Efficiency and purity in particle identification

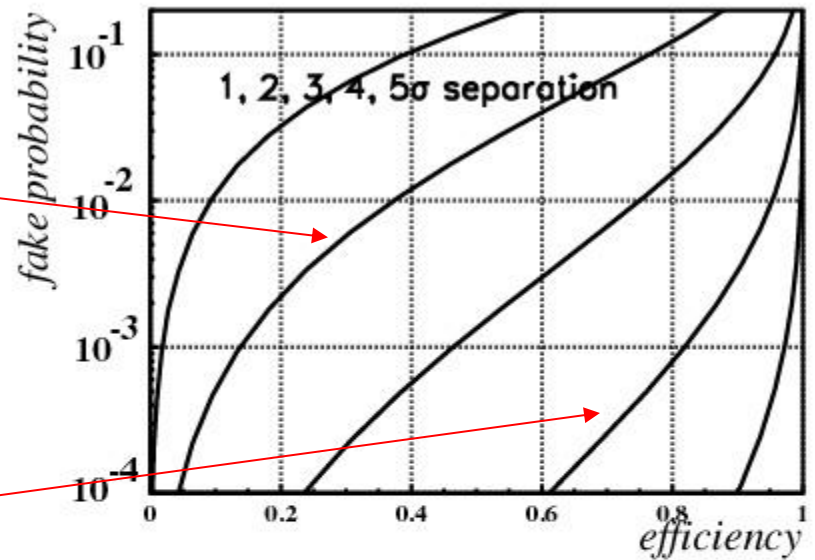
Efficiency and purity are tightly coupled!

Two examples:

particle type 1 type 2



eff. vs fake probability



some discriminating variable

Time-of-flight measurement (TOF)

Measure time difference over a known distance, determine velocity

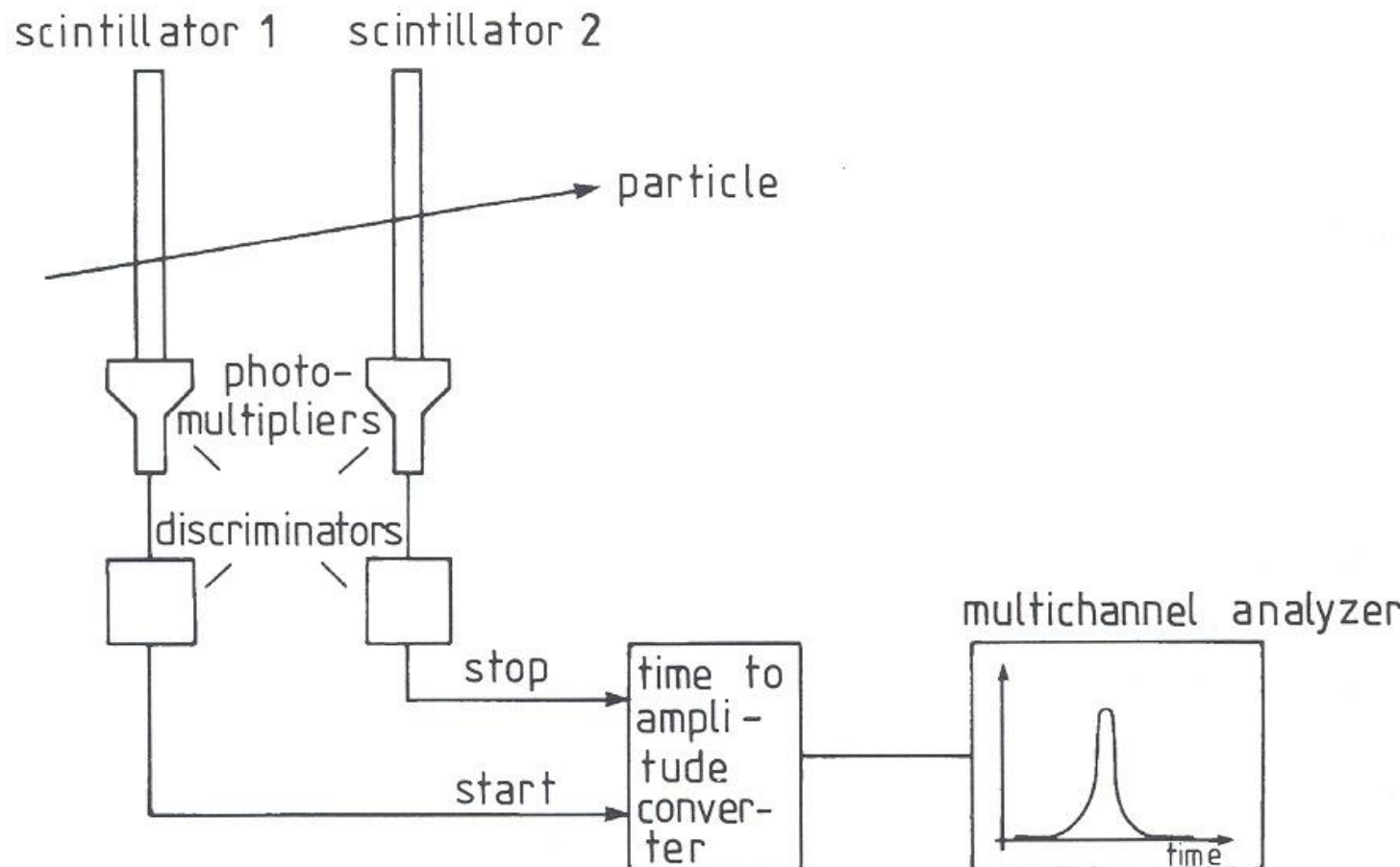


Fig. 6.5. Working principle of time-of-flight measurement.

Time-of-flight measurement 2

Required resolution, example:

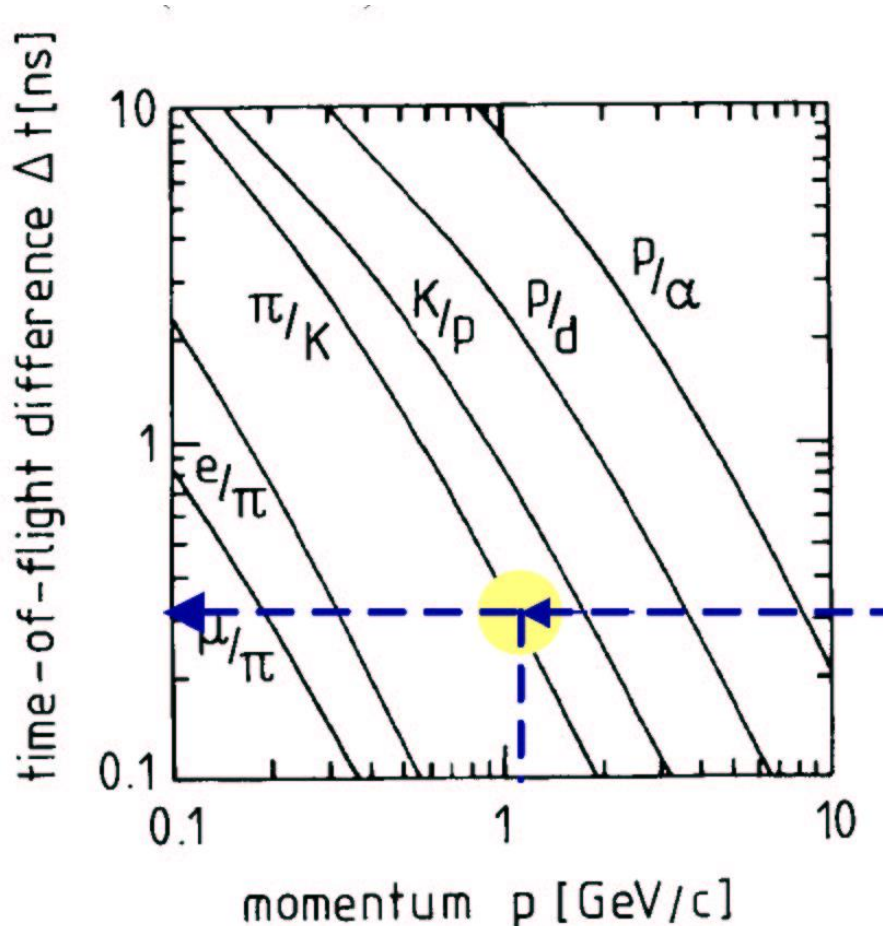
π/K difference at $1\text{GeV}/c$: 300ps

For a 3σ separation need
 $\sigma(\text{TOF})=100\text{ps}$

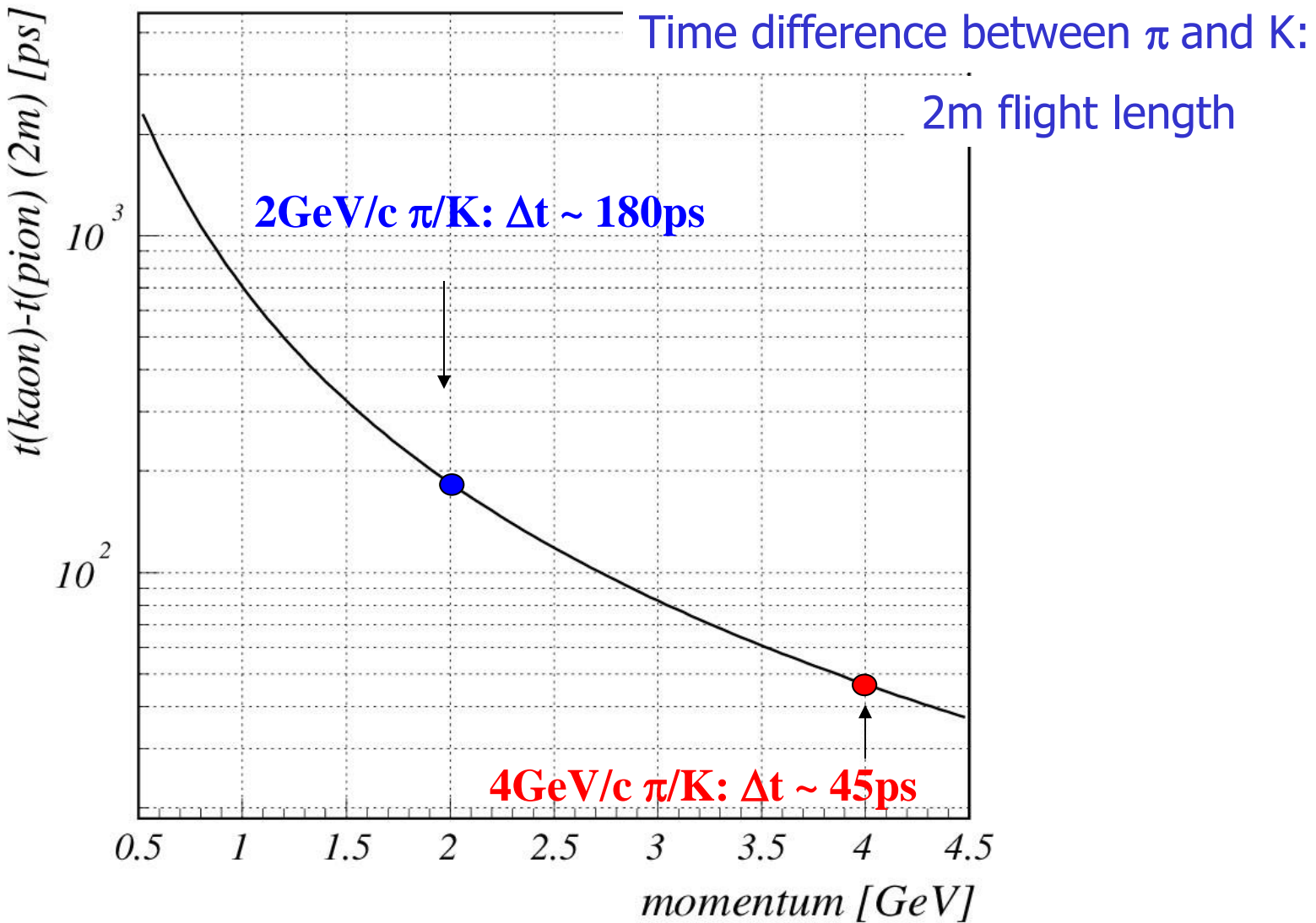
Resolution contributions:

- PMT: transient time spread (TTS)
- Path length variation
- Momentum uncertainty
- Decay time of the scintillator

Time difference between two particle species for path length=1m



Time-of-Flight (TOF) counters



Time-of-flight measurement 3

Resolution of a PMT: transient time spread (TTS), time variation for single photons

Tubes for TOF have to be optimized for small TTS.

Main contribution after the optimisation: photoelectron time spread before it hits the first dynode.

Estimate: take two cases, one with $T=1\text{eV}$ and the other with $T=0$ after the photoelectron leaves the photocathode; take $U=200\text{V}$ and $d=10\text{mm}$

$$T=1\text{eV}: v_0 = \sqrt{(2T/m)} = 0.002 c, \quad a=F/m=200\text{eV}/(10\text{mm} \cdot 0.5 \cdot 10^6\text{eV/c}^2)$$

$$d = v_0 t + at^2/2 \rightarrow t = \sqrt{(2d/a + (v_0/a)^2)} - v_0/a$$

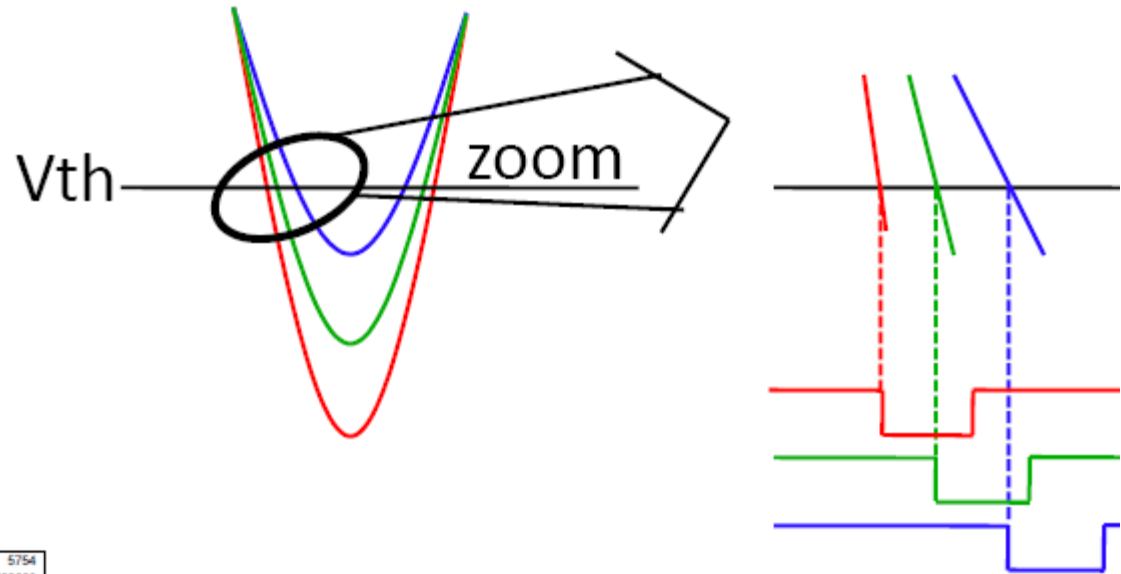
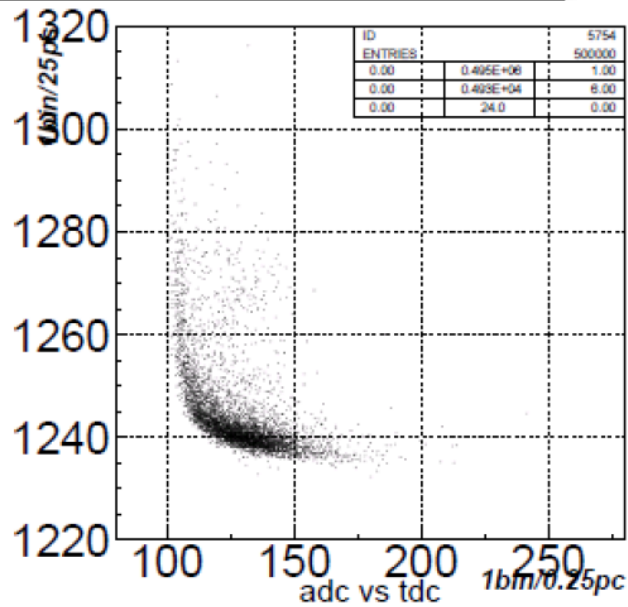
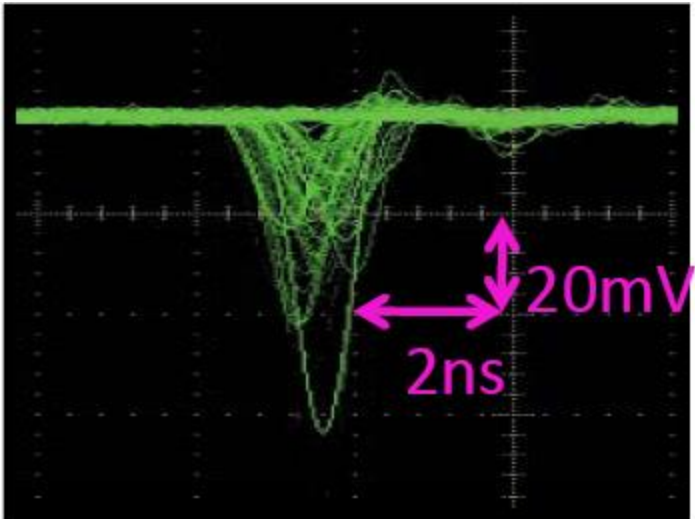
$$T=0\text{eV} : v_0 = 0 \rightarrow t = \sqrt{(2d/a)} = 2.3\text{ns}$$

Time difference: 170ps is a typical value.

Good tubes: $\sigma(\text{TTS})=100\text{ps}$

For N photons: $\sigma \sim \sigma(\text{TTS}) / \sqrt{N}$

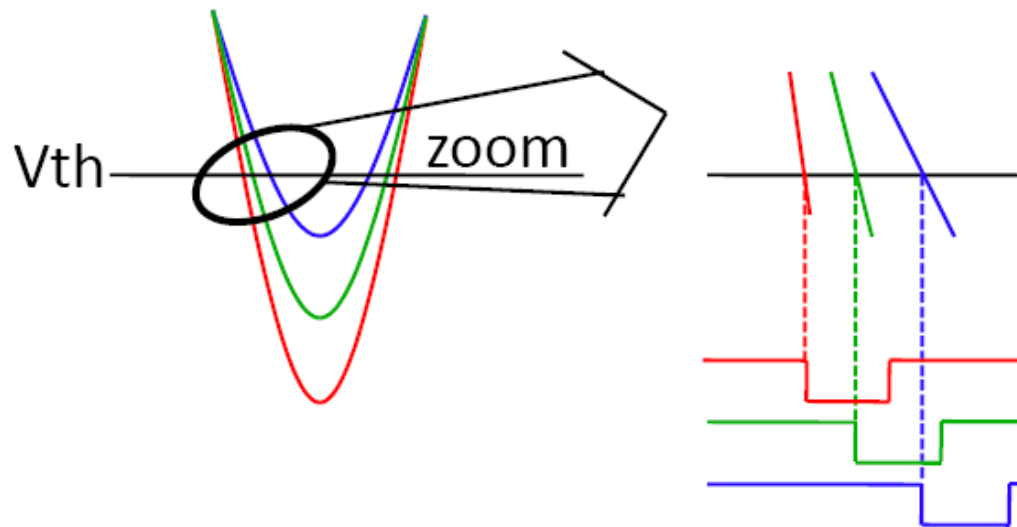
Read out: time walk with a leading edge discriminator



Variation of time determined with a leading edge discriminator: **smaller pulses give a delayed signal**

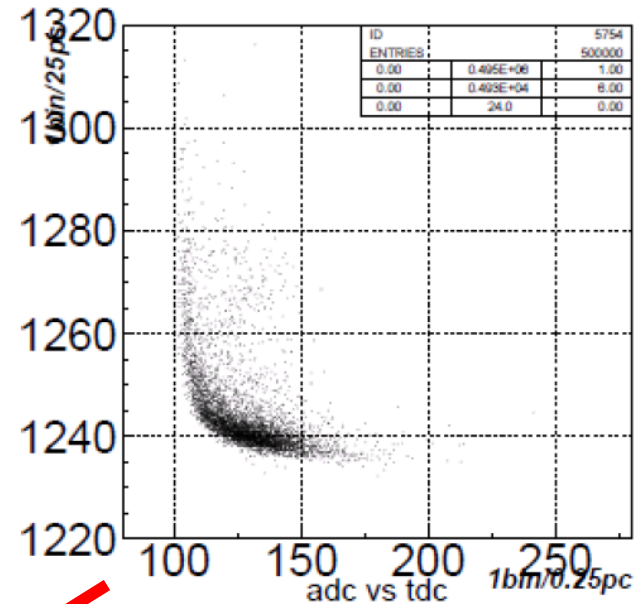
→ Has to be corrected!

Time walk correction 1



One possibility: measure both time (TDC) and amplitude (ADC)

→ Correct time of arrival by using a $\Delta T(\text{ADC})$ correction

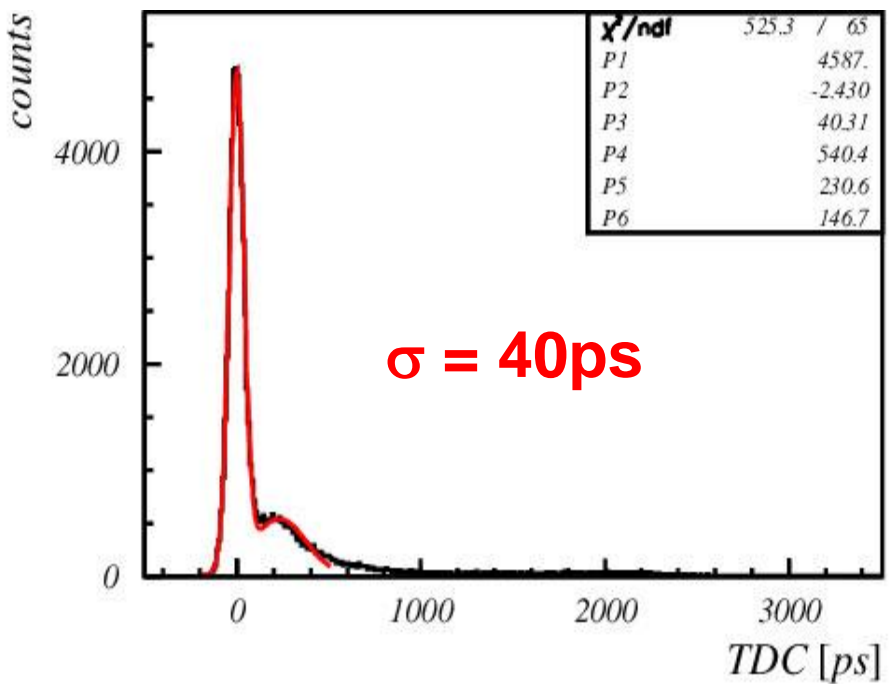
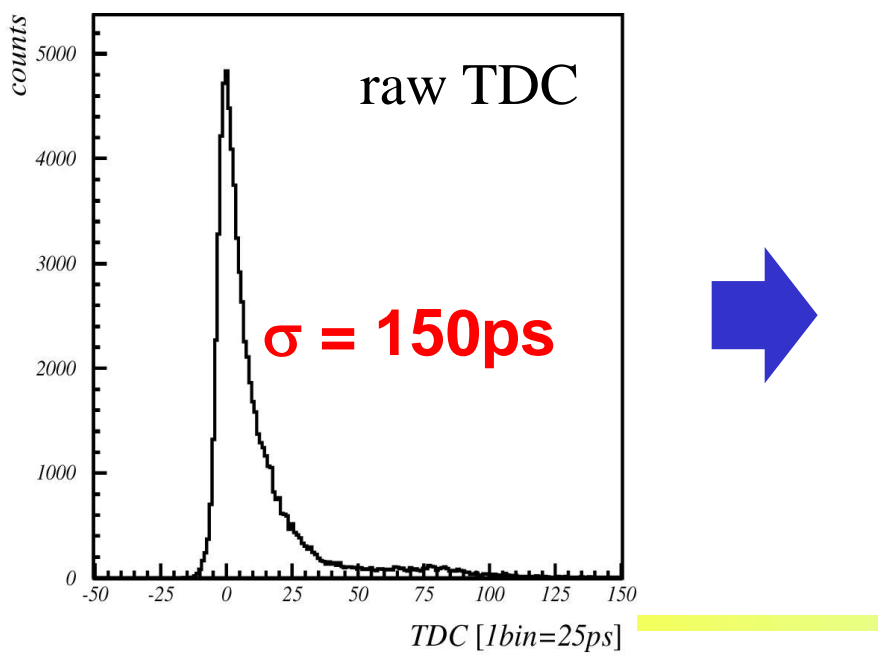


Time walk correction

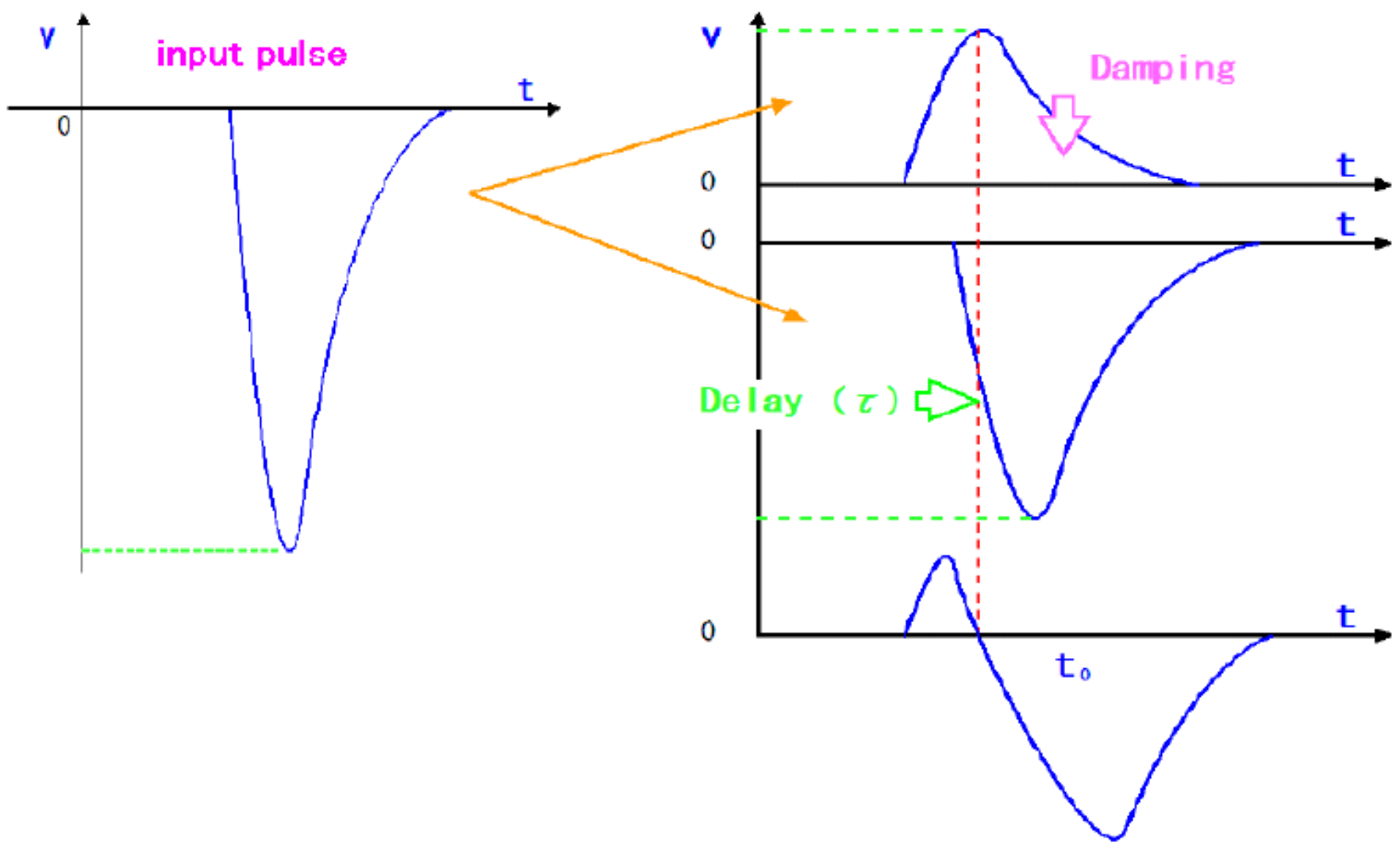
TDC vs. ADC correlation is fitted with

$$TDC = P1 + \sqrt{\frac{P2}{ADC - P3}}$$

and used for TDC correction

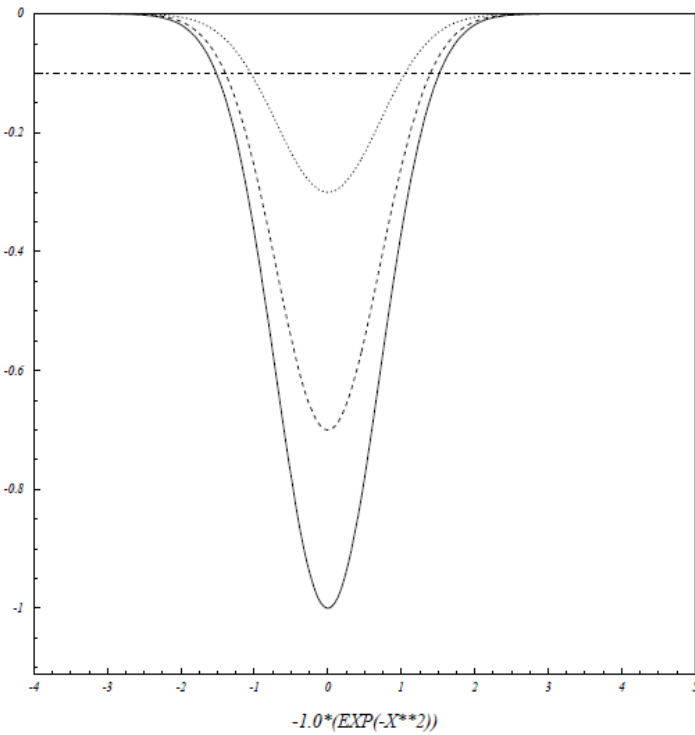


Time walk correction 2: constant fraction discriminator

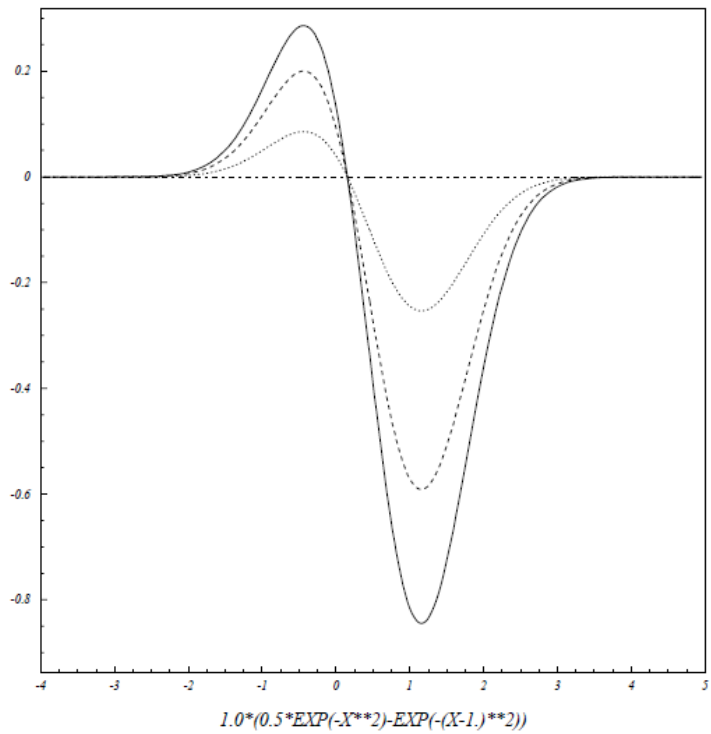


Leading edge discrimination vs constant fraction discrimination

LE discrimination

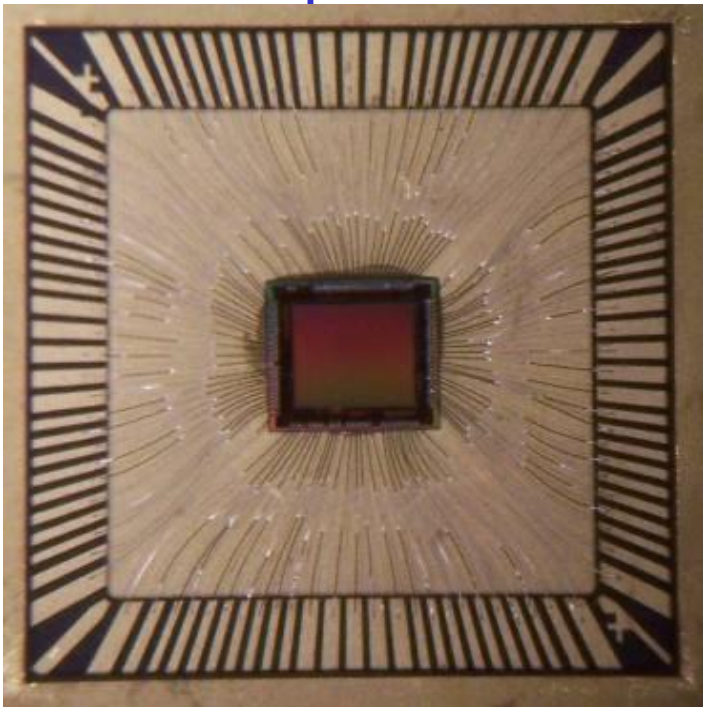


CF discrimination



Read out: waveform sampling

Example: Buffered LABRADOR (BLAB1) ASIC



3mm x 2.8mm, TSMC 0.25um

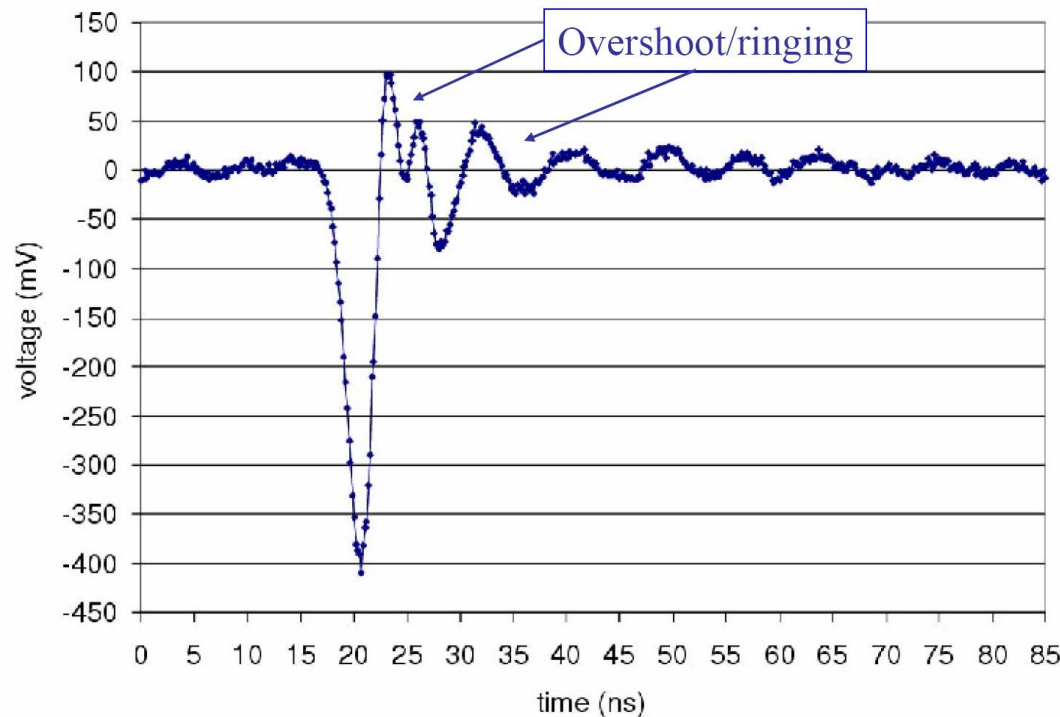
- 64k samples deep
- Multi-MSa/s to Multi-GSa/s

Gary Varner, Larry Ruckman (Hawaii)

Variant of the LABRADOR 3

Successfully flew on ANITA in Dec 06/Jan 07 (≤ 50 ps timing)

Typical single p.e. signal [Burle]



Time-of-Flight (TOF) counters

Traditionally: plastic scintillator + PMTs

Typical resolution: ~ 100 ps \rightarrow pion/K separation up to $\sim 1\text{GeV}$.

To go beyond that: need faster detectors:

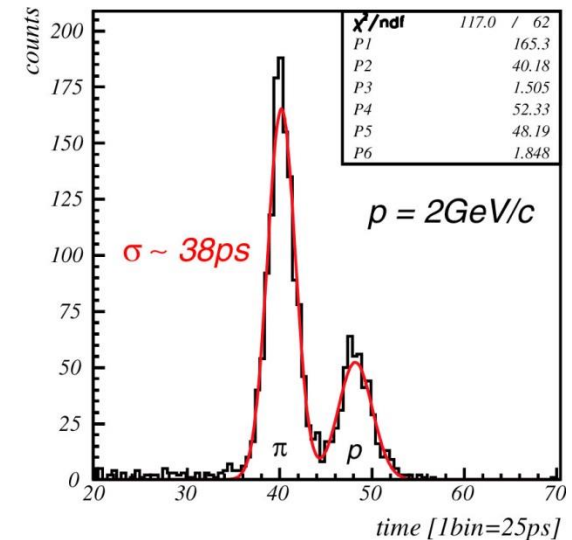
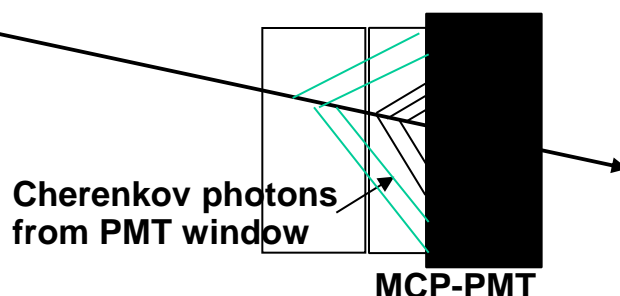
- use Cherenkov light (prompt) instead of scintillations
- use a fast gas detector (Multi gap RPC)

However: make sure you also know the interaction time very precisely...

TOF with Cherenkov light

Idea: detect Cherenkov light with a very fast photon detector (MCP PMT).

Cherenkov light is produced in a quartz plate in front of the MCP PMT and in the PMT window.



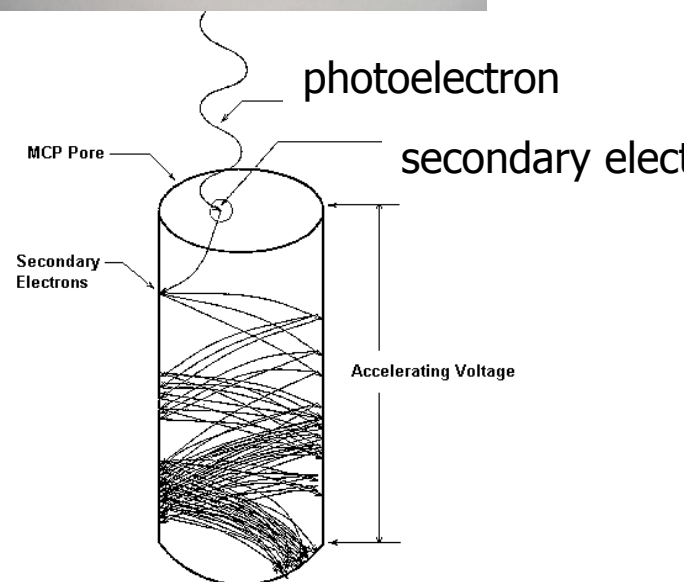
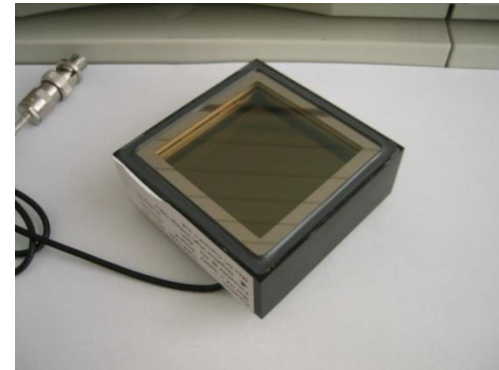
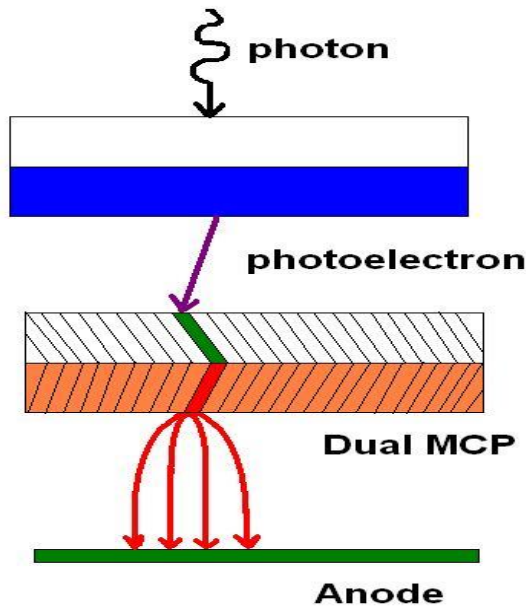
Proof of principle: beamt test with pions and protons at $2\text{ GeV}/c$.

Only photons from the window

Distance between start counter and MCP-PMT was only 65cm

Very fast: MCP-PMT

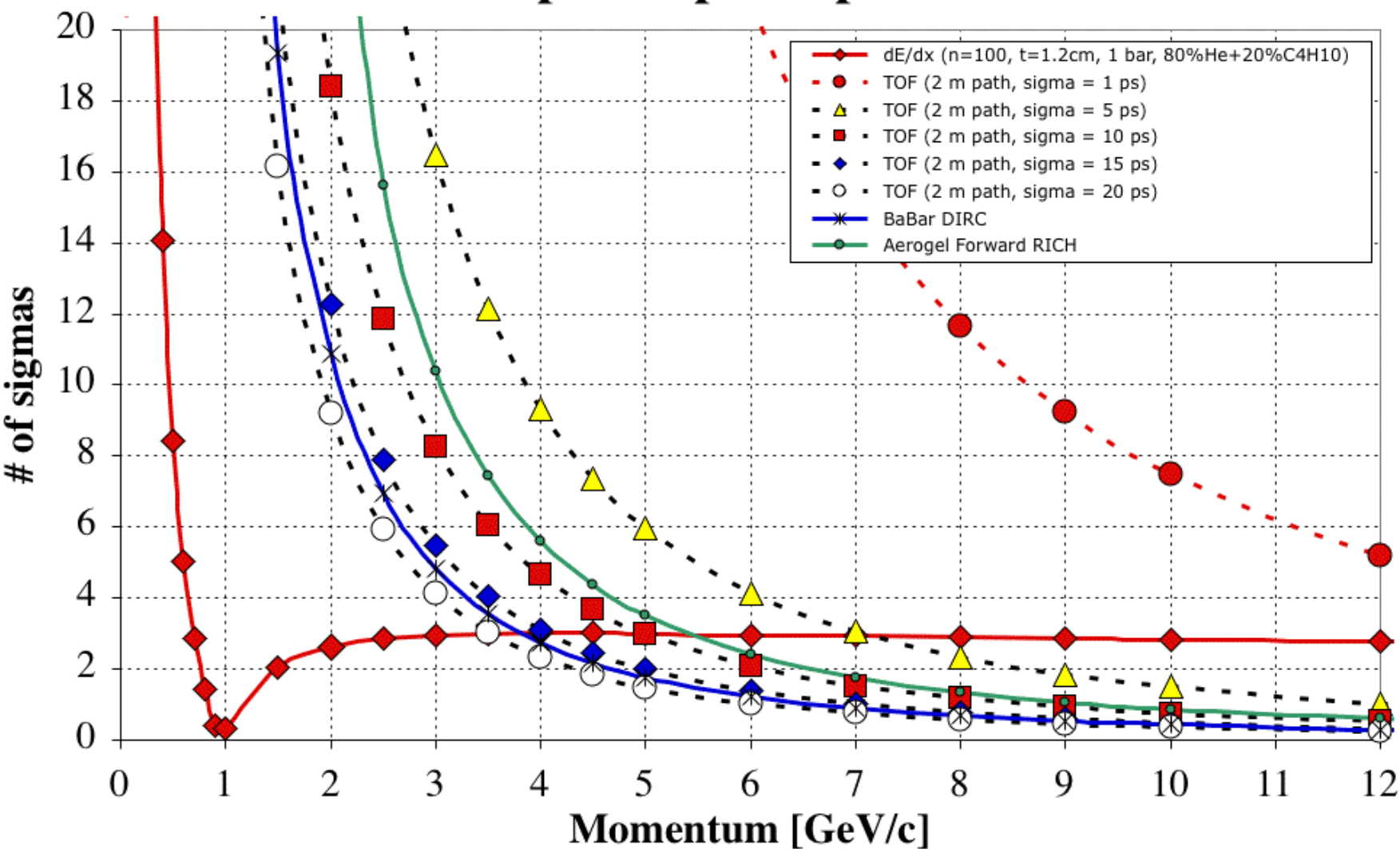
BURLE 85011 microchannel plate (MCP) PMT: multi-anode PMT with two MCP stages



→ very fast ($\sigma=40\text{ps}$ for single photons)

Time-of-flight with fast photon detectors

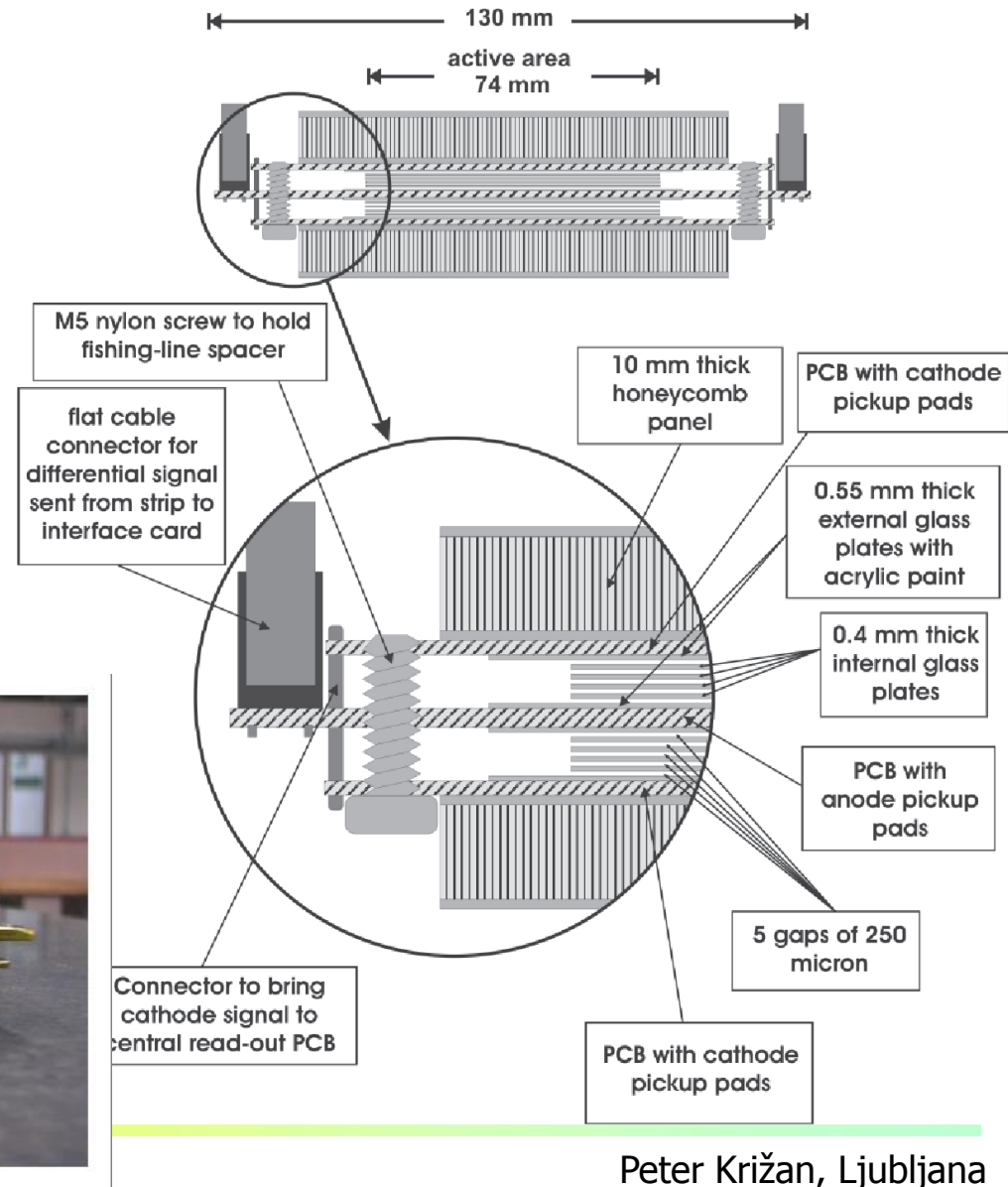
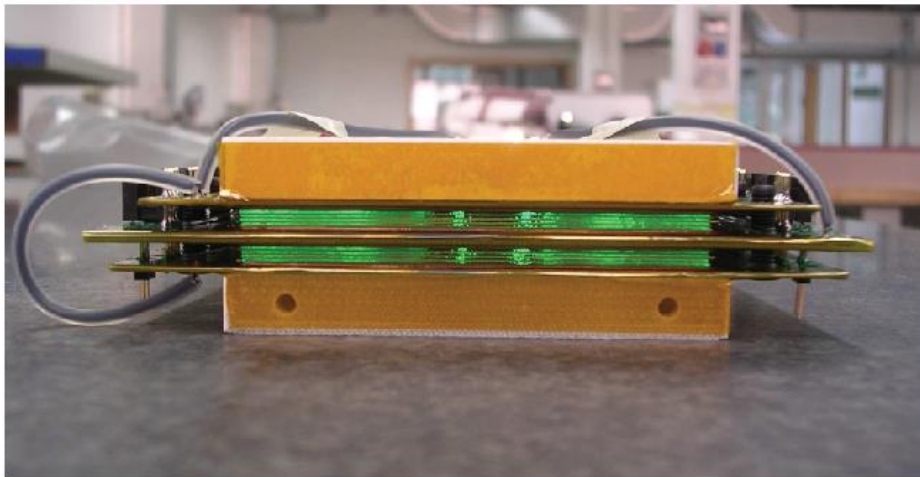
Expected p/K separation



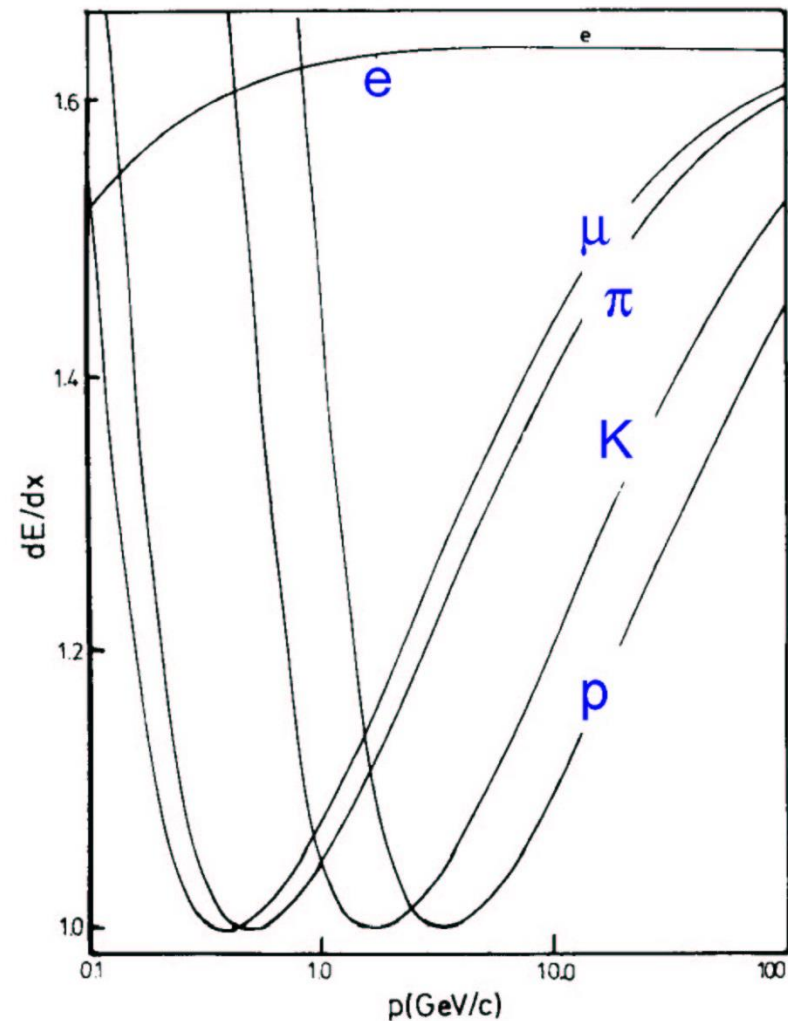
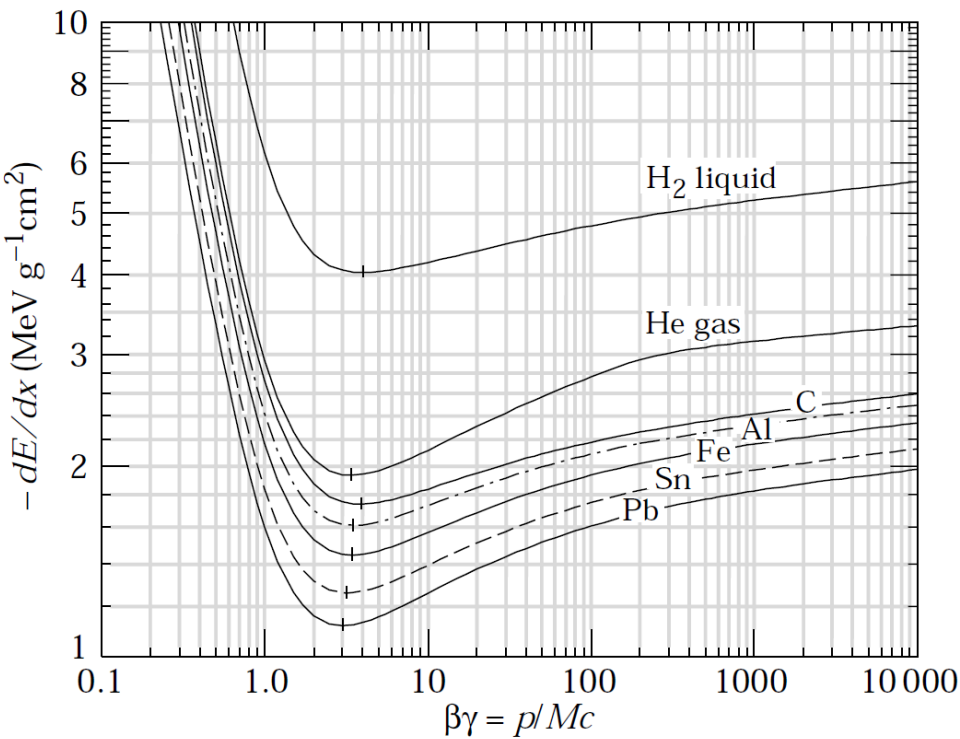
ALICE TOF

Very fast large area (140m^2)
particle detector:
→ MRPC, multi-gap RPC

$\sigma=50\text{ps}$ (incl. read-out)
 π/K separation (3σ) up to 2.5
GeV/c at large track densities



Identification with the dE/dx measurement



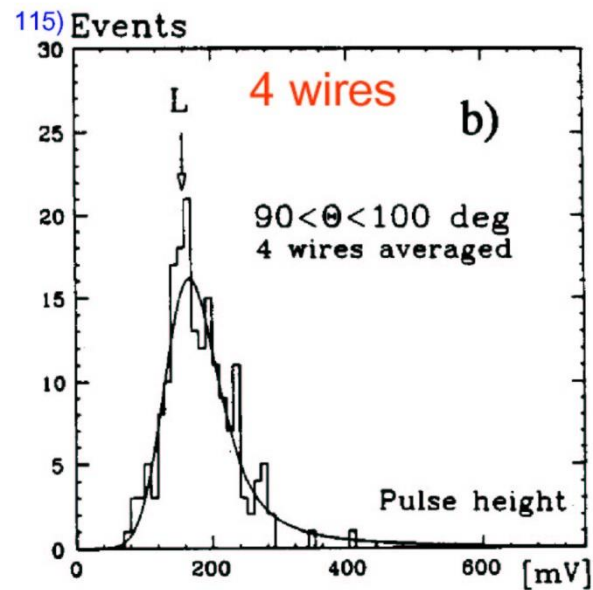
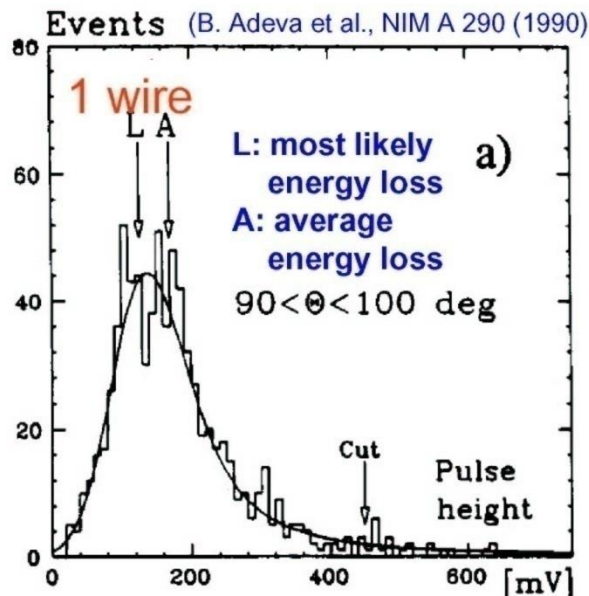
dE/dx is a function of velocity β

For particles with different mass the Bethe-Bloch curve gets displaced if plotted as a function of p

For good separation: resolution should be $\sim 5\%$

Identification with dE/dx measurement 2

Problem: long tails (Landau distribution, not Gaussian)

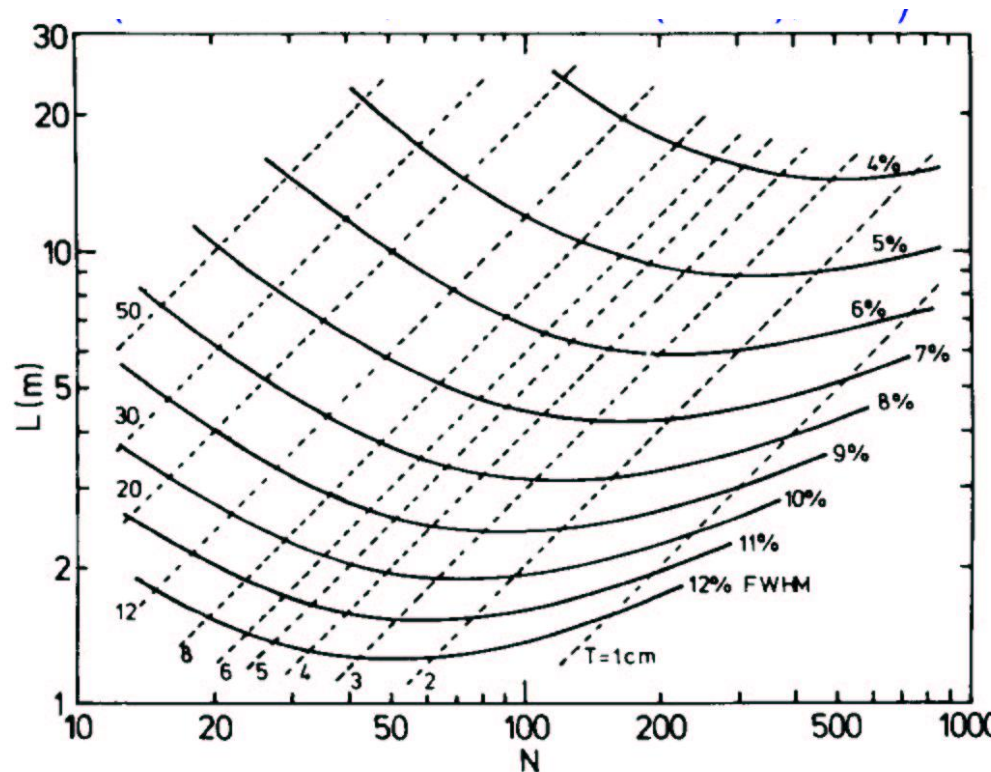


Identification with dE/dx measurement 3

Optimisation of the counter: length L, number of samples N, resolution (FWHM)

If the distribution of individual measurements were Gaussian, only the total sample thickness would be relevant.

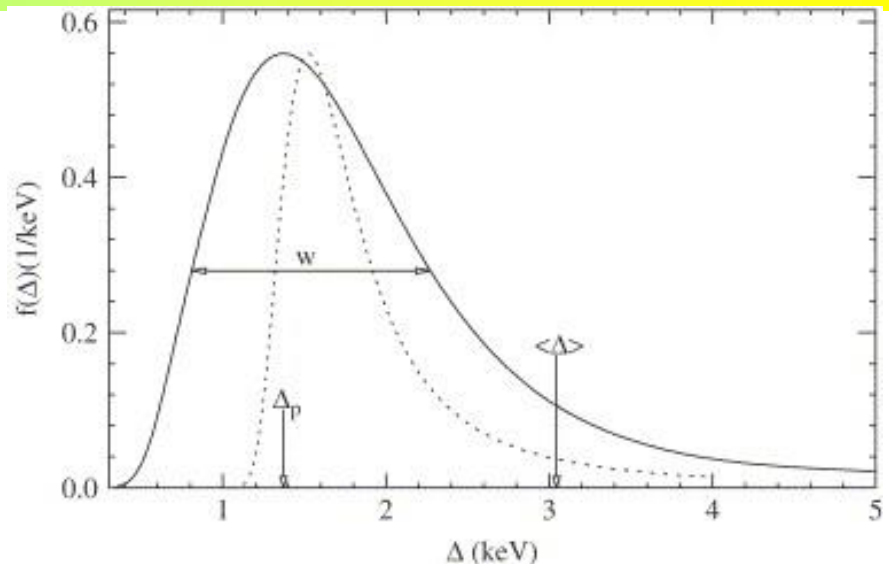
Tails: eliminate the largest 30% values → the optimum depends also on the number of samples.



Identification with dE/dx measurement

Problem: long tails (not Gaussian!)

Energy loss distribution for particles with $\beta\gamma=3.6$ traversing 1.2 cm of Ar gas (solid line).



Parameters describing $f(\Delta)$ are the most probable energy loss $\Delta_p(x, \beta\gamma) =$ the position of the maximum at 1371 eV, and w , the full-width-at-half-maximum (FWHM) of 1463 eV. The mean energy loss is 3044 eV.
Dotted line: the original Landau function.

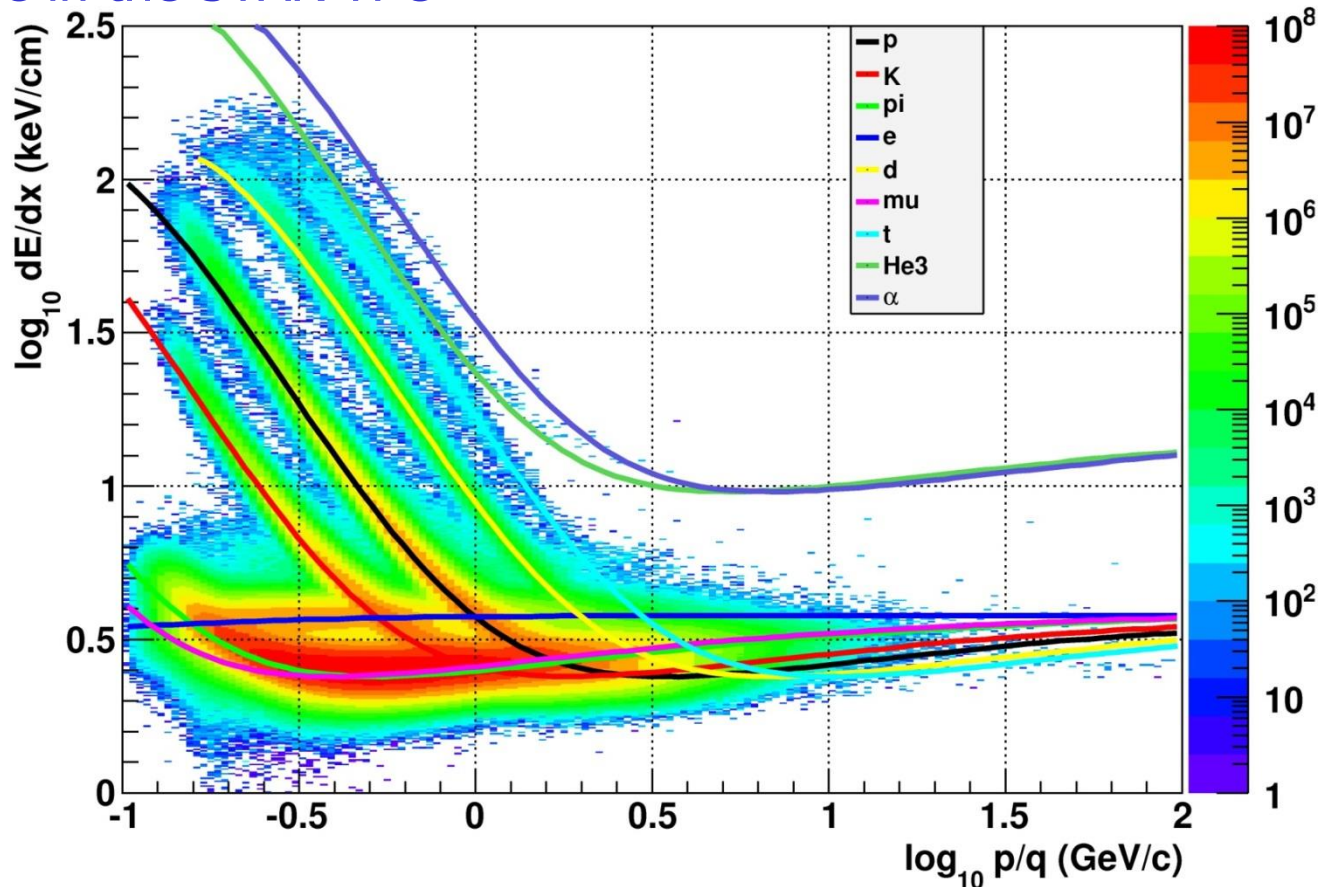
→ Many samples along the track (~100 in ALICE TPC), remove the largest ~40% values (reduce the influence of the long tail) → truncated mean

→ Hans Bichsel: A method to improve tracking and particle identification in TPCs and silicon detectors, NIM A562 (2006) 154

Identification with dE/dx measurement

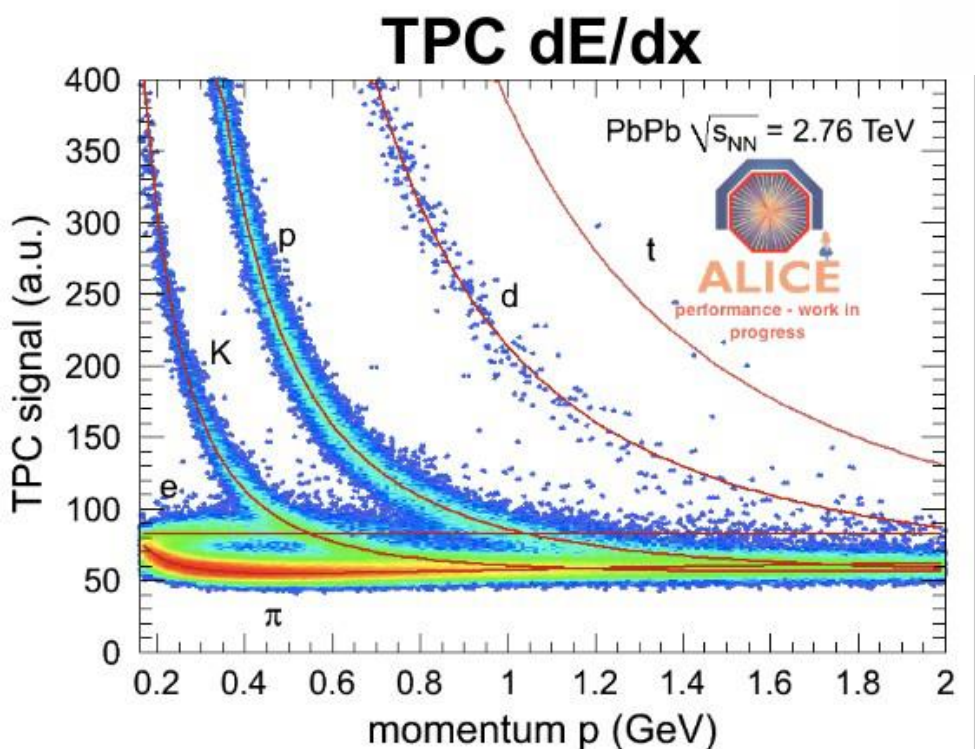
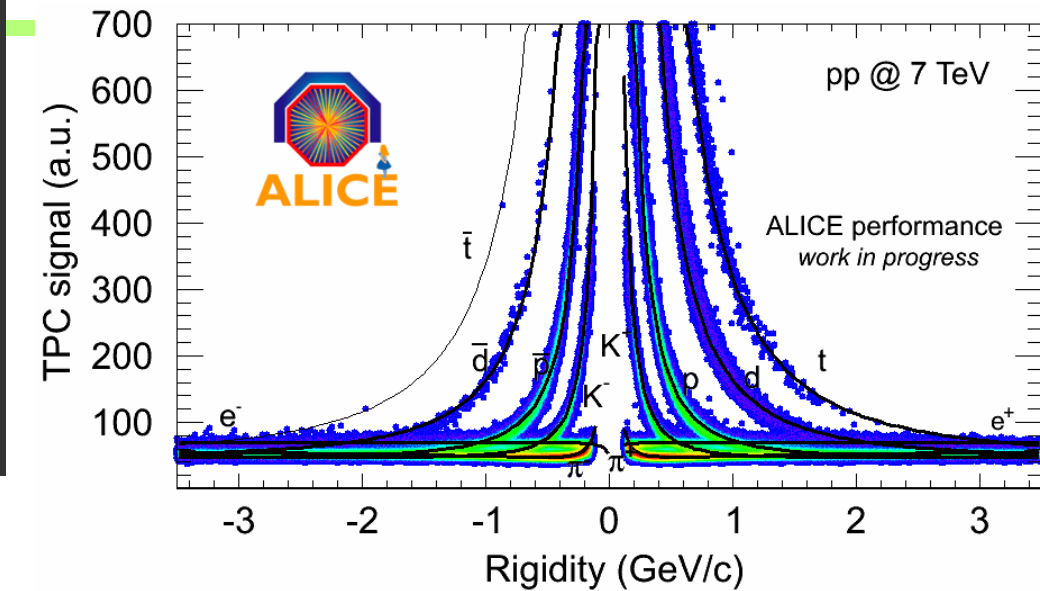
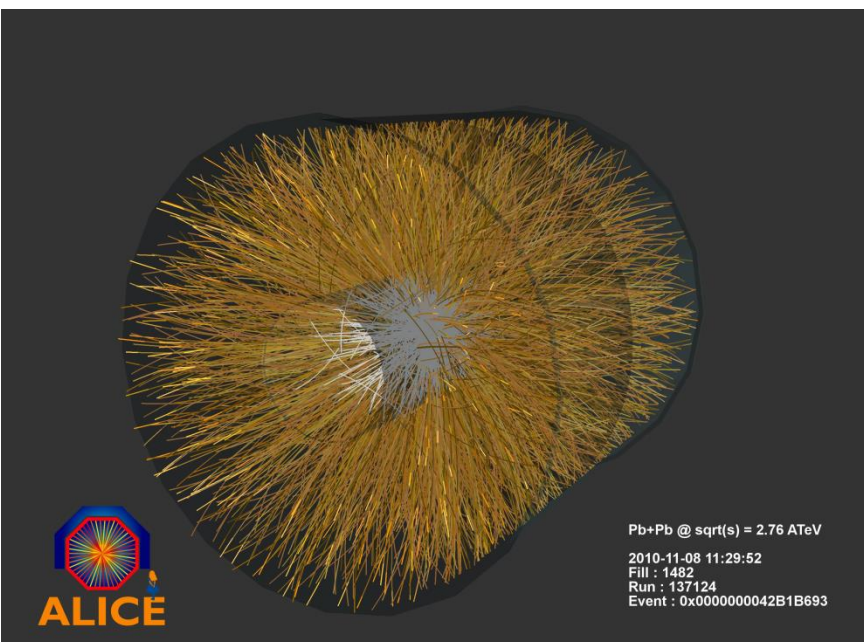
gold-gold
collisions

dE/dx performance in the STAR TPC

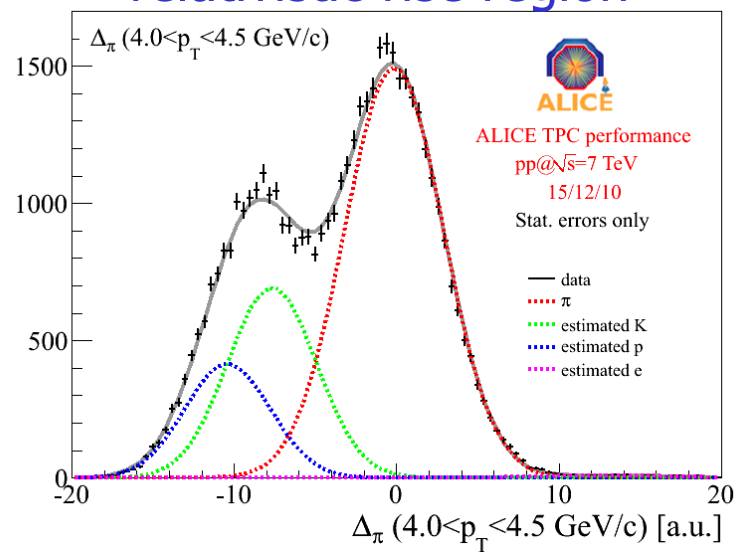


Energy loss in the STAR TPC: truncated mean as a function of momentum. The curves are Bichsel model predictions.

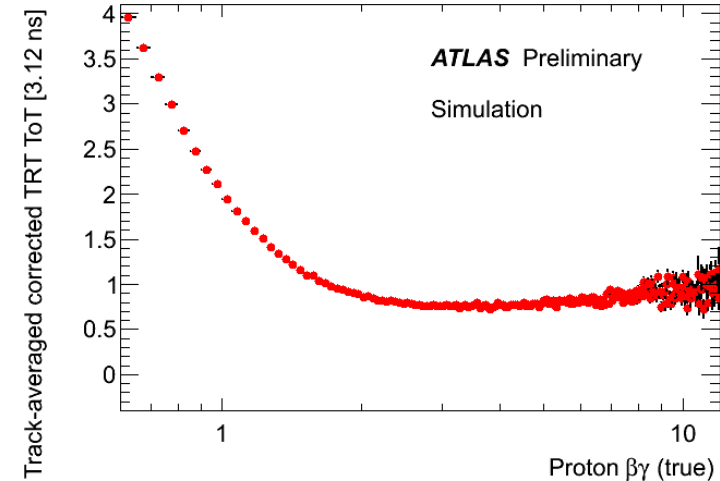
dE/dx in ALICE



relativistic rise region

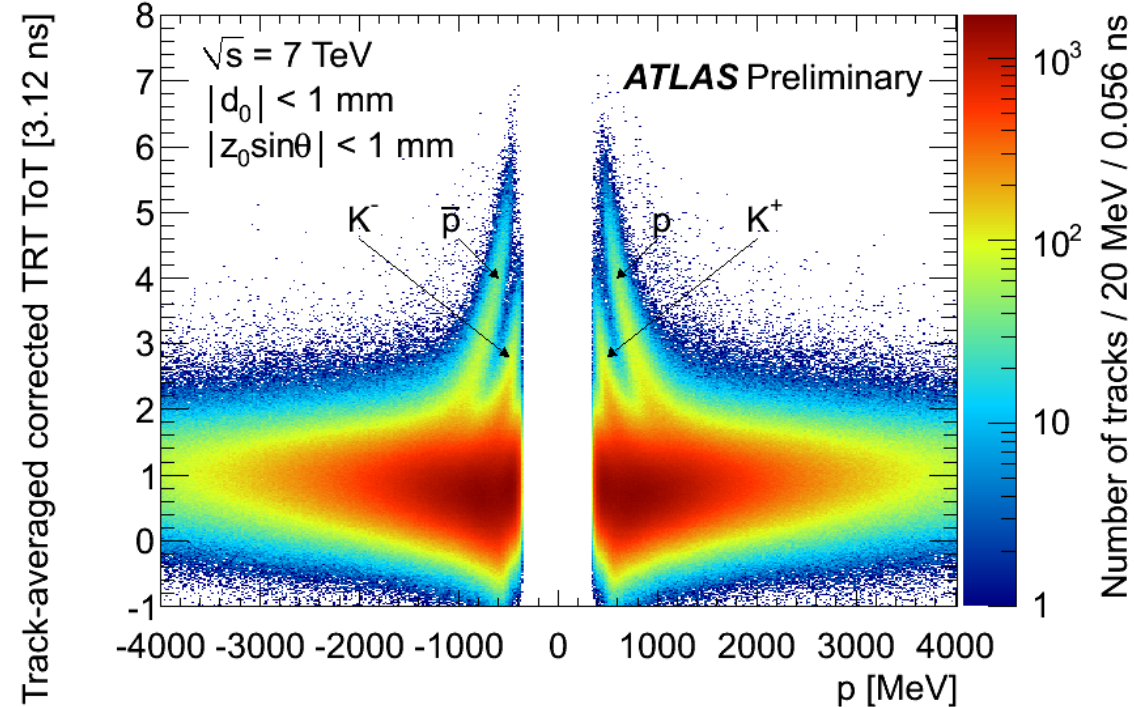


Time-over-Threshold (ToT): dE/dx in ATLAS TRT



2010 data: The track-averaged ToT distribution as a function of the track momentum.

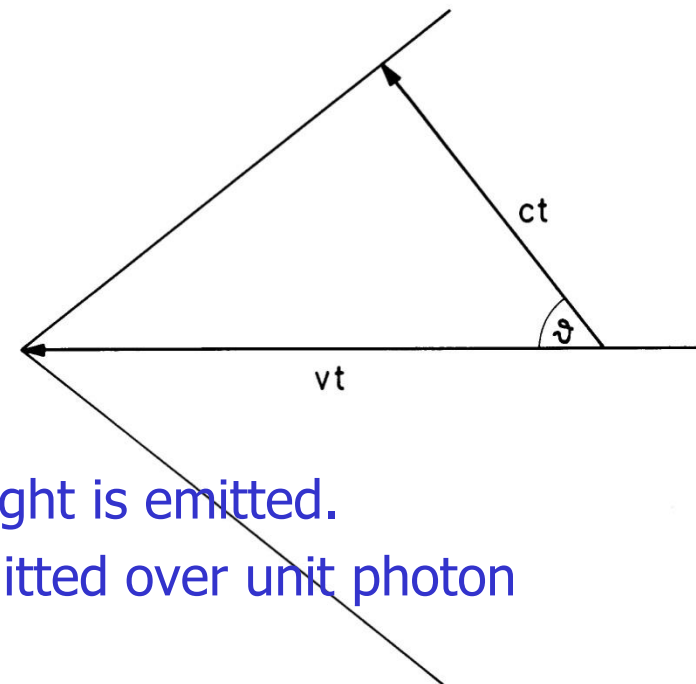
The relation between the track ToT measurement and the track $\beta\gamma$, obtained from MC studies.



Cherenkov radiation

A charged track with velocity $v=\beta c$ exceeding the speed of light c/n in a medium with refractive index n emits polarized light at a characteristic (Cherenkov) angle,

$$\cos\theta = c_0/nv = 1/\beta n$$



Two cases:

→ $\beta < \beta_t = 1/n$: below threshold no Cherenkov light is emitted.

→ $\beta > \beta_t$: the number of Cherenkov photons emitted over unit photon energy $E=h\nu$ in a radiator of length L :

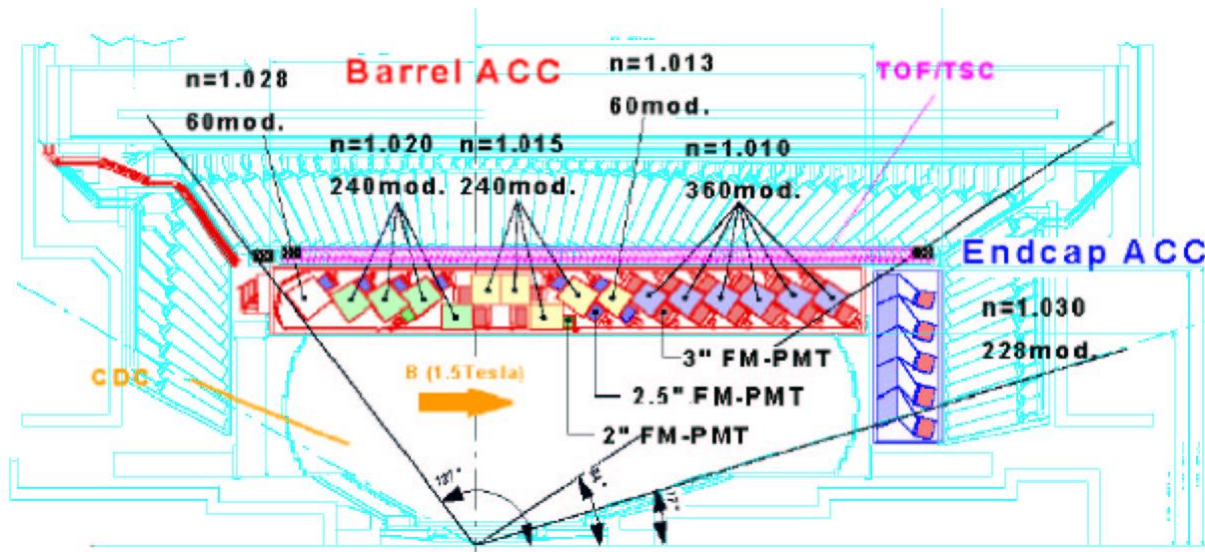
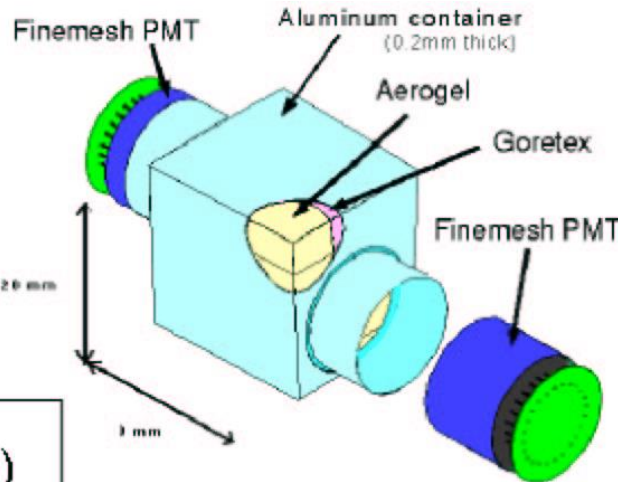
$$\frac{dN}{dE} = \frac{\alpha}{\hbar c} L \sin^2 \theta = 370(cm)^{-1}(eV)^{-1} L \sin^2 \theta$$

→ Few detected photons

Belle: threshold Cherenkov counter, ACC (aerogel Cherenkov counter)

K (below threshold) vs. π (above) by properly choosing n for a given kinematic region (more energetic particles fly in the 'forward region')

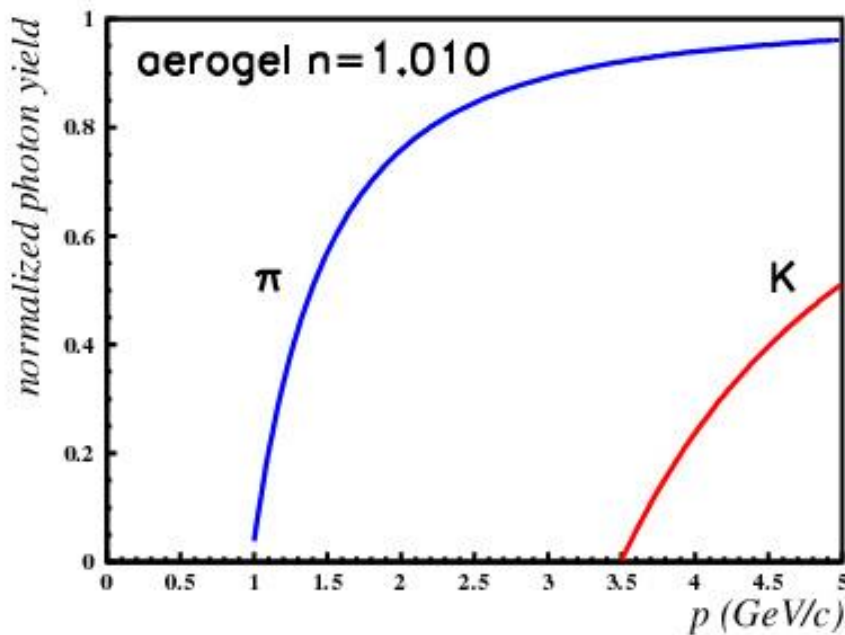
Detector unit: a block of aerogel and two fine-mesh PMTs



Fine-mesh PMT: works in high B fields (1.5 T)

Belle ACC : threshold Cherenkov counter

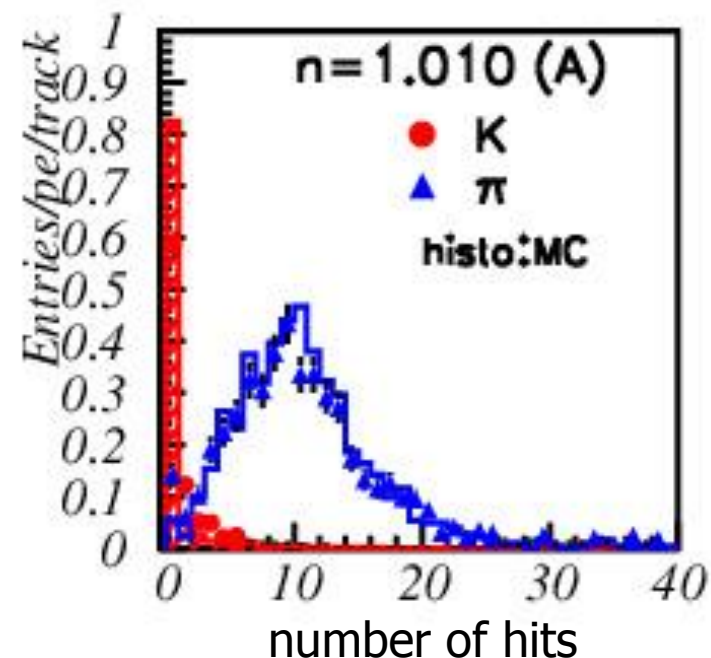
expected yield vs p



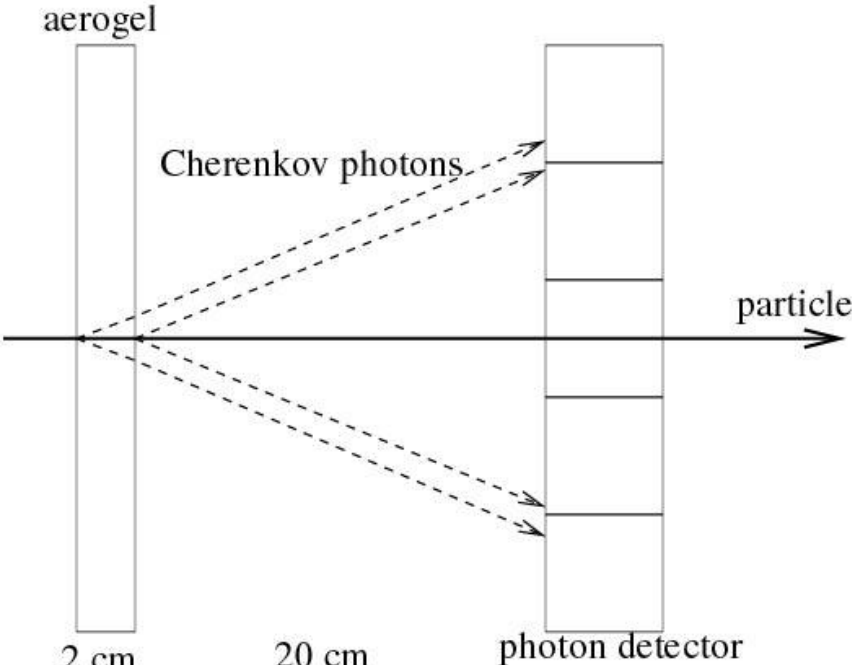
→ Good separation between pions (light) and kaons (no light) between ~ 1.5 GeV/c and 3.5 GeV/c

NIM A453 (2000) 321

yield for $2\text{GeV} < p < 3.5\text{GeV}$:
expected and measured
number of hits



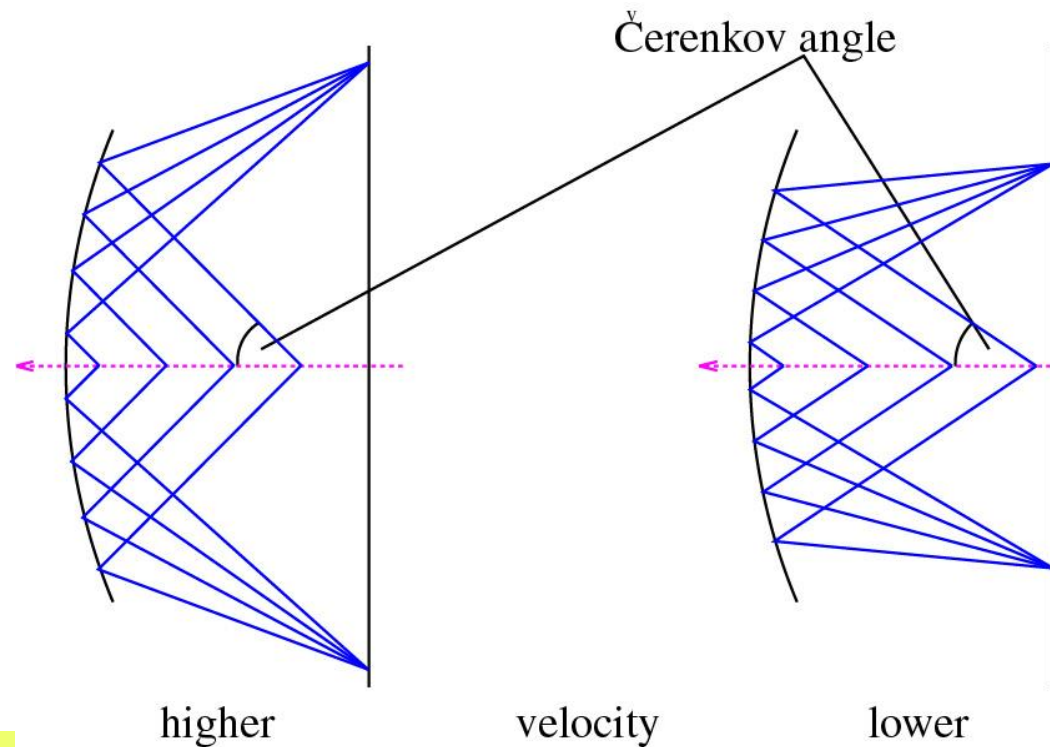
Measuring Cherenkov angle



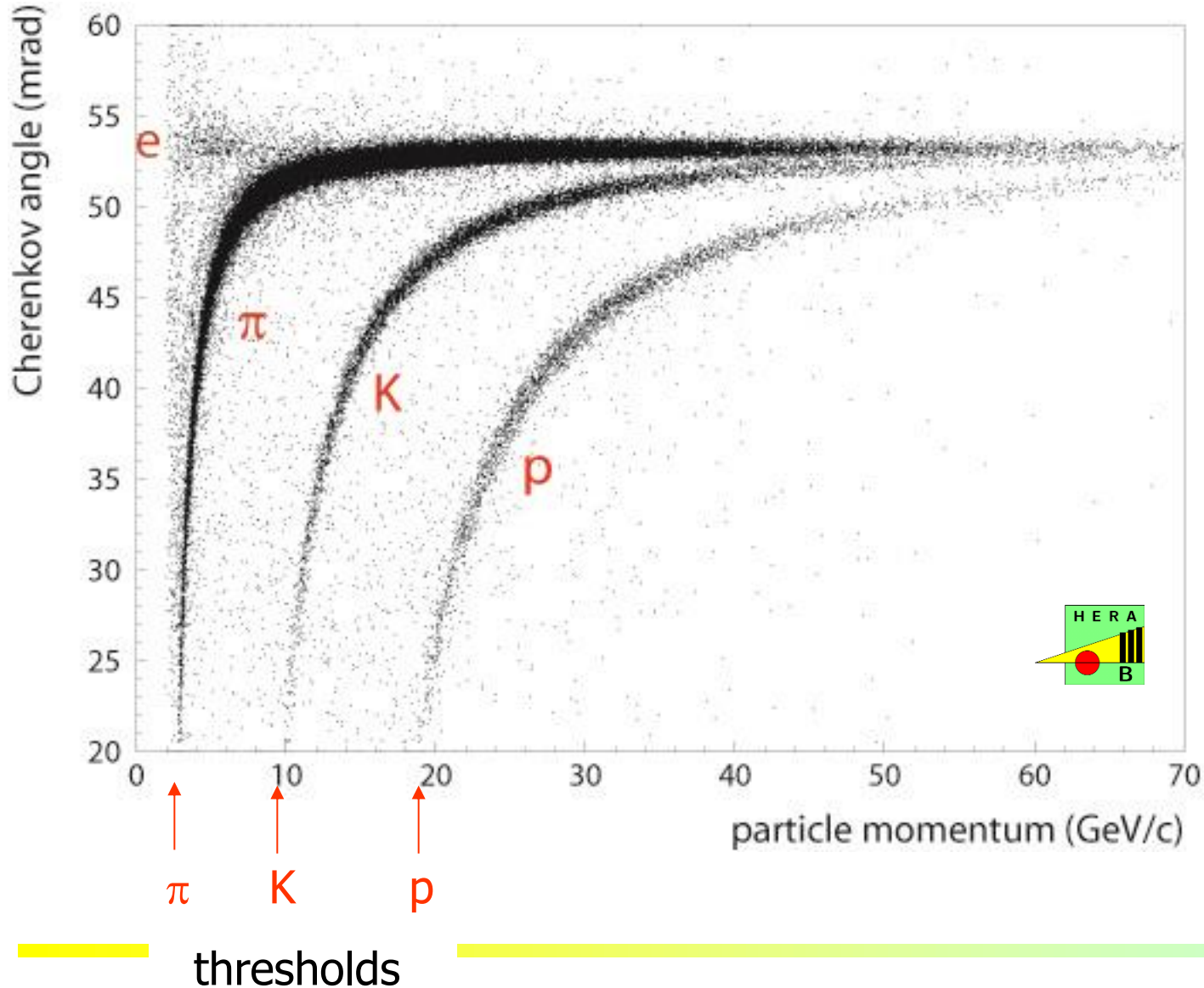
Proximity focusing RICH

RICH with a focusing mirror

Idea: transform the direction into a coordinate →
ring on the detection plane
→ Ring Imaging Cherenkov



Measuring Cherenkov angle

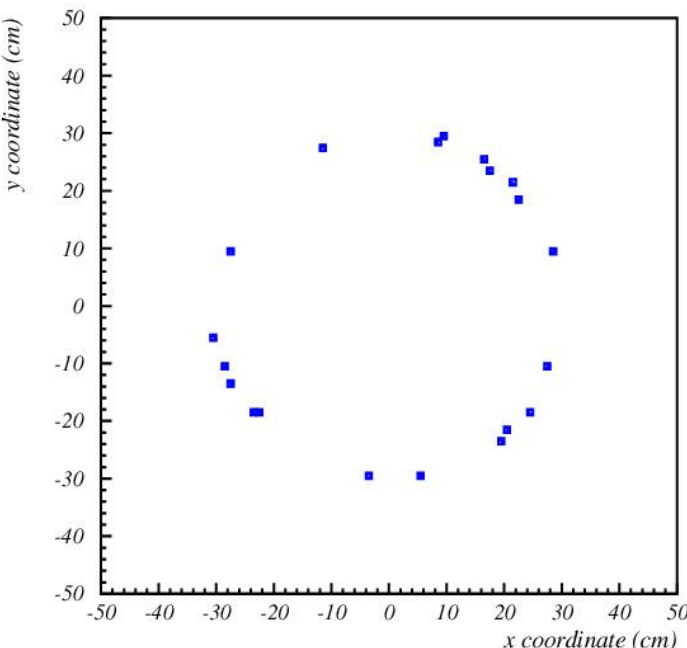


Photon detection in RICH counters

RICH counter: measure photon impact point on the photon detector surface

→ detection of **single** photons with

- sufficient **spatial resolution**
- **high efficiency** and **good signal-to-noise ratio** (few photons!)
- over a **large area** (square meters)



Special requirements:

- Operation in magnetic field
- High rate capability
- Very high spatial resolution
- Excellent timing (time-of-arrival information)

Resolution of a RICH counter

Determined by:

- Photon impact point resolution (~photon detector granularity)
- Emission point uncertainty (not in a focusing RICH)
- Dispersion: $1/\beta = n(\lambda) \cos\theta$
- Errors of the optical system
- Uncertainty in track parameters

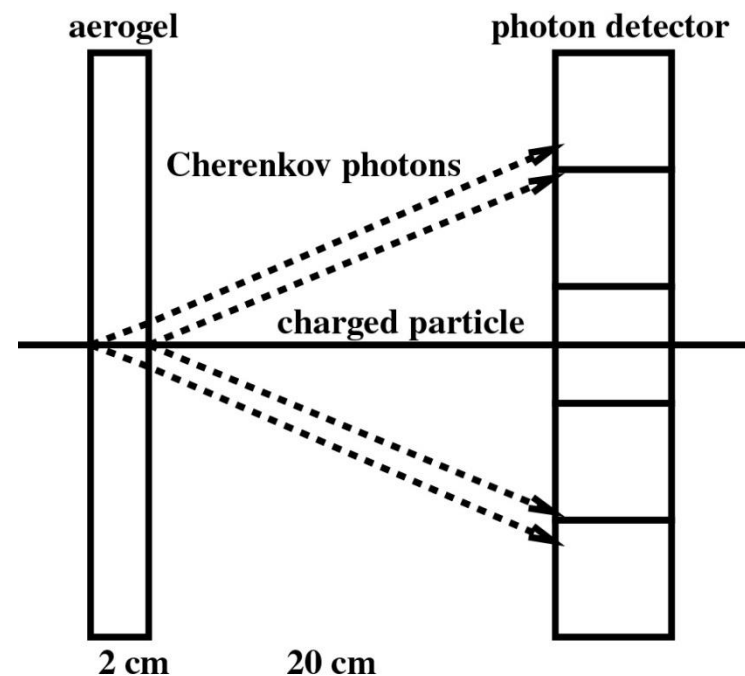
Resolution per track:

$$\sigma_{track} = \frac{\sigma_0}{\sqrt{N_{pe}}}$$

single photon
resolution

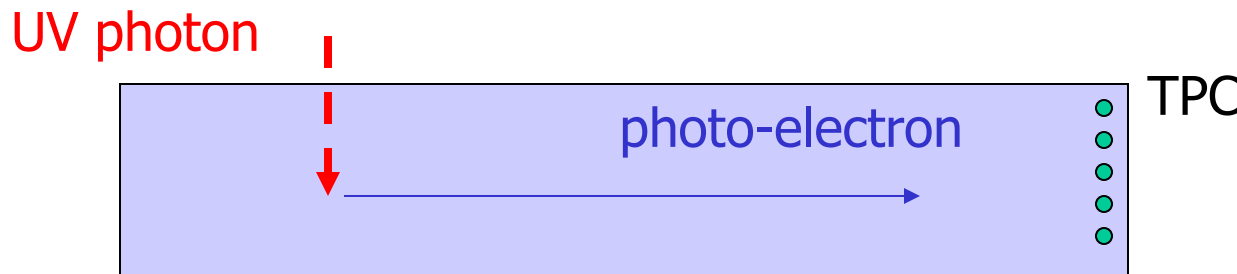
of detected
photons

(in the case of low background)

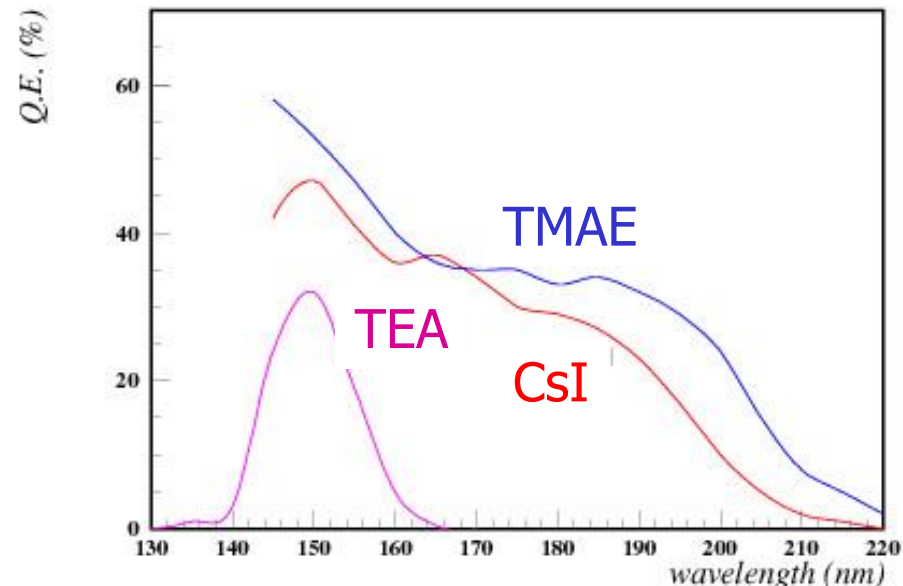


First generation of RICH counters

DELPHI, SLD, OMEGA RICH counters: all employed wire chamber based photon detectors (UV photon → photo-electron → detection of a single electron in a TPC)

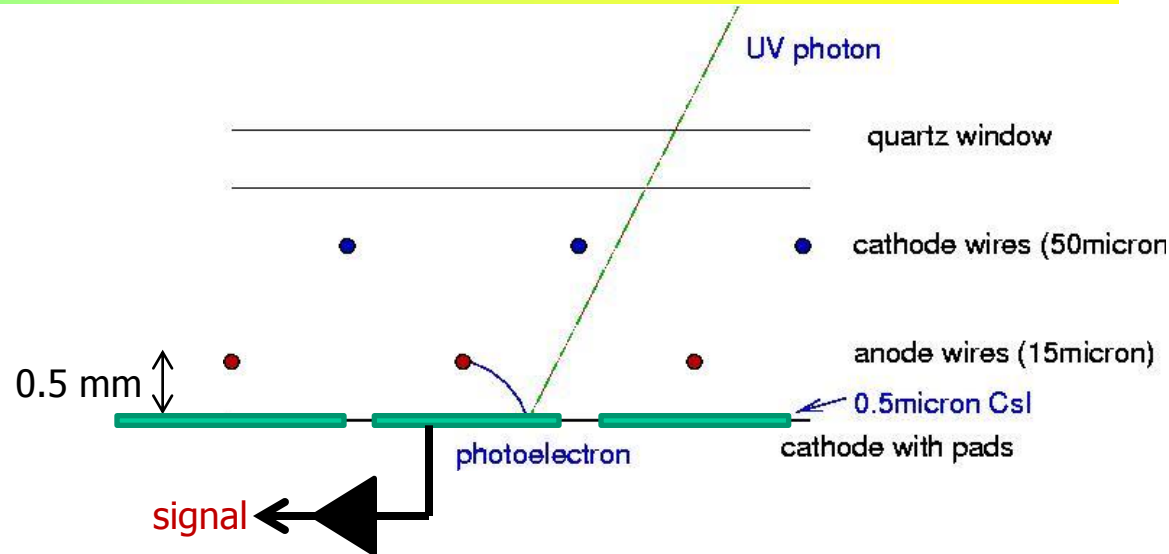


Photosensitive component:
TMAE added to the gas mixture



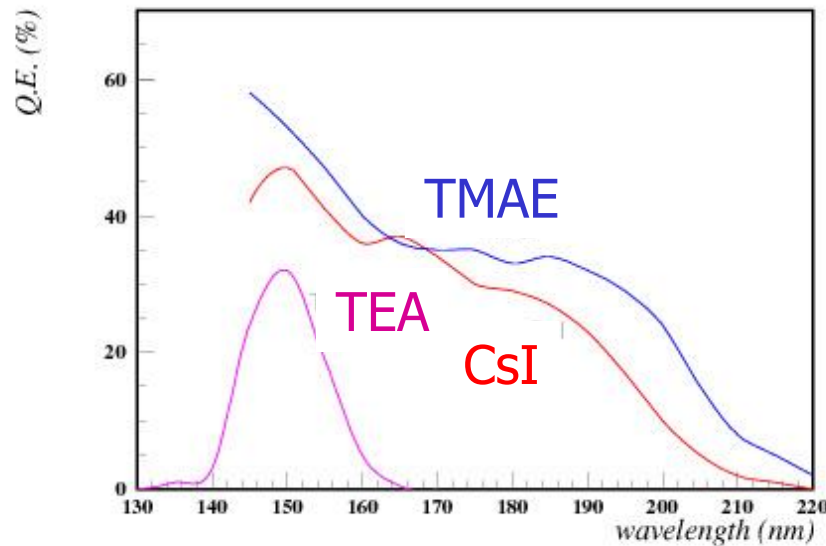
Fast RICH counters with wire chambers

Multiwire chamber with cathode pad read-out:
→ short drift distances,
fast detector



Photosensitive component:

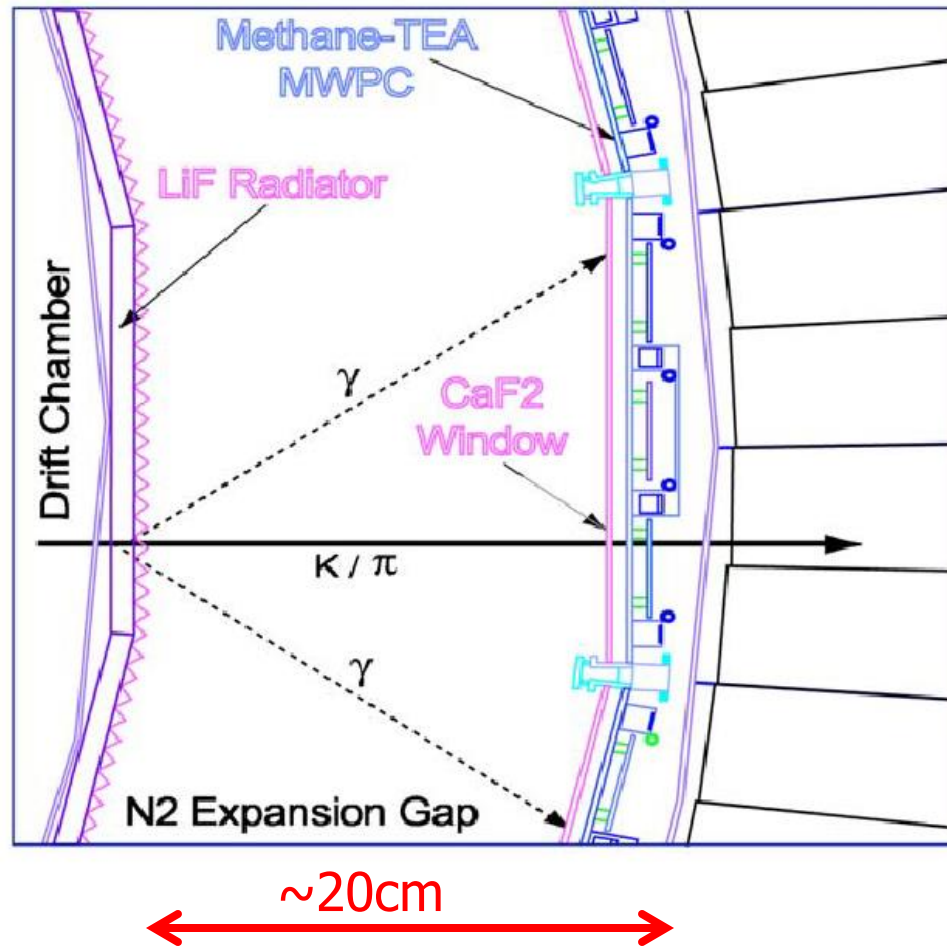
- in the gas mixture (**TEA**):
CLEOIII RICH
- or a layer on one of the cathodes
(**CsI** on the printed circuit cathode with pads) →



Works in high magnetic field!

CLEOIII RICH

Photon detection in a wire chamber with a methane+TEA mixture.
Technique pioneered by T. Ypsilantis and J. Seguinot

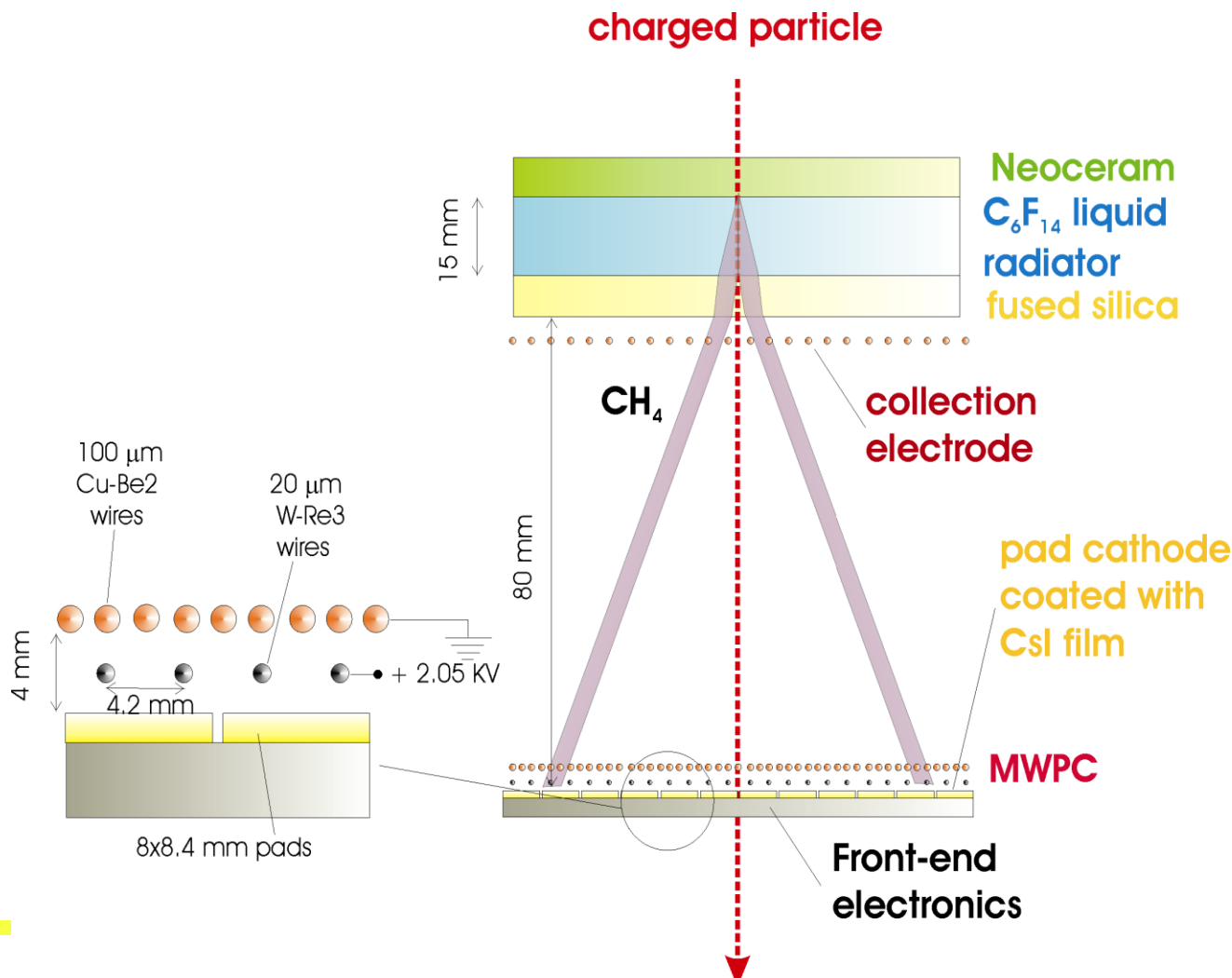


CsI based RICH counters: HADES, COMPASS, ALICE

HADES and COMPASS RICH: gas radiator + CsI photocathode – long term experience in operation

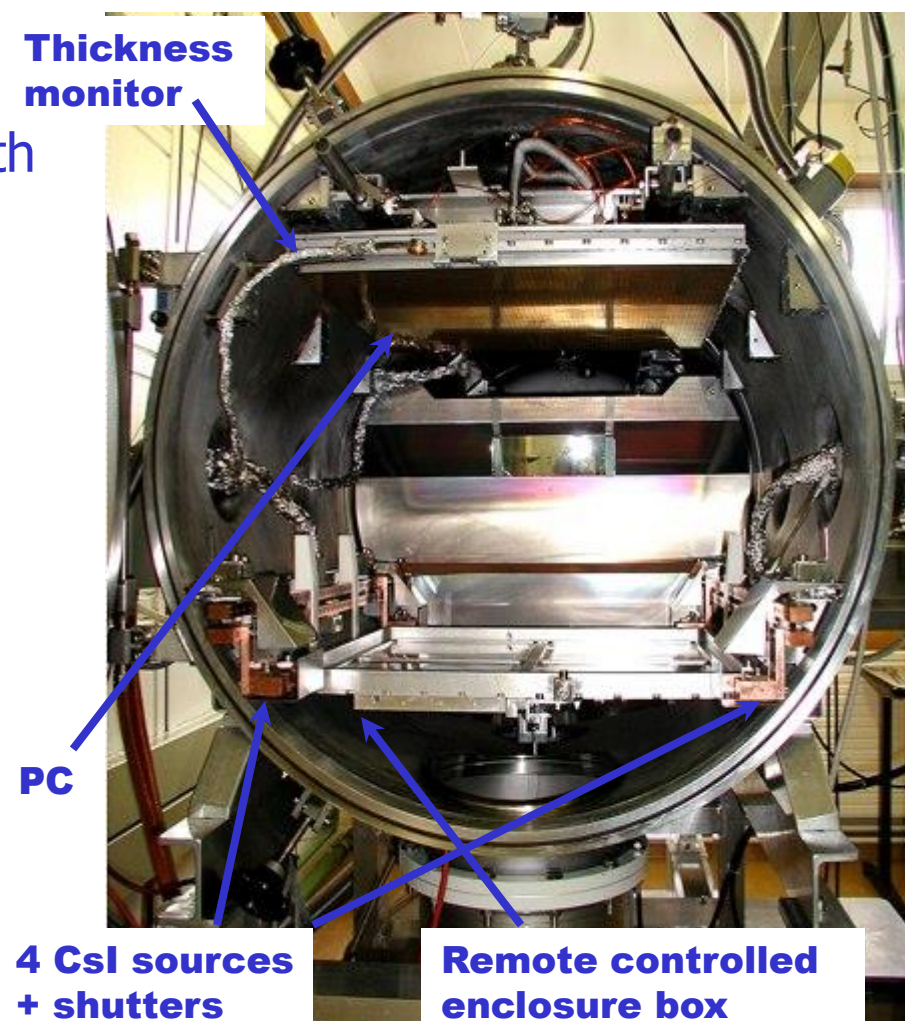
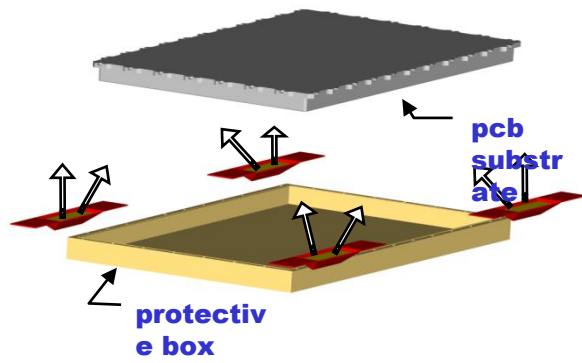
ALICE:

- liquid radiator
- proximity focusing



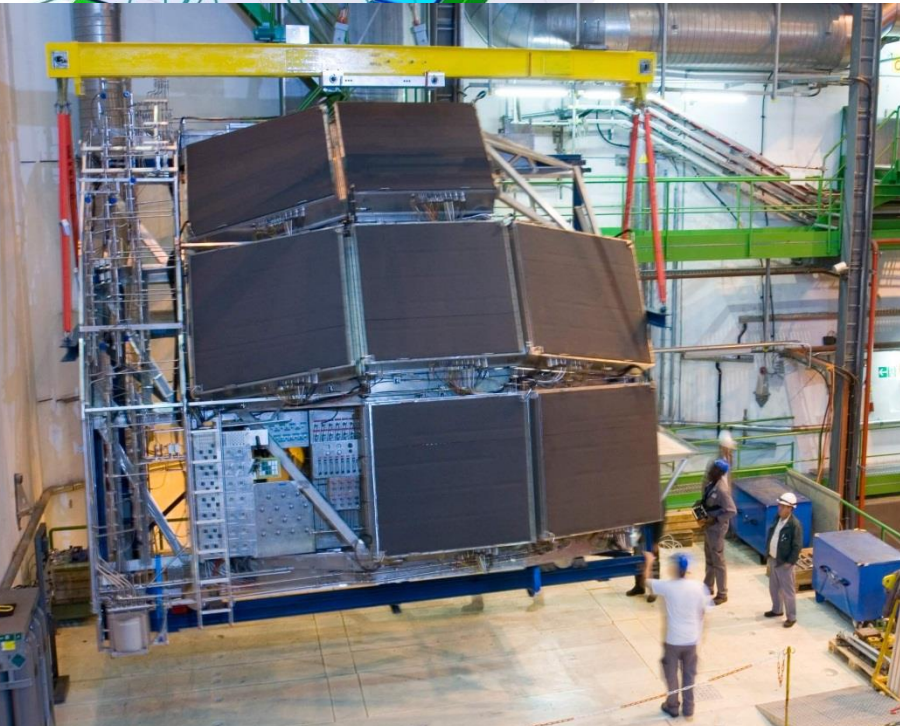
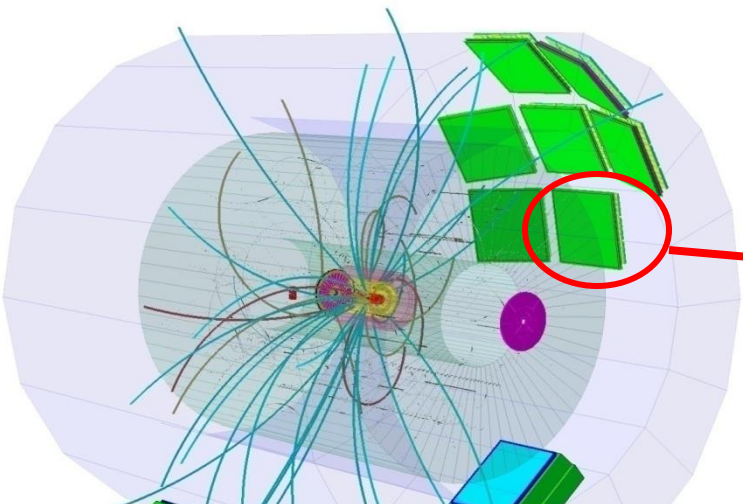
CERN CsI deposition plant

Photocathode produced with a well defined, several step procedure, with CsI vacuum deposition and subsequent heat conditioning

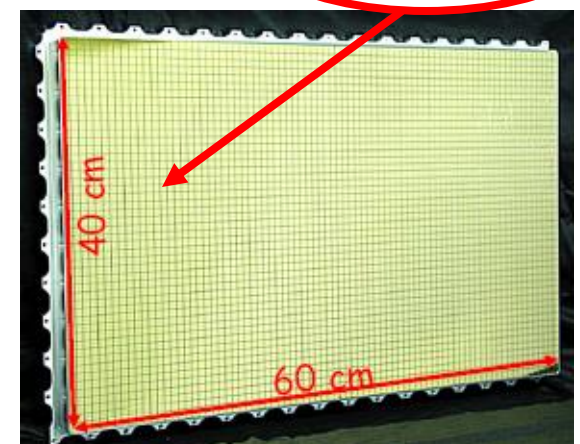
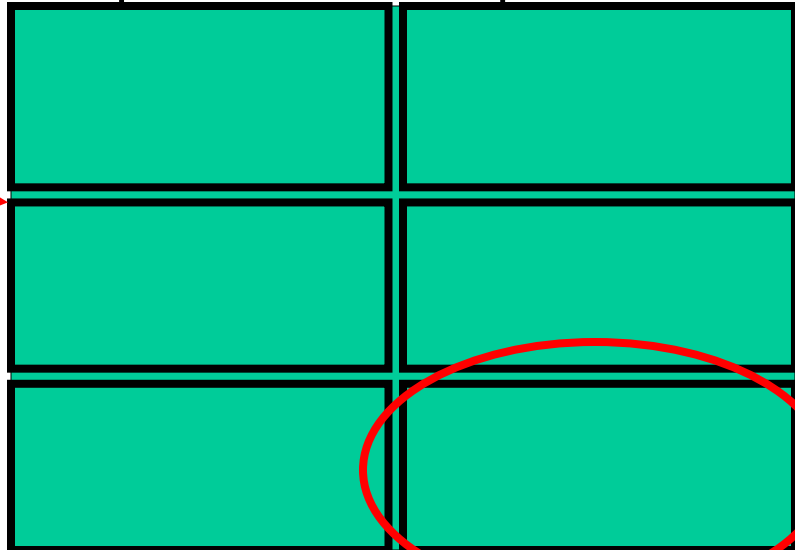


ALICE RICH = HMPID

The largest scale (11 m^2) application of CsI photo-cathodes in HEP!

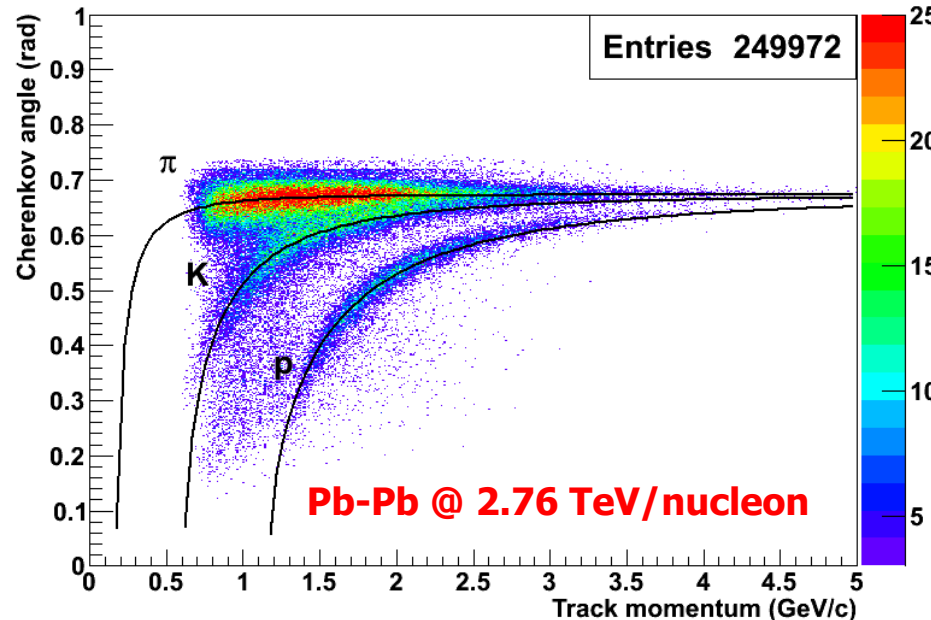
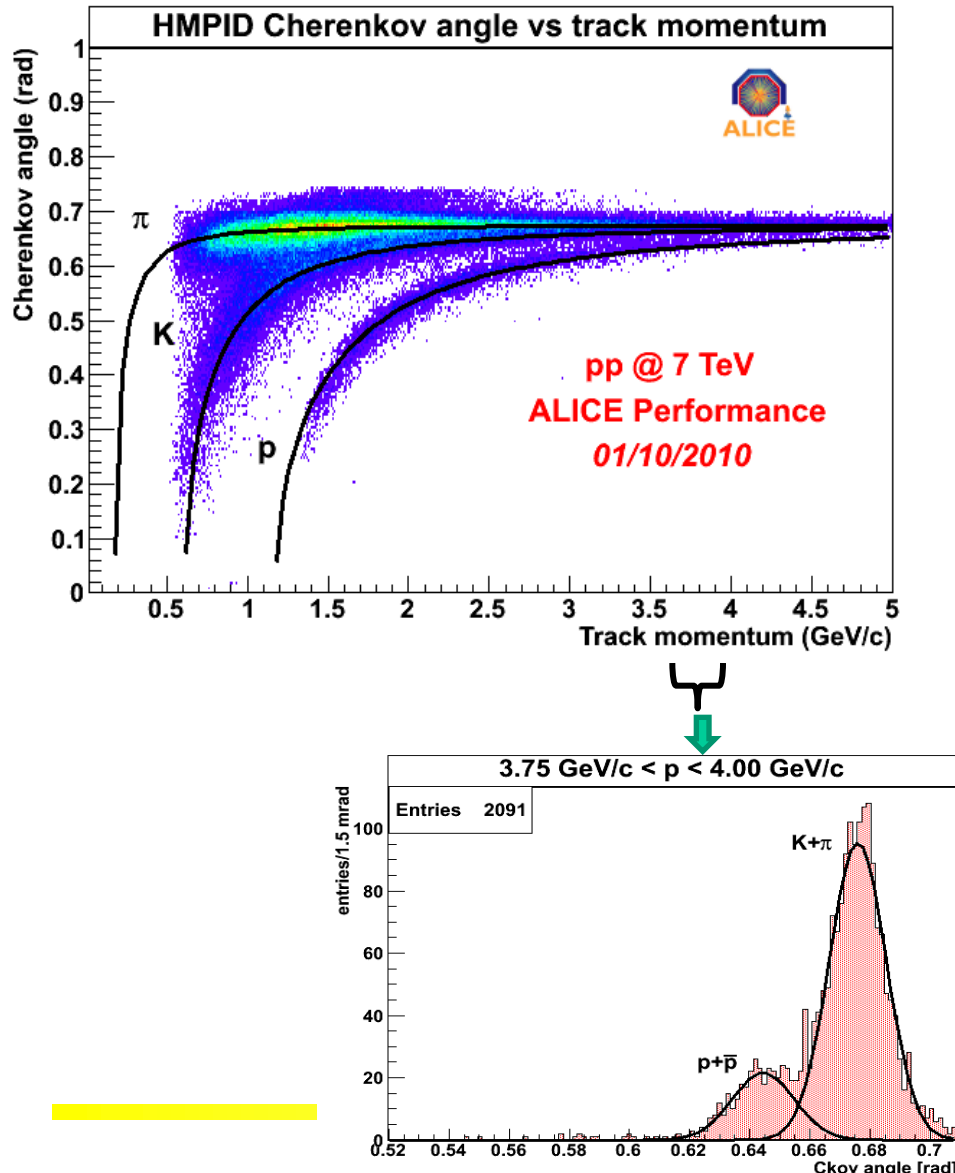


Six photo-cathodes per module



CsI photo-cathode is segmented in $0.8 \times 0.84\text{ cm}$ pads

ALICE HMPID performance



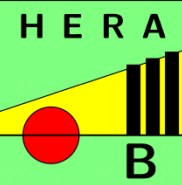
Cherenkov counters with vacuum based photodetectors

Some applications: operation at high rates over extended running periods (years) → wire chamber based photon detectors were found to be unsuitable (problems in high rate operation, ageing, only UV photons, difficult handling in 4π spectrometers)

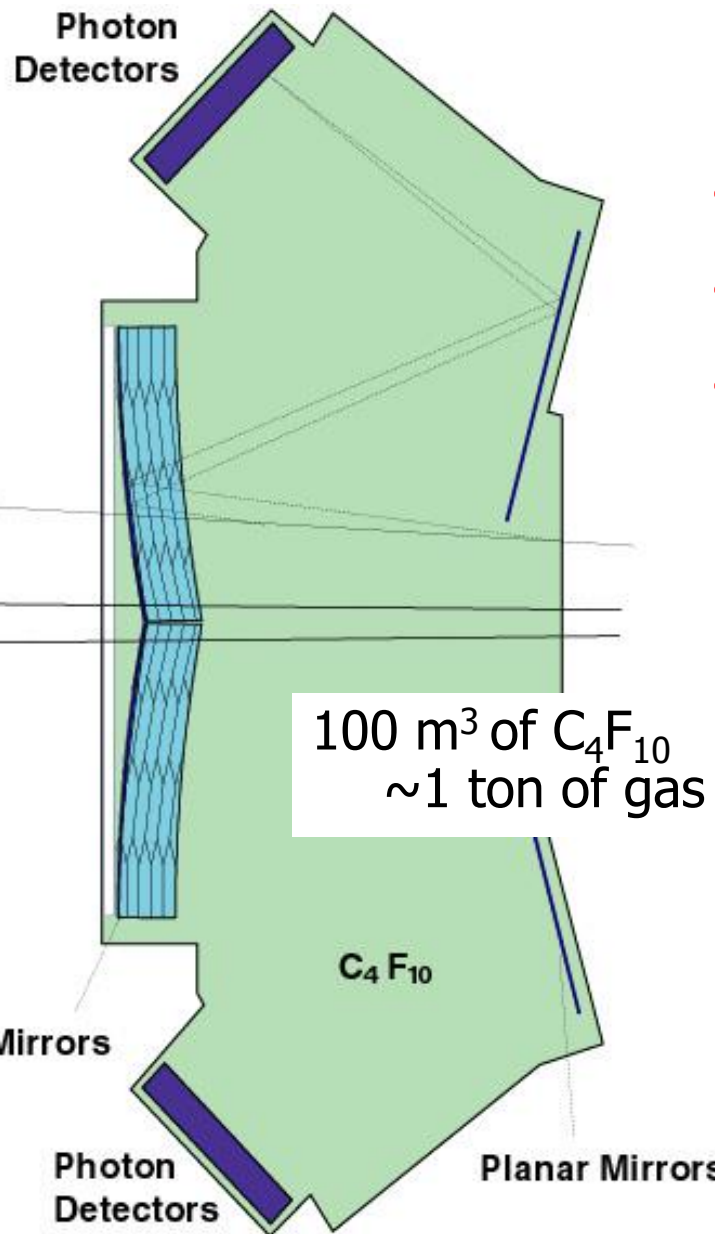
→ Need **vacuum based photon detectors** (e.g. PMTs)

Good spacial resolution (pads with ~ 5 mm size)

→ Need **multianode** PMTs

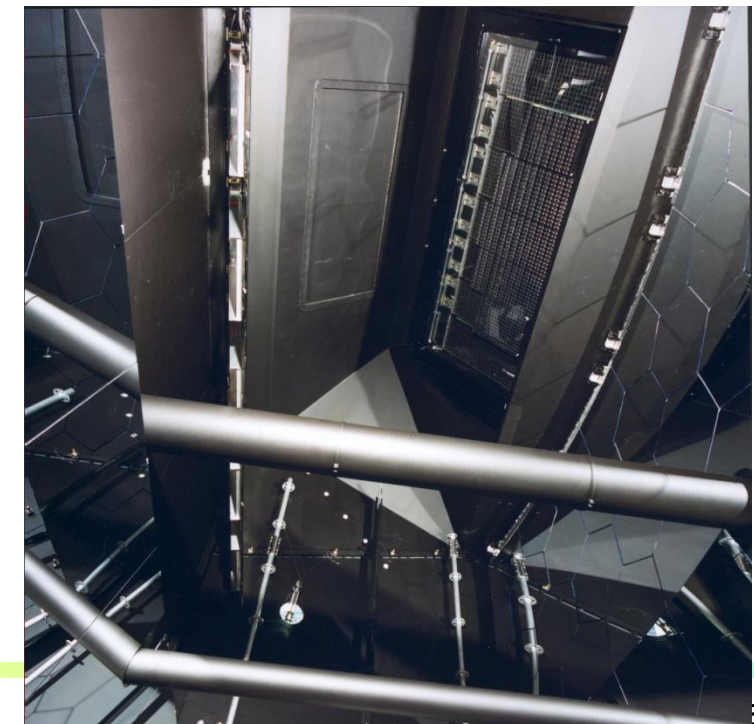


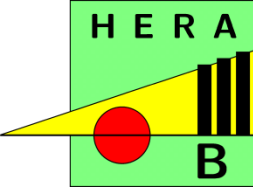
HERA-B RICH



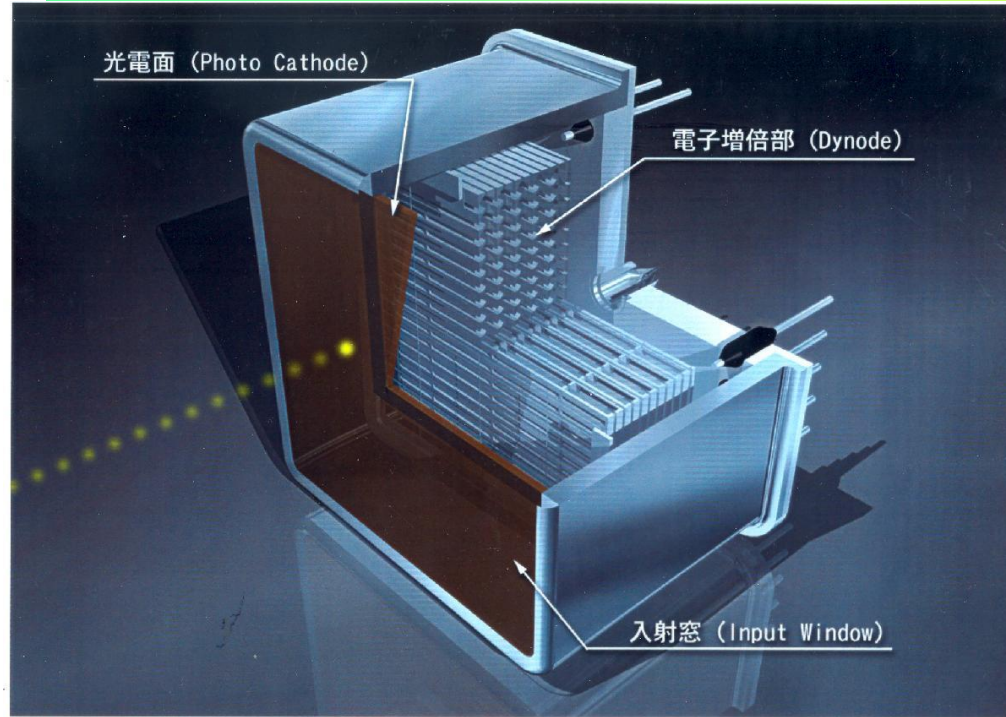
Photon detector requirements:

- High QE over $\sim 3\text{m}^2$
- Rates $\sim 1\text{MHz}$
- Long term stability





Multianode PMTs



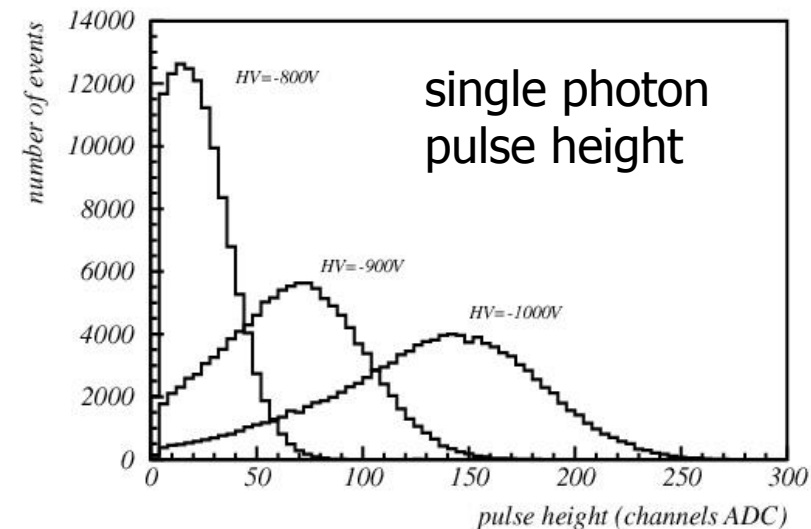
Multianode PMTs with metal foil dynodes and 2x2, 4x4 or 8x8 anodes
Hamamatsu R5900 (and follow up types 7600, 8500)

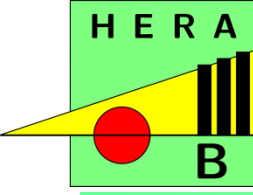
→ Excellent single photon pulse height spectrum

→ Low noise (few Hz/ch)

→ Low cross-talk (<1%)

→ NIM A394 (1997) 27

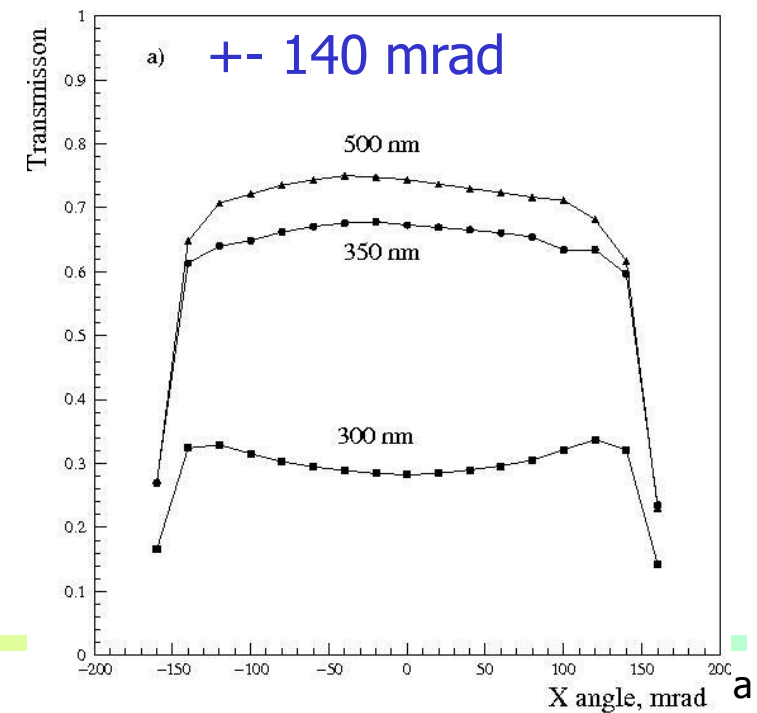
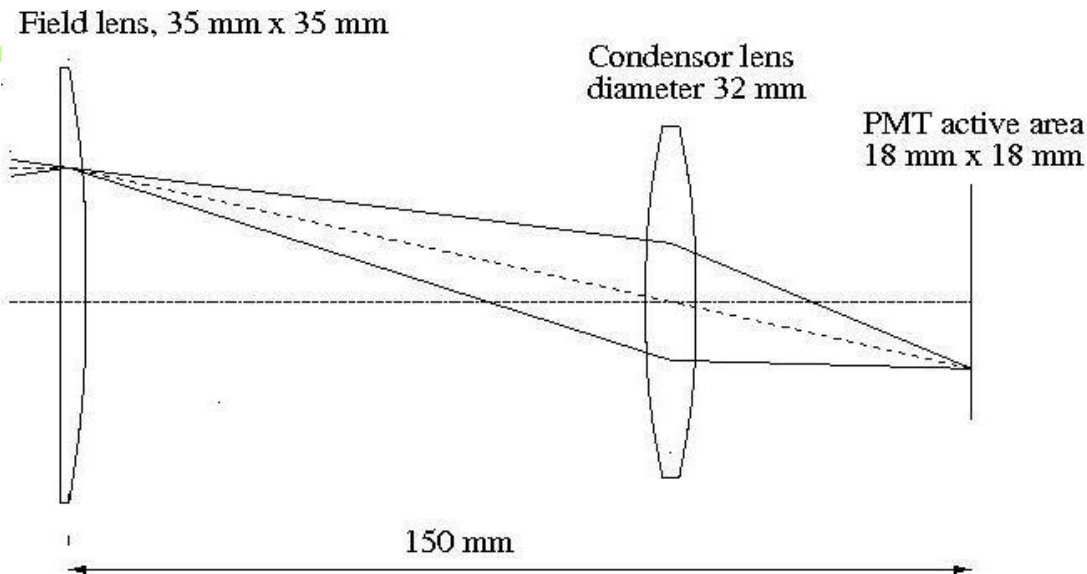
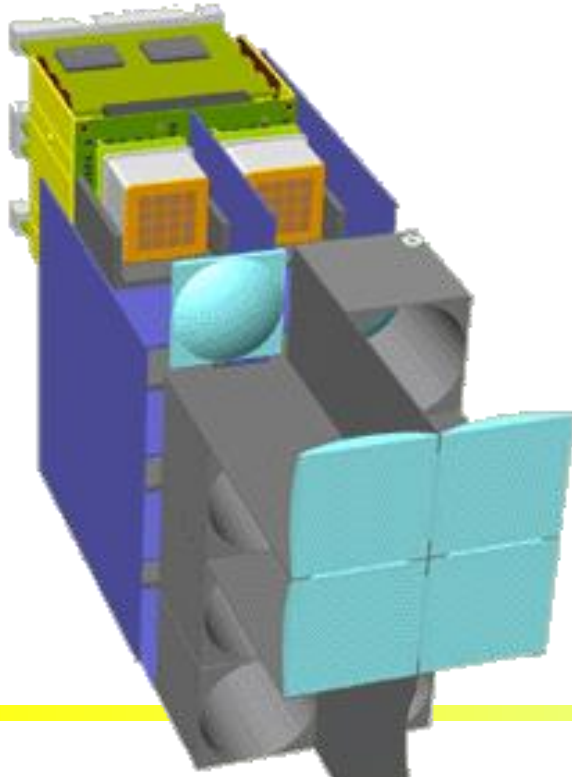




HERA-B RICH photon detector

Light collection system
(imaging!) to:

- Eliminate dead areas
- Adapt the pad size

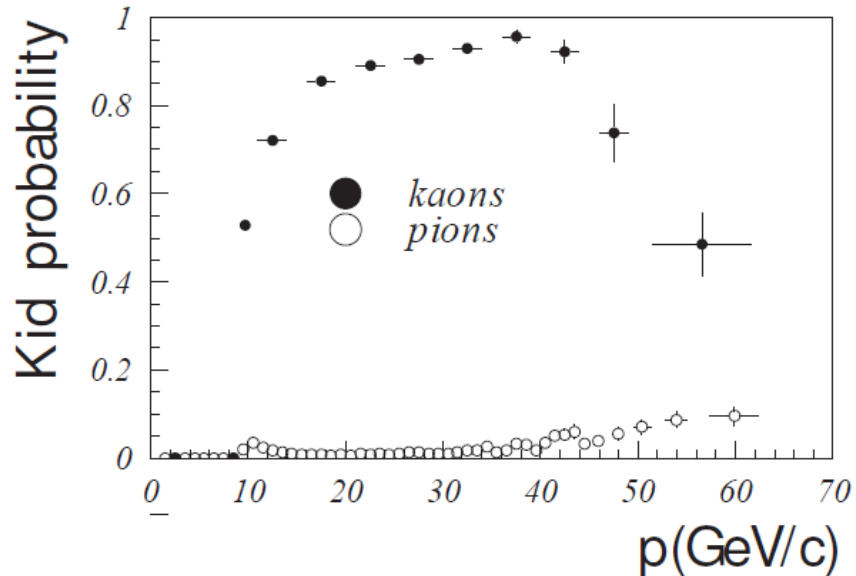
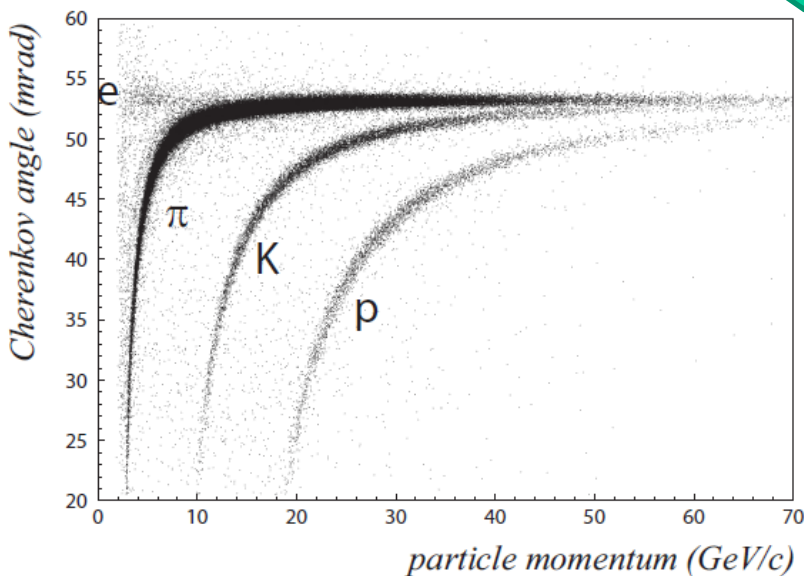


HERA-B RICH

← Little noise, ~30 photons per ring

Typical event →

Worked very well!



Kaon efficiency and
pion fake probability

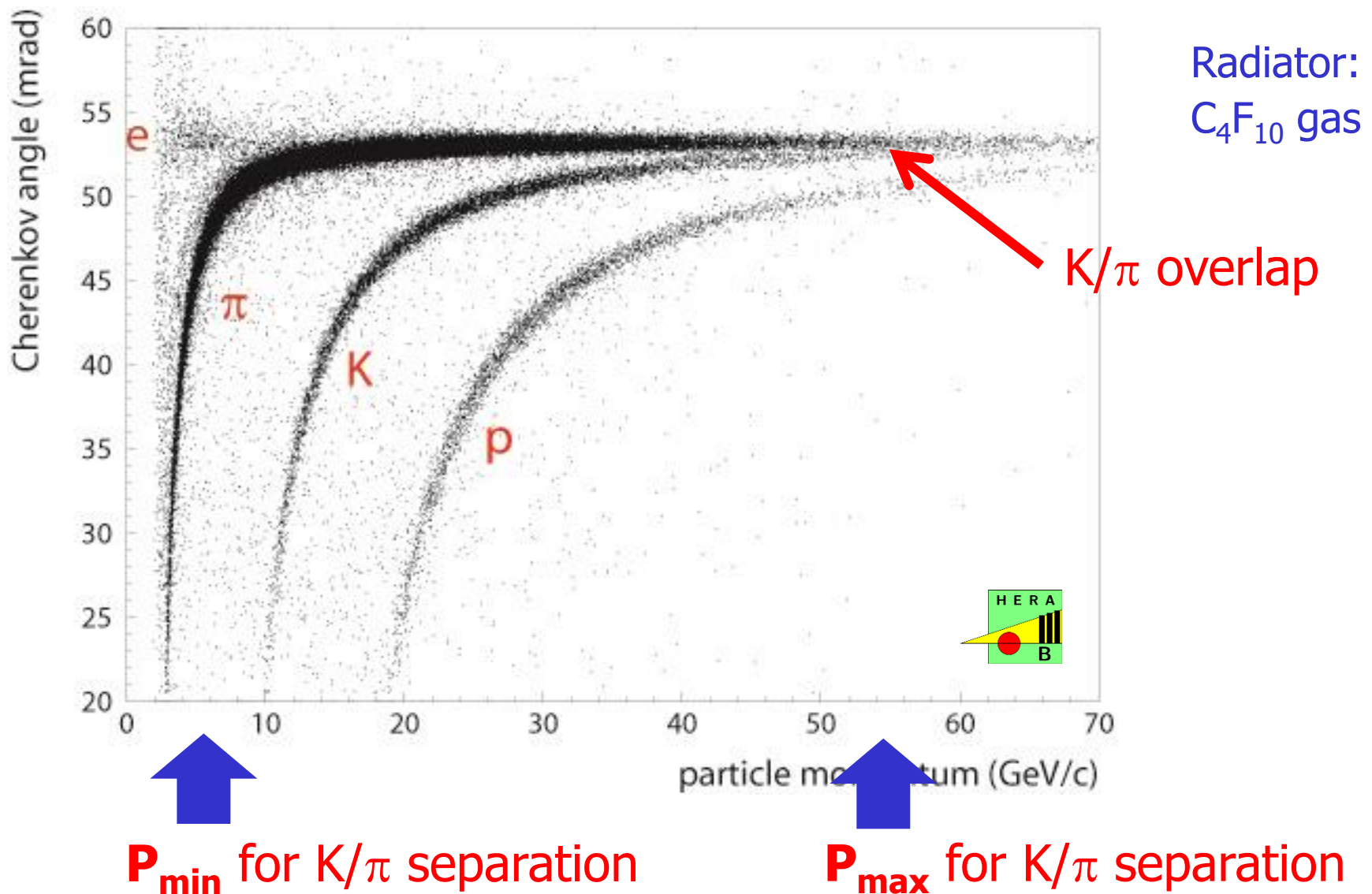
Ljubljana

Limits of the RICH technique

The choice of RICH radiator medium in case of a specific experiment depends on the particles we would like to identify, and their kinematics:

- the threshold momentum for the lighter of the two particles we want to separate: $\mathbf{p}_t = \beta_t \gamma_t \mathbf{m} \mathbf{c}$, $\beta_t = 1/n$ should coincide with the lower limit of momentum spectrum p_{\min} . Typically
$$\mathbf{p}_{\min} = \sqrt{2} \mathbf{p}_t$$
- the resolution in Čerenkov angle should allow for a separation up to the upper limits of kinematically allowed momenta \mathbf{p}_{\max}

Limits of a RICH detector



π/K separation example:

Limiting performance at the high momentum side: irreducible contribution to the resolution - dispersion.

radiator	LiF solid	C ₆ F ₁₄ liquid	C ₅ F ₁₂ gas	N ₂ gas	He gas
σ_θ (mrad)	7.0	3.9	0.45	0.40	0.13
σ_N (mrad)	2.2	1.2	0.14	0.13	0.04
p_{max} (GeV/c) for $3\sigma \pi/K$	3.5	6.9	50	100	330
p_{min} (GeV/c)	0.6	0.9	11	28	83

photon detector: TMAE, 10 det. photons assumed

Summary:

$$\mathbf{p_{max}/p_{min} \sim 4-7}$$

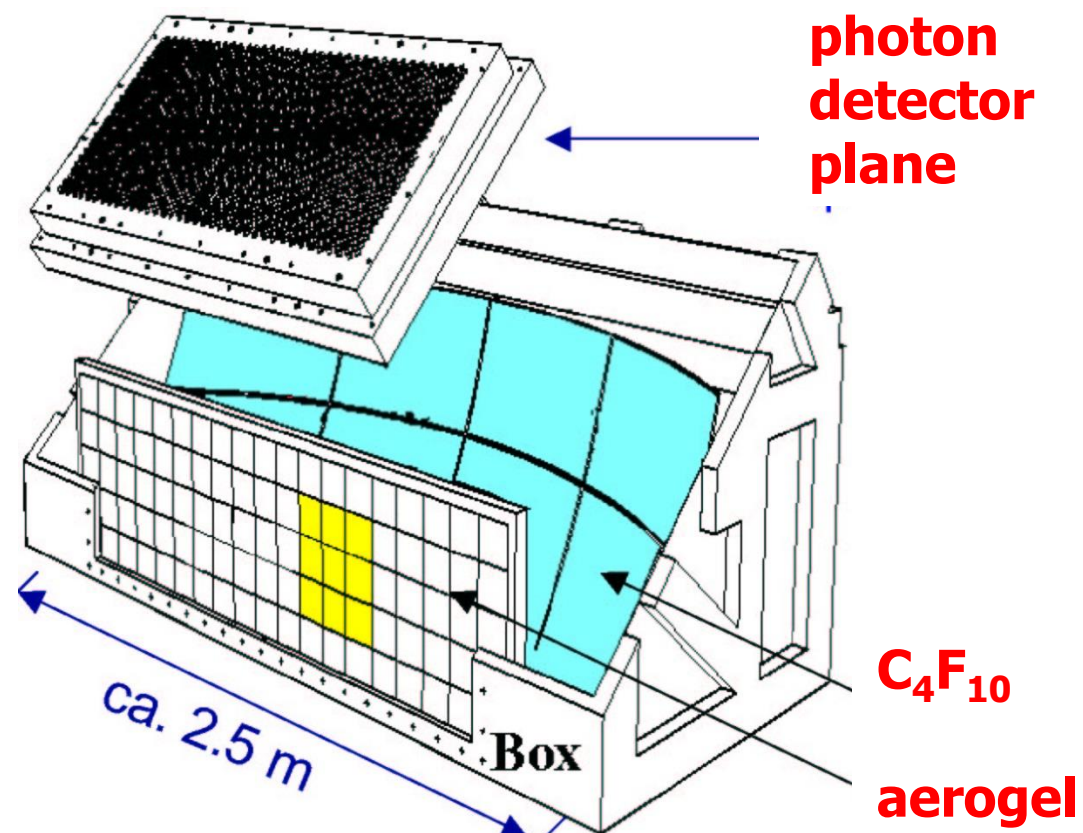
for a 3σ separation between the two particles

For a larger kinematic region **2 radiators are needed!**

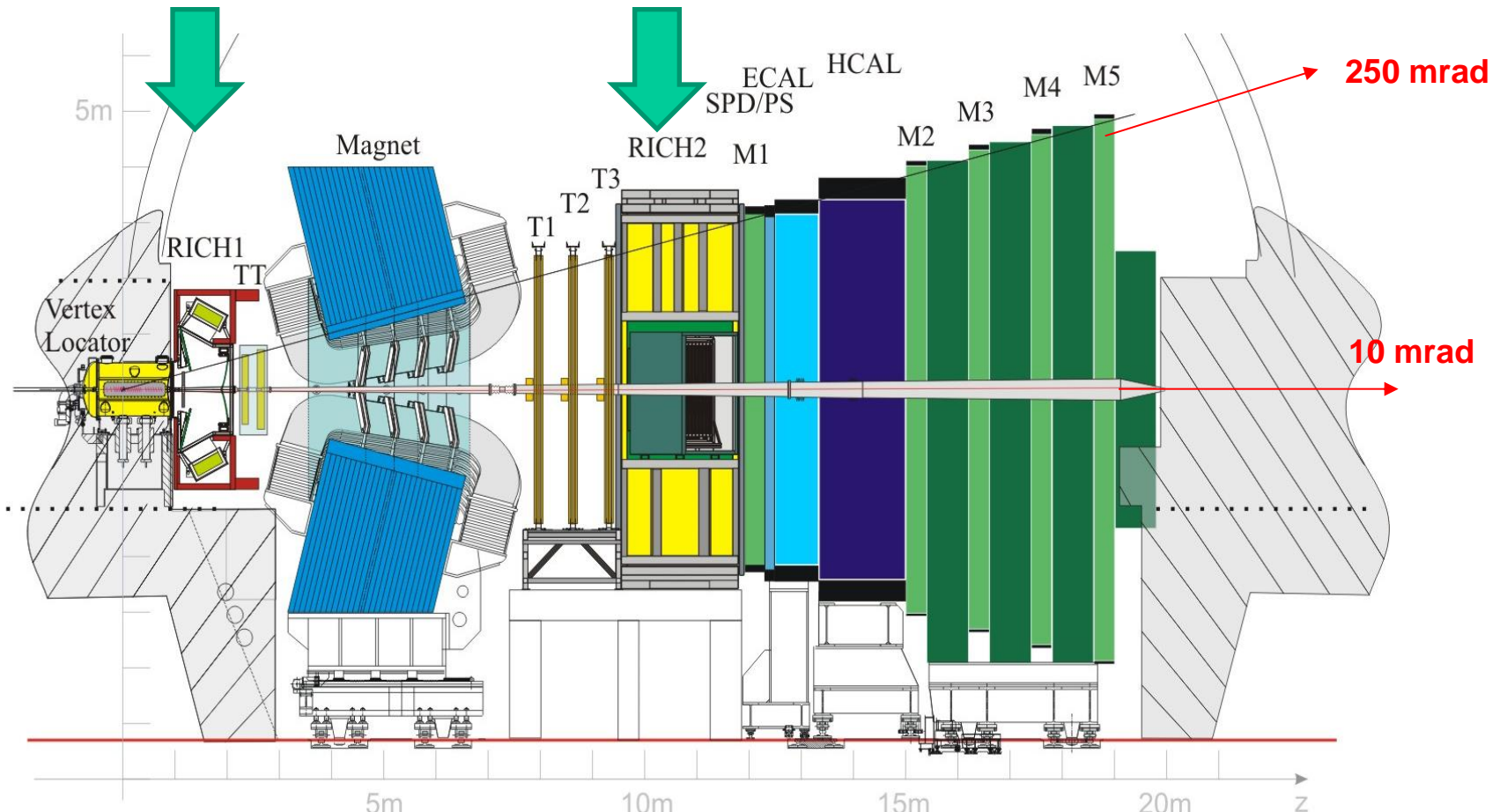
RICHes with several radiators

Extending the kinematic range → need more than one radiator

- DELPHI, SLD (liquid +gas)
- HERMES (aerogel+gas)



The LHCb RICH counters



**Vertex
reconstruction:**
VELO

Trigger:
Muon Chambers
Calorimeters
Tracker

PID:
RICHes
Calorimeters
Muon Chambers

Kinematics:
Magnet
Tracker
Calorimeters

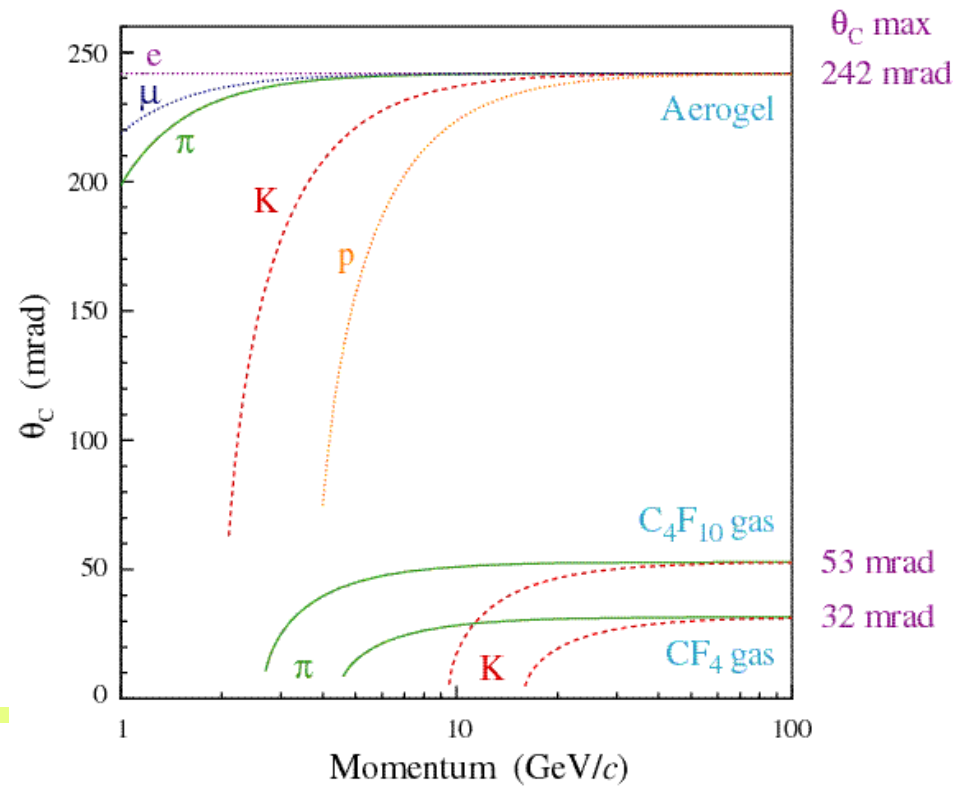
LHCb RICHes

Need:

- Particle identification for momentum range ~2-100 GeV/c
- Granularity 2.5x2.5mm²
- Large area (2.8m²) with high active area fraction
- Fast compared to the 25ns bunch crossing time
- Have to operate in a small B field

→ 3 radiators

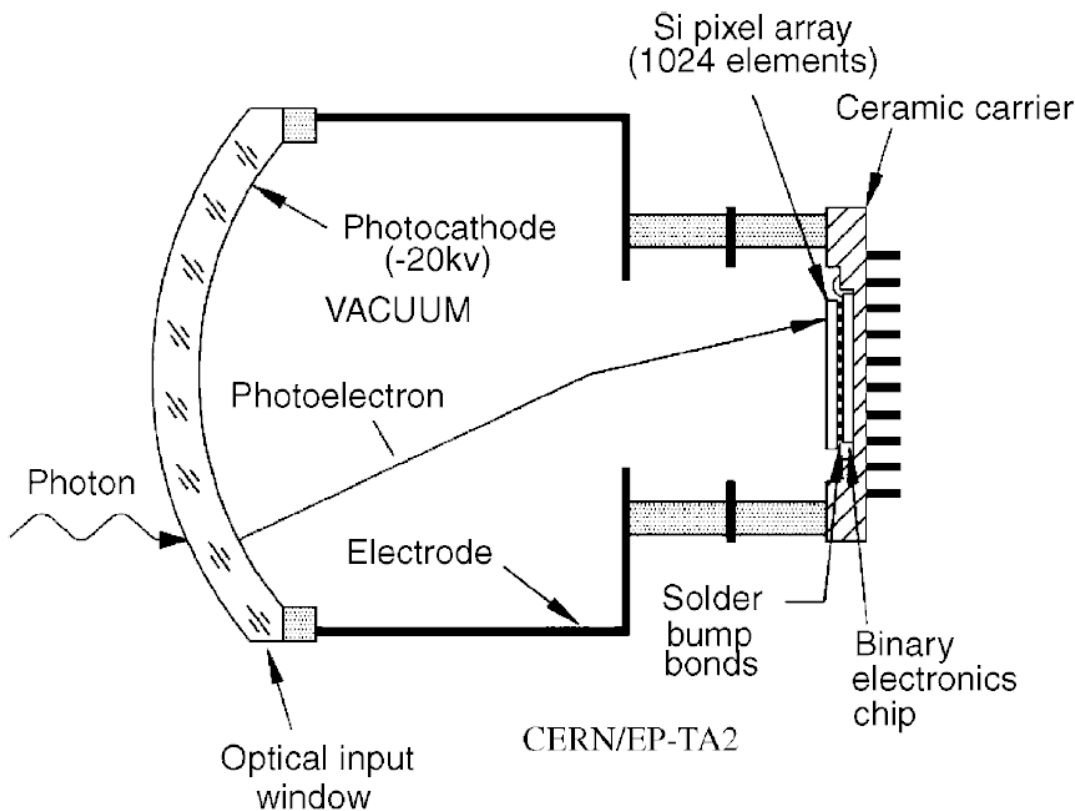
- Aerogel
- C₄F₁₀
- CF₄



LHCb RICHes

Photon detector: hybrid PMT (R+D with DEP) with 5x demagnification (electrostatic focusing).

Hybrid PMT: accelerate photoelectrons in electric field ($\sim 20\text{kV}$), detect it in a pixelated silicon detector.



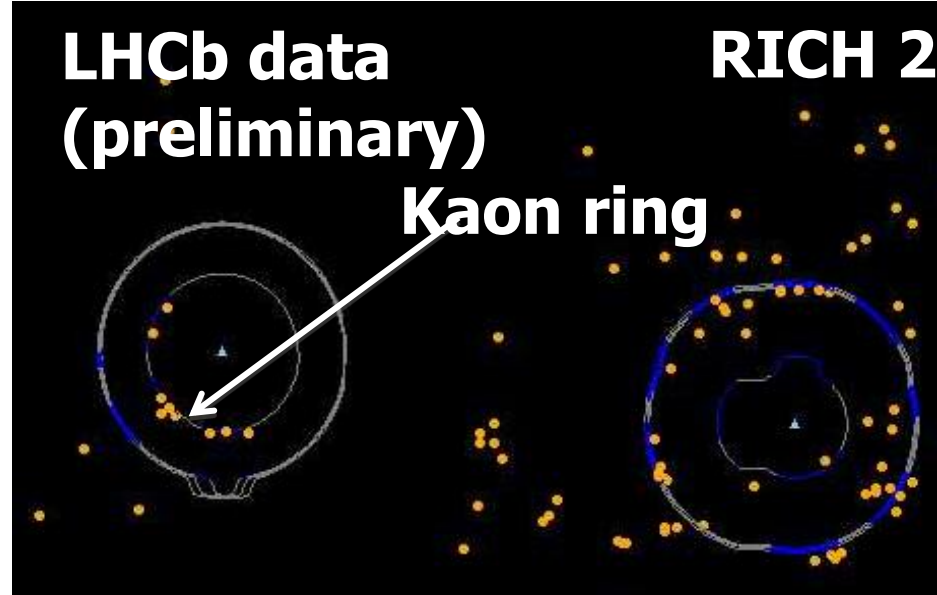
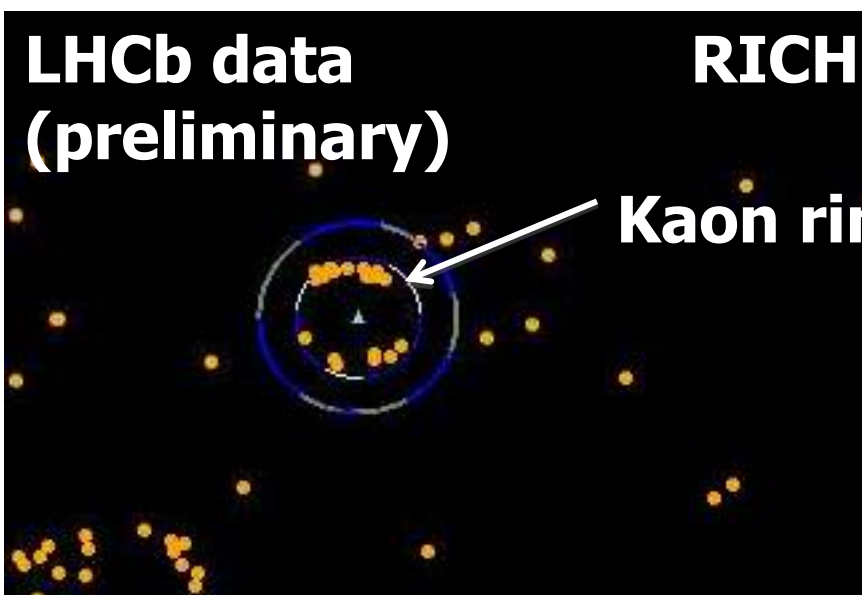
NIM A553 (2005) 333

LHCb Event Display

RICH1

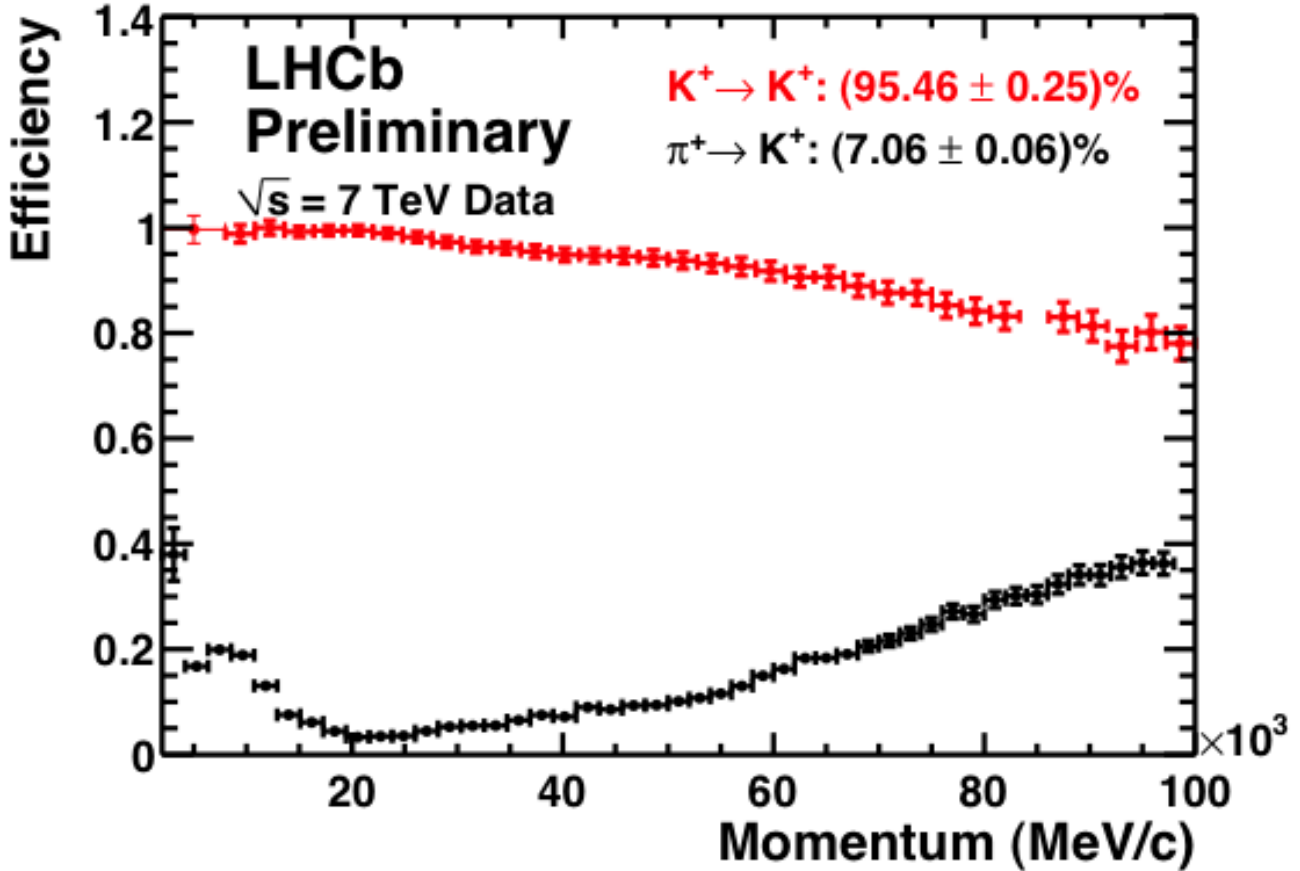
Early data, Nov/Dec 2009
LHC beams $\sqrt{s} = 900 \text{ GeV}$

RICH2

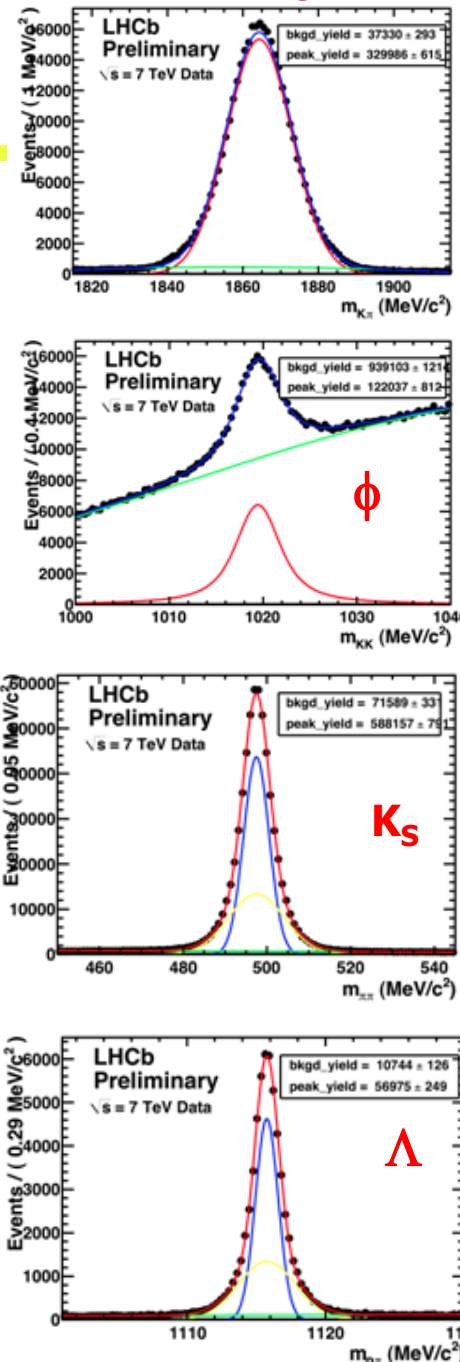


- Orange points → photon hits
- Continuous lines → expected distribution for each particle hypothesis

LHCb RICHes: performance



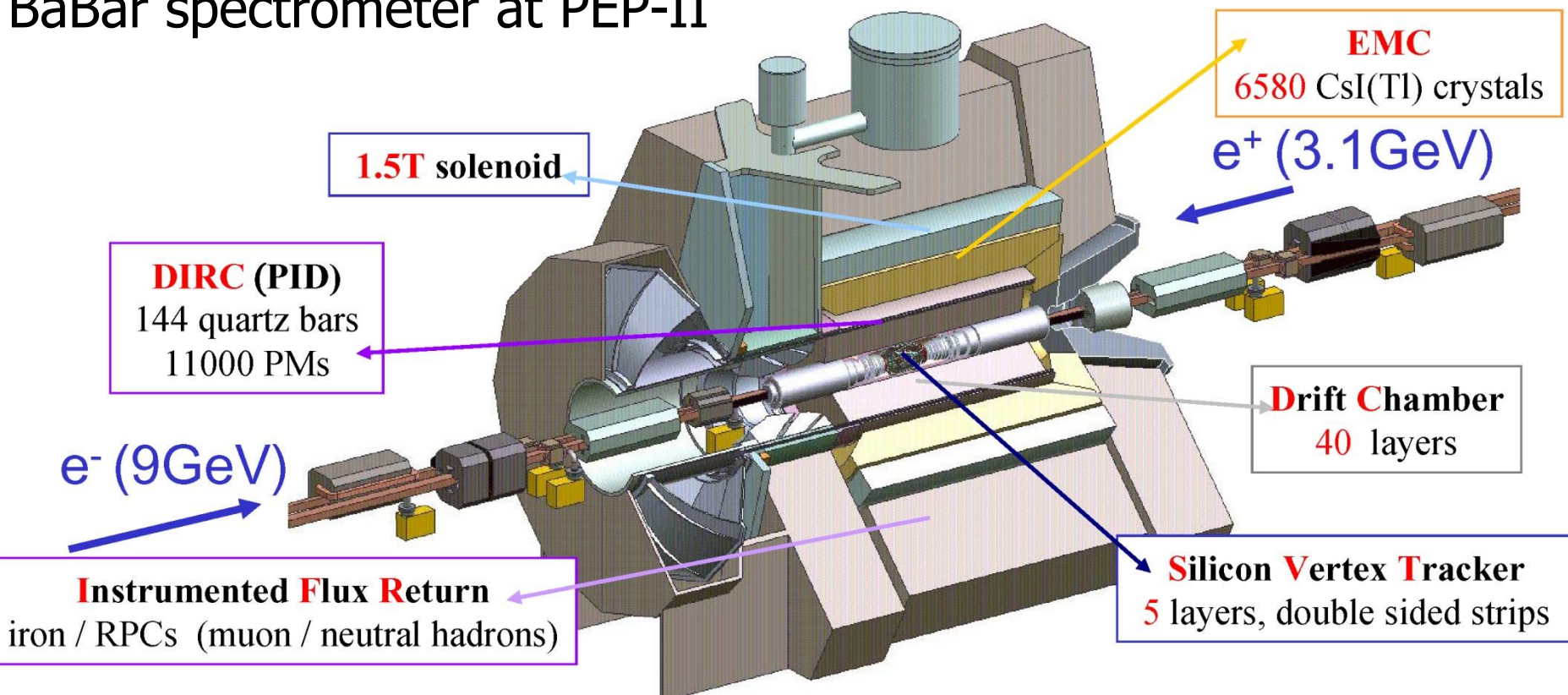
Efficiency and purity from data → excellent agreement with MC



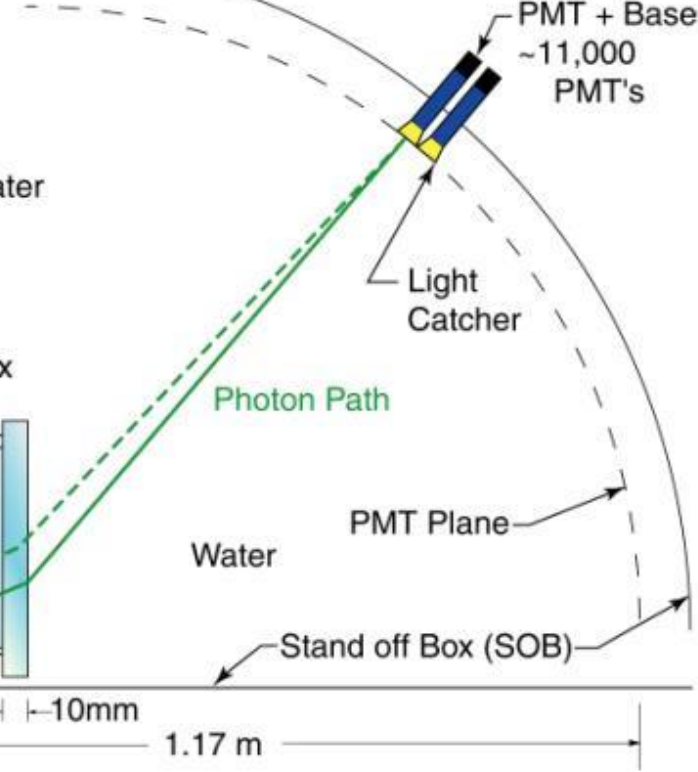
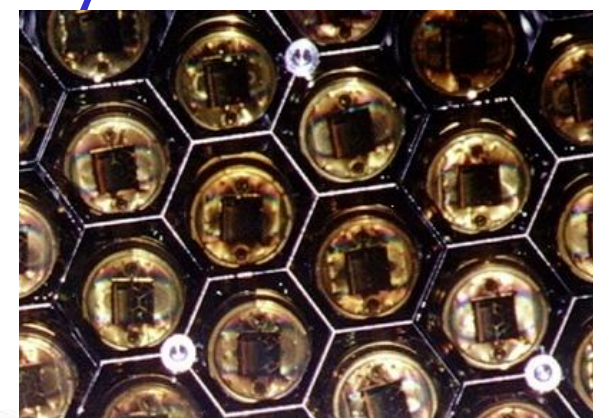
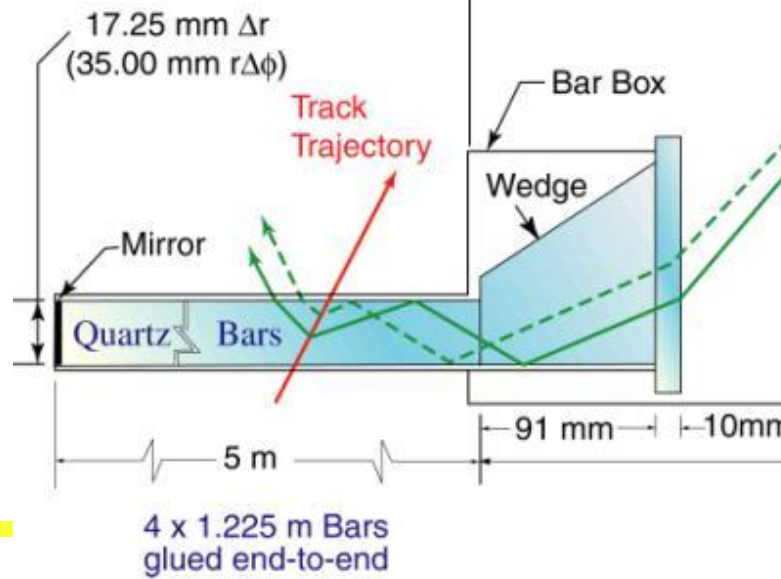
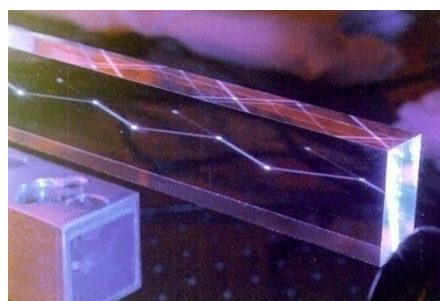
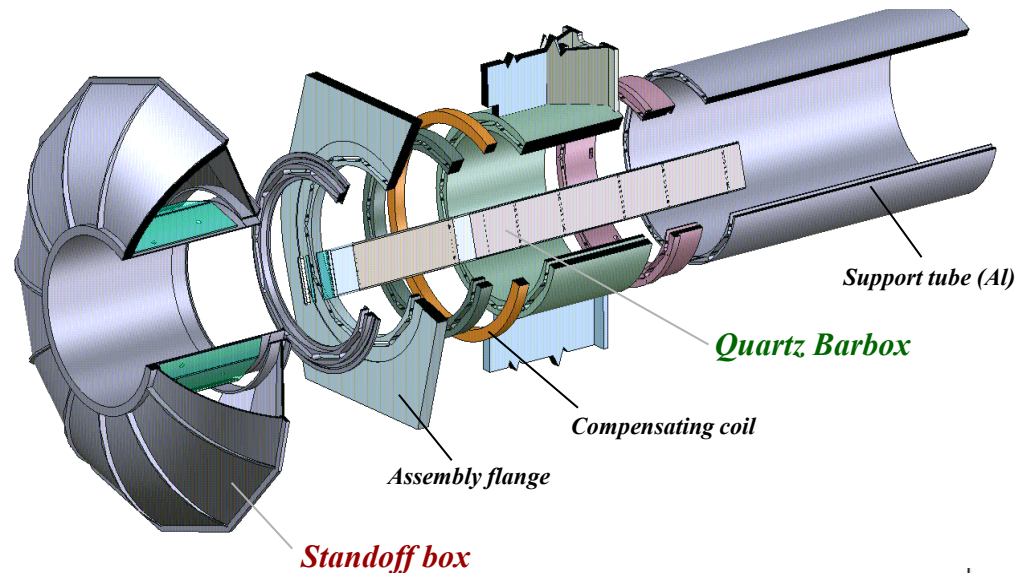


DIRC - detector of internally reflected Cherenkov light

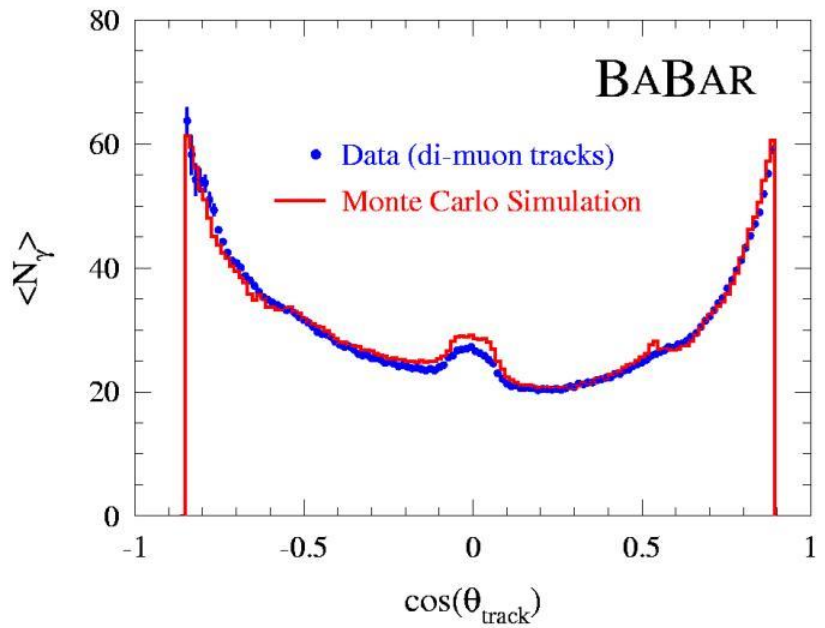
BaBar spectrometer at PEP-II



DIRC (@BaBar) - detector of internally reflected Cherenkov light

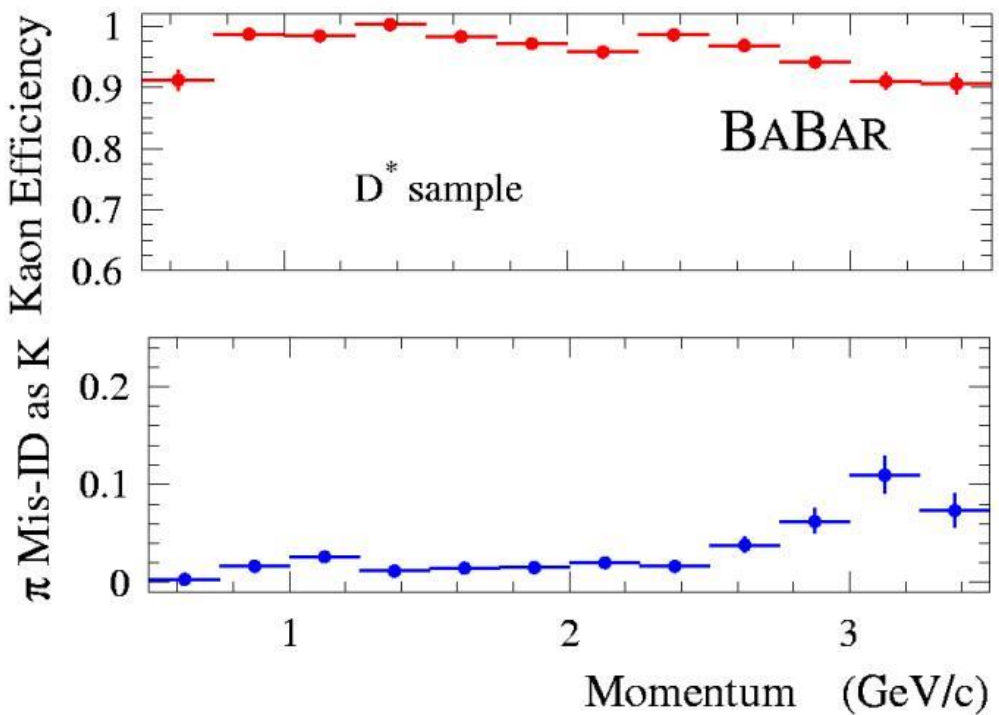


DIRC performance



← Lots of photons!

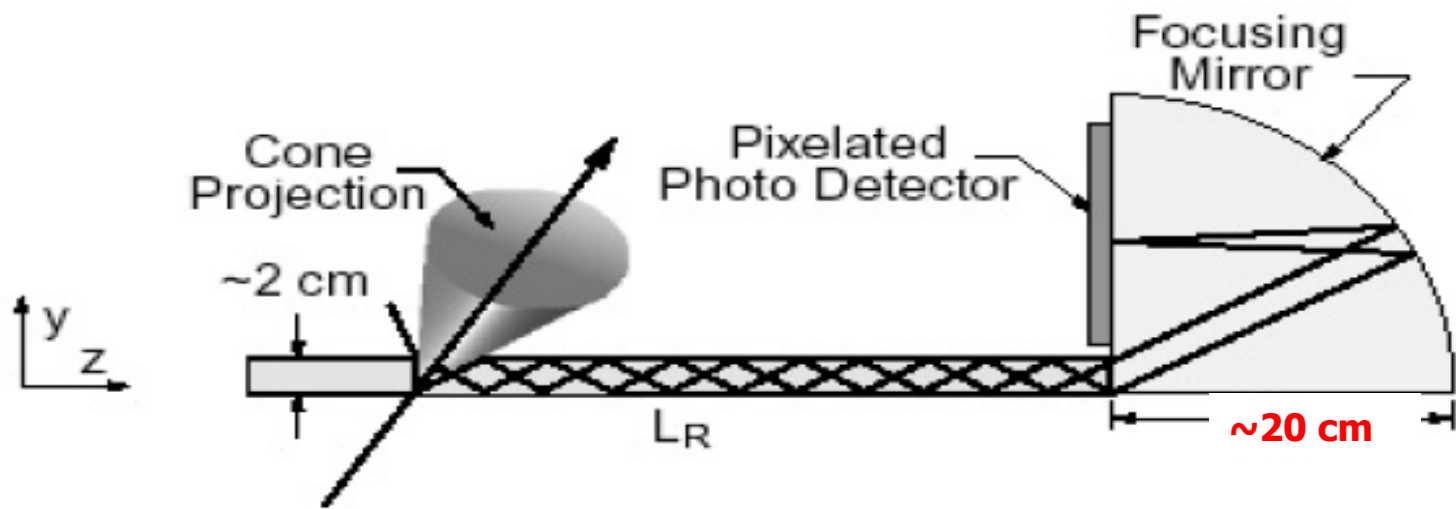
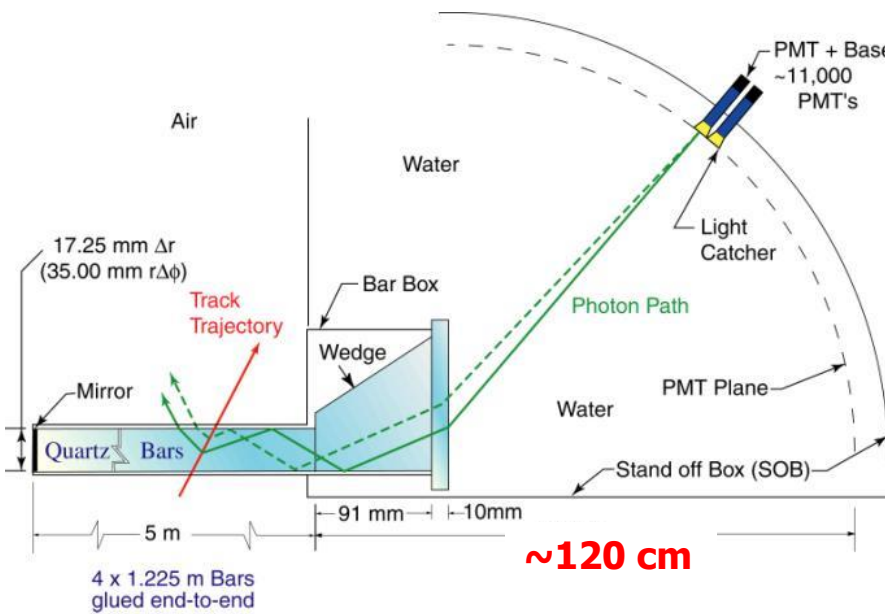
Excellent π/K separation





Focusing DIRC

Upgrade: step further, remove the stand-off box →





Focusing DIRC

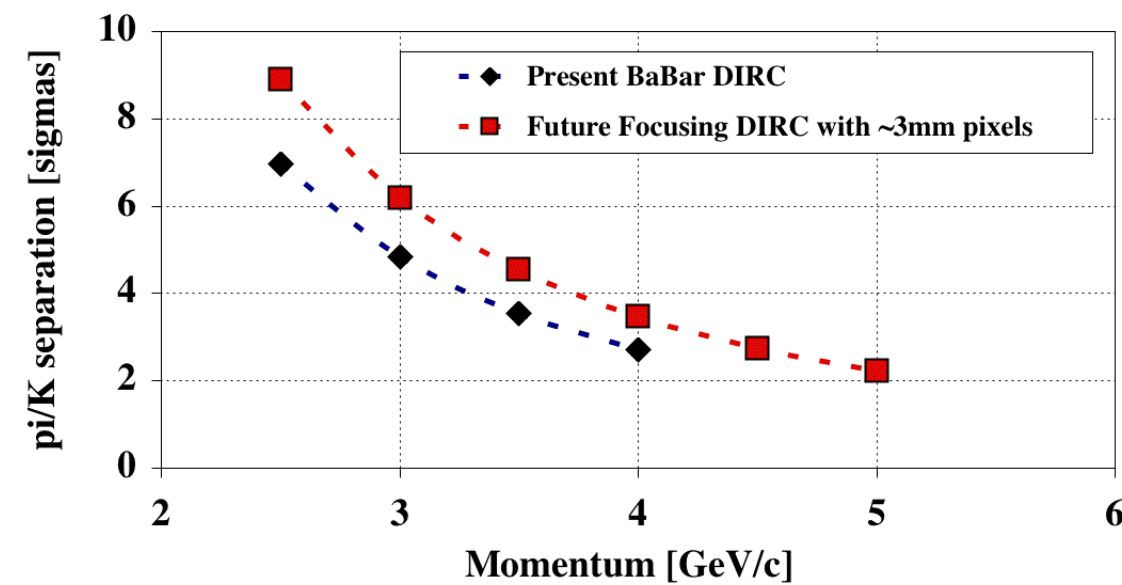
Super-B factory: 100x higher luminosity => DIRC needs to be smaller and faster

Focusing and smaller pixels can reduce the expansion volume by a factor of 7-10

Timing resolution improvement: $\sigma \sim 1.7\text{ns}$ (BaBar DIRC) $\rightarrow \sigma \leq 150\text{-}200\text{ps}$ ($\sim 10\text{x}$ better) allows a measurement of the photon group velocity $c_g(\lambda)$ to correct the chromatic error of θ_c .

Photon detector:

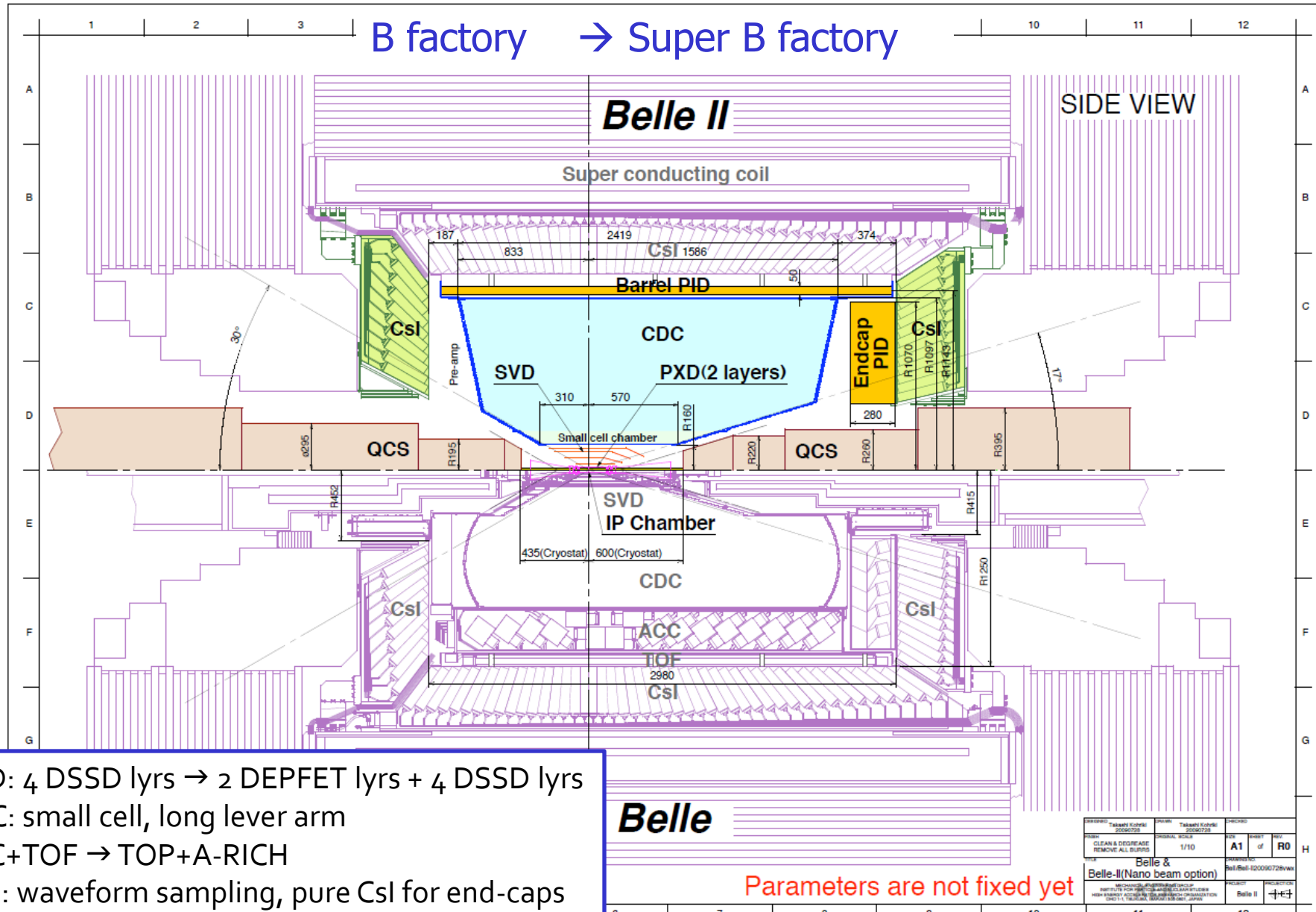
- Pad size <5mm
- Time resolution $\sim 50\text{-}100\text{ps}$



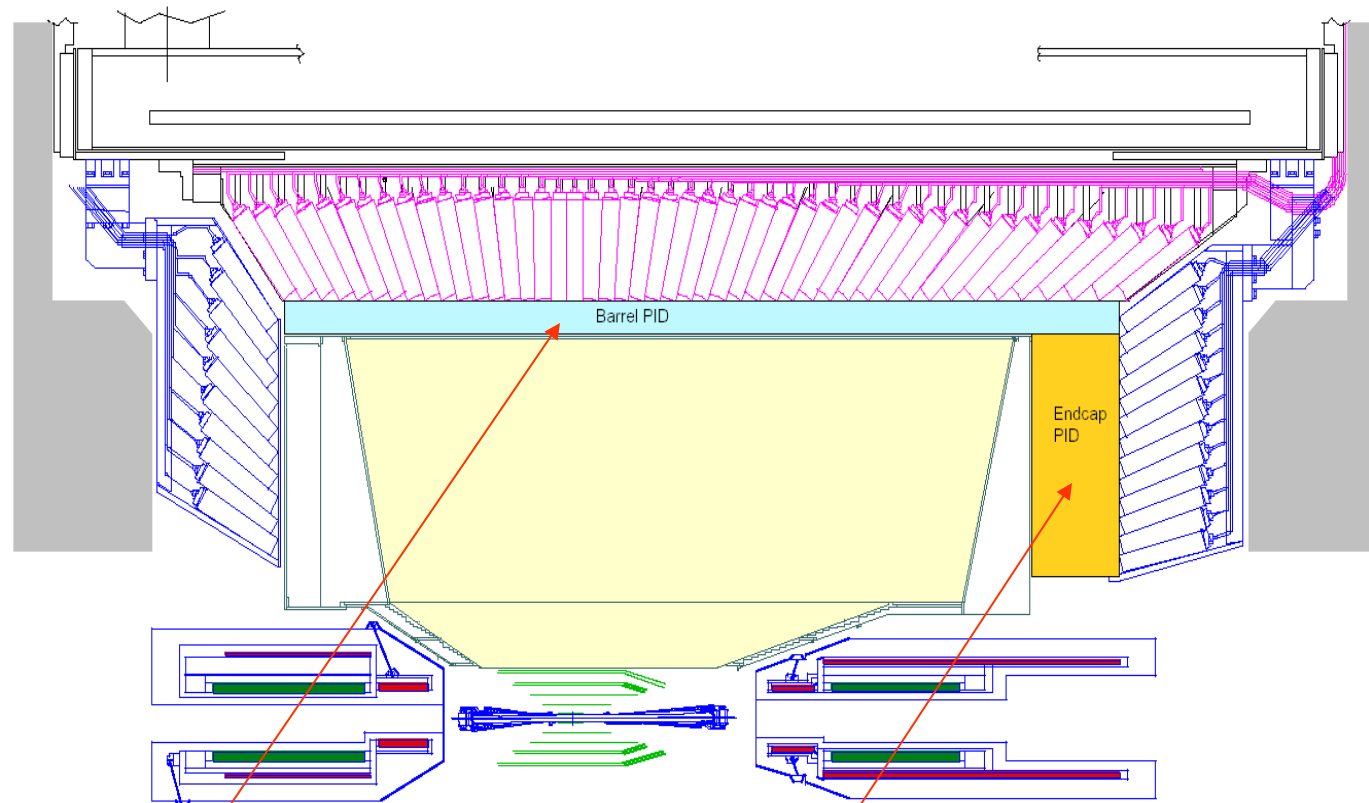
Belle → Belle II

B factory

→ Super B factory



Belle II PID systems – side view

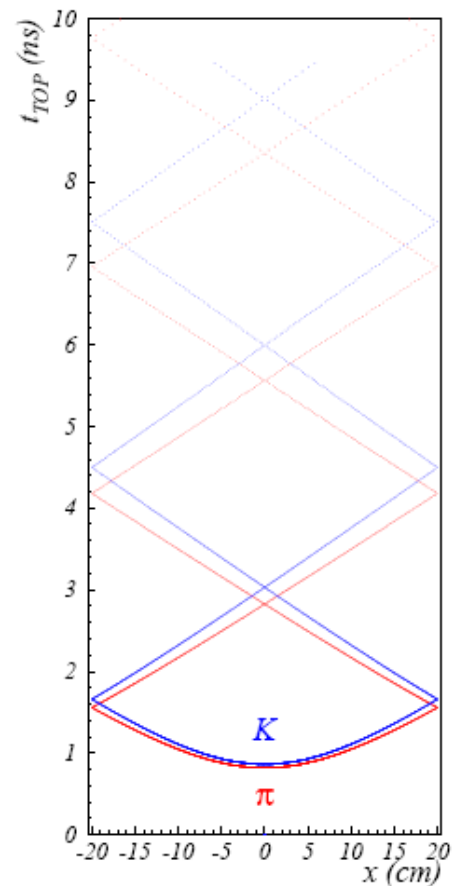
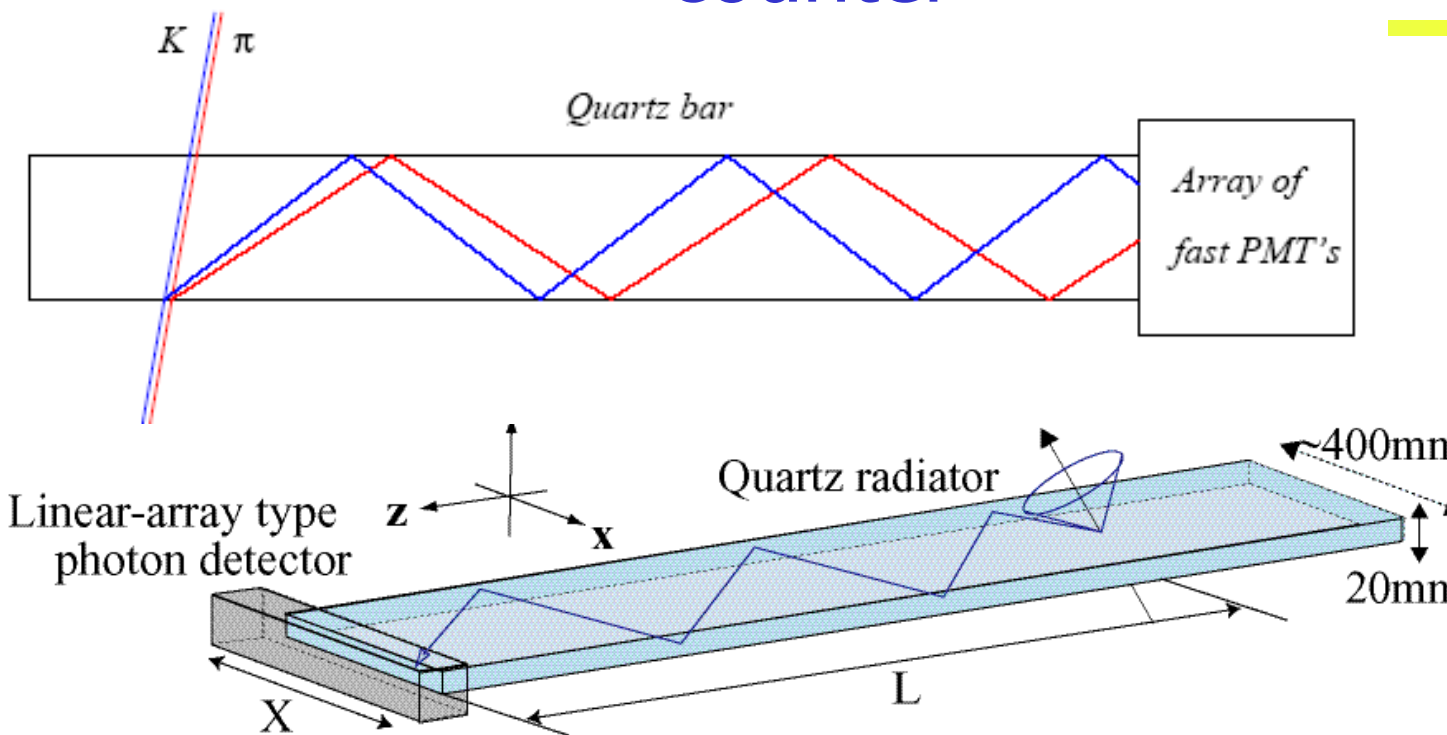


Two new particle ID devices, both RICHes:

Barrel: time-of-propagation (TOP) counter

Endcap: proximity focusing RICH

Time-Of-Propagation (TOP) counter



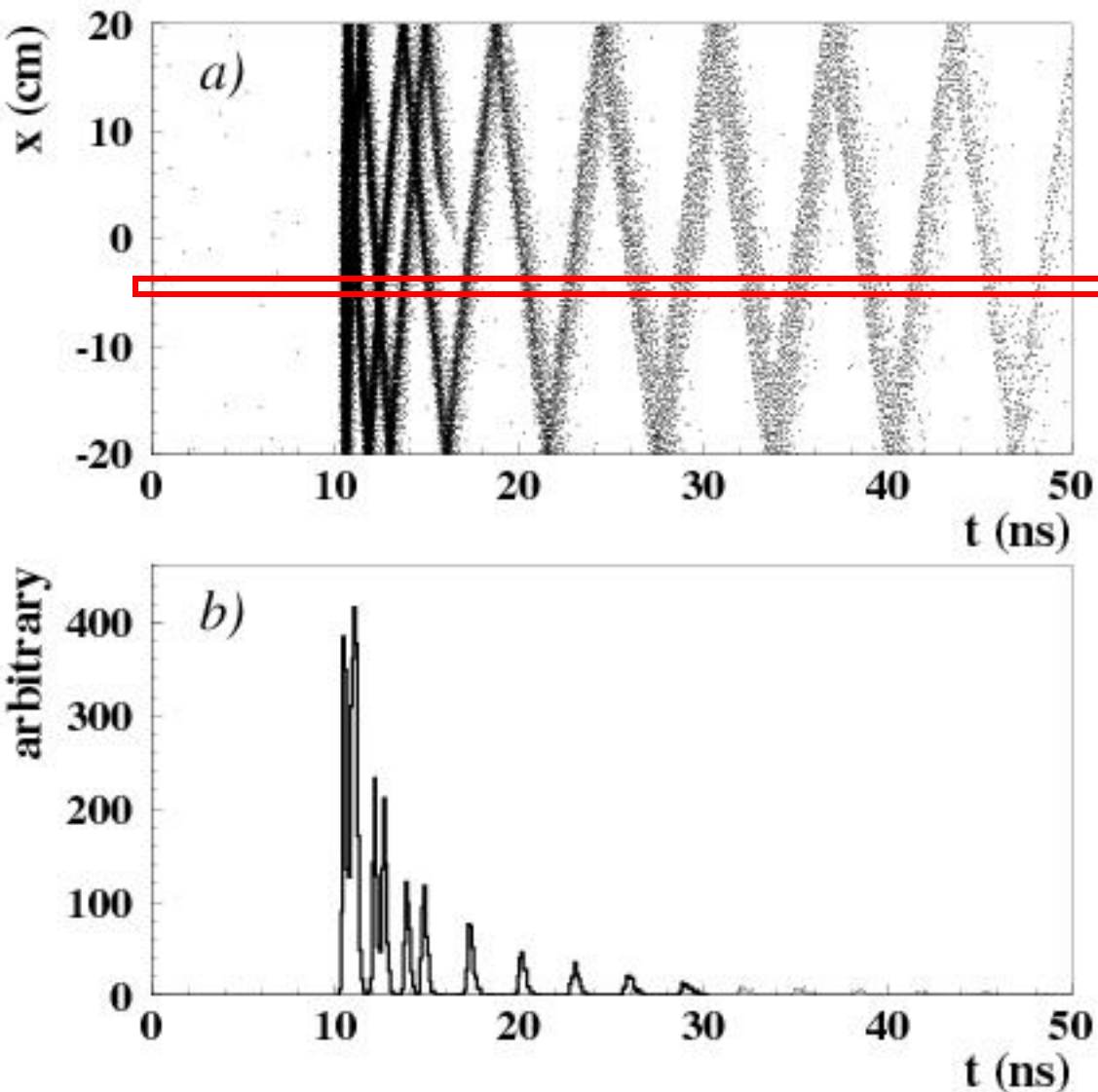
Similar to DIRC, but instead of two coordinates measure:

- One (or two coordinates) with a few mm precision
- Time-of-arrival
- Excellent time resolution < ~ 40 ps
required for single photons in 1.5T B field



Hamamatsu
SL10 MCP-PMT

TOP image

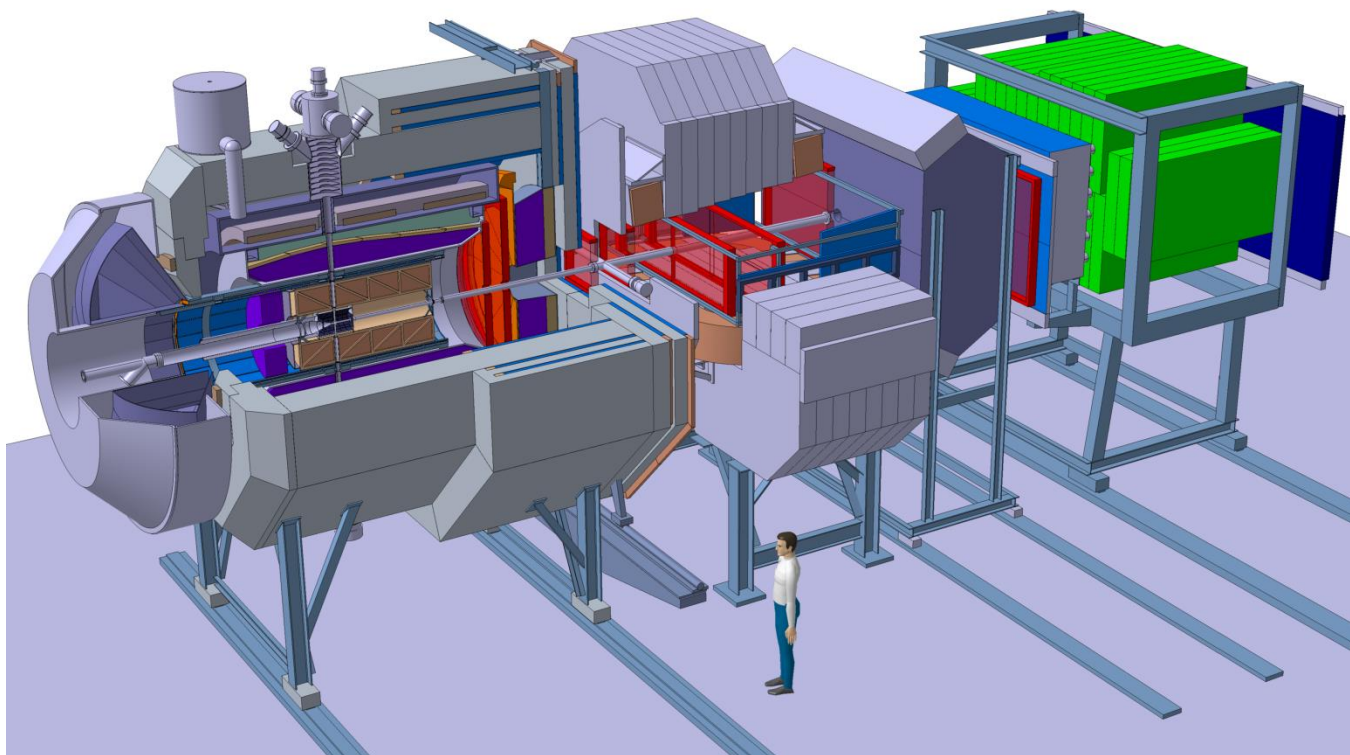


Pattern in the coordinate-time space ('ring') of a pion hitting a quartz bar with ~ 80 MAPMT channels

Time distribution of signals recorded by one of the PMT channels: different for π and K

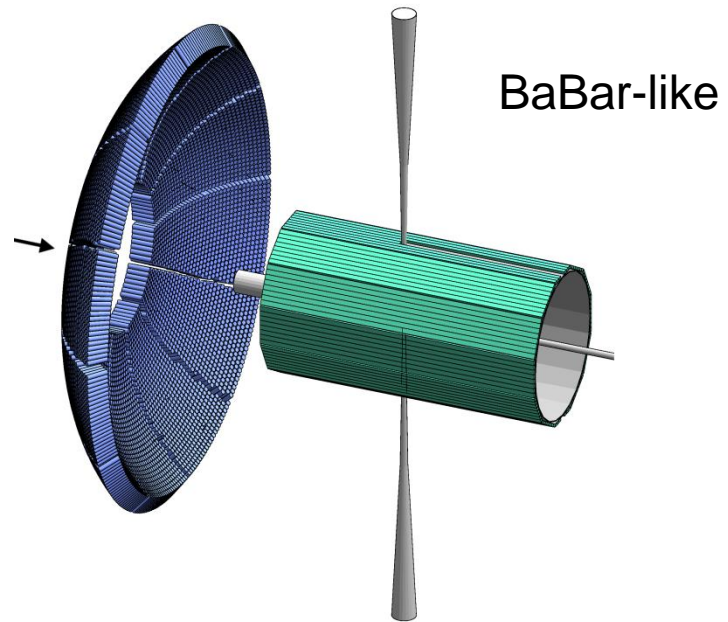
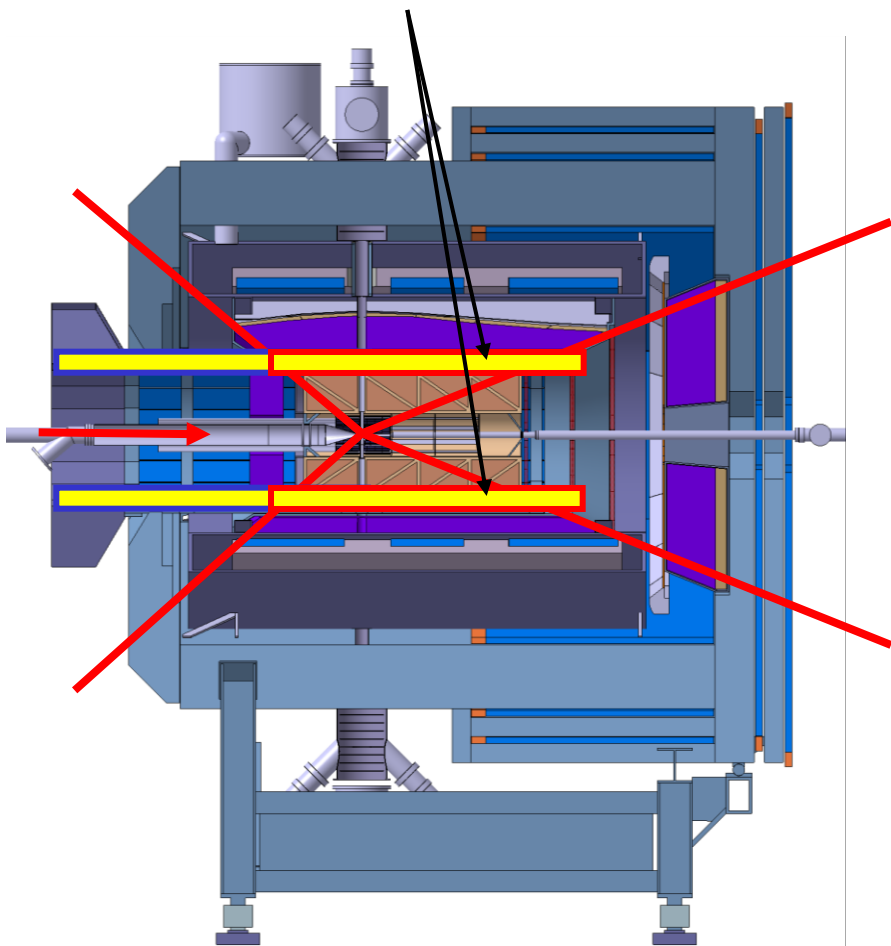
DIRC counters for PANDA (FAIR, GSI)

Two DIRC-like counters are considered for the PANDA experiment



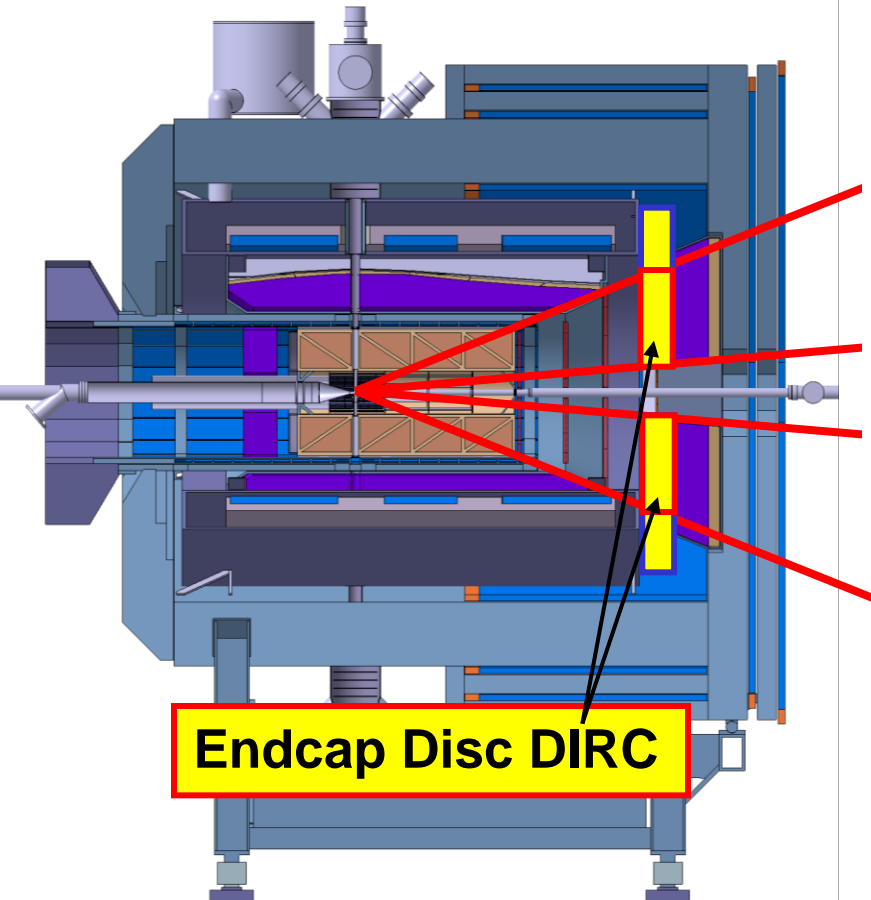
PANDA barrel DIRC

Barrel-DIRC

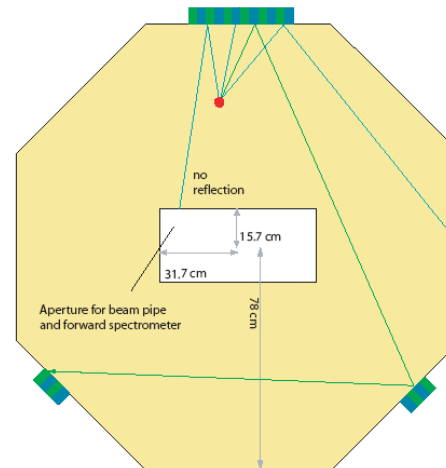


PANDA endcap DIRC

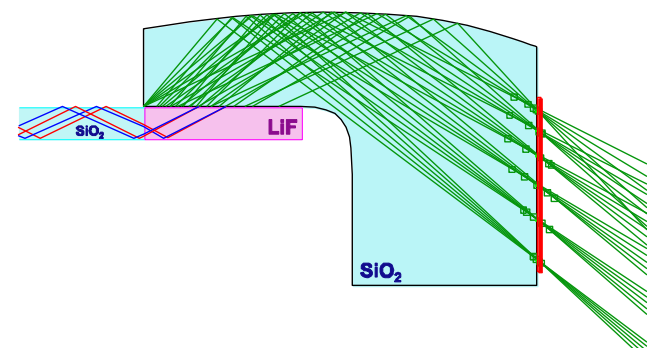
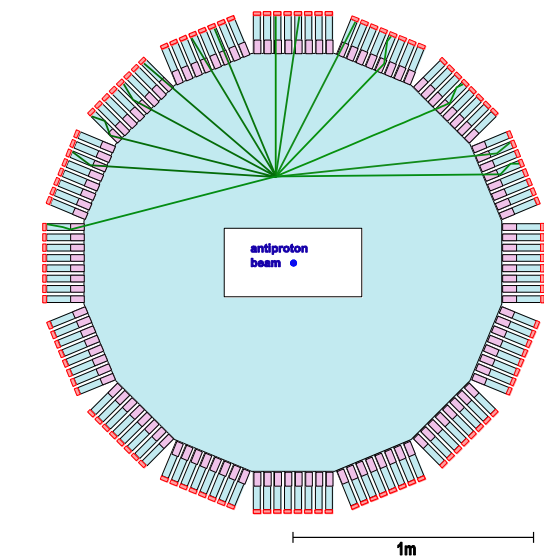
Two different readout designs:



Time-of-Propagation

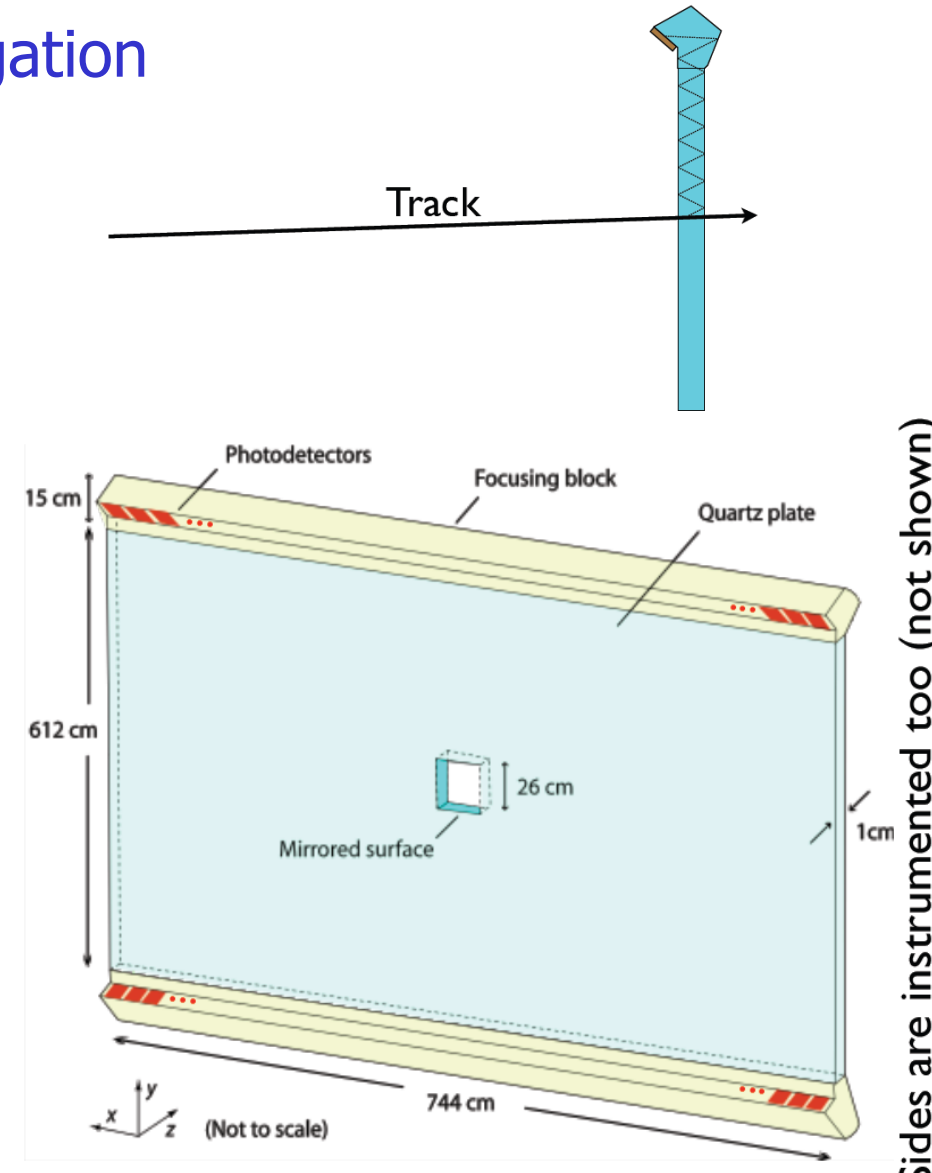
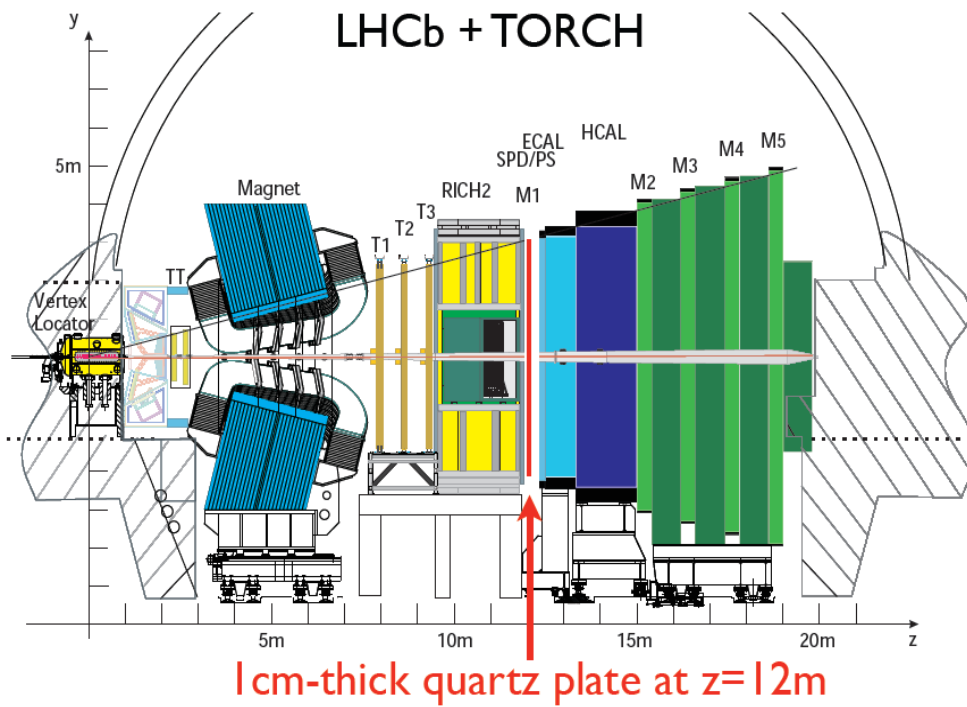


Focussing light guide

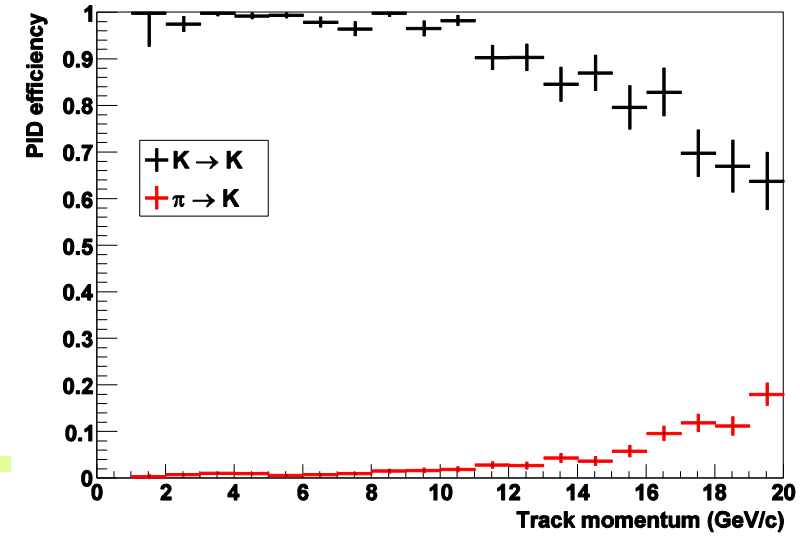
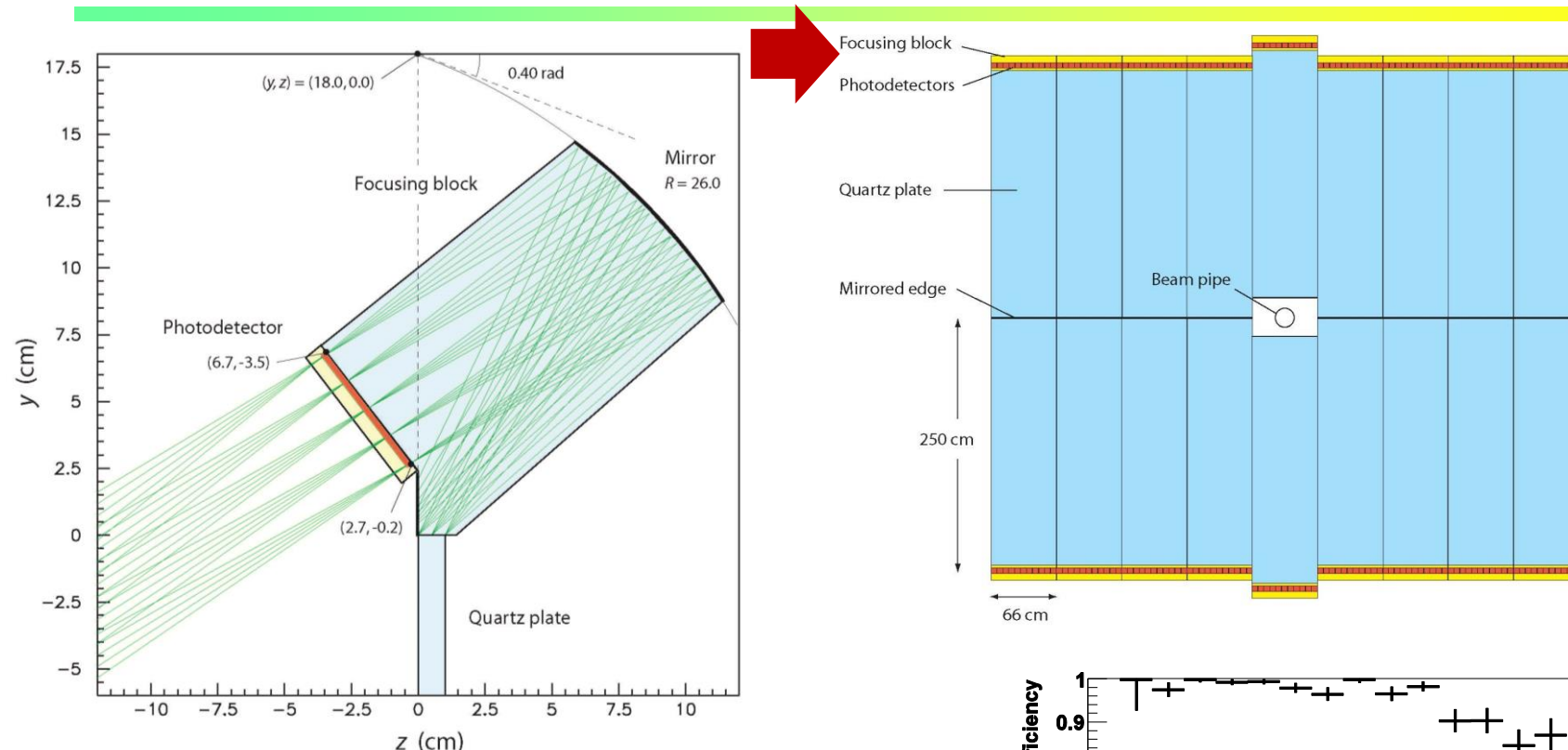


LHCb PID upgrade: TORCH

A special type of Time-of-Propagation counter for the LHCb upgrade

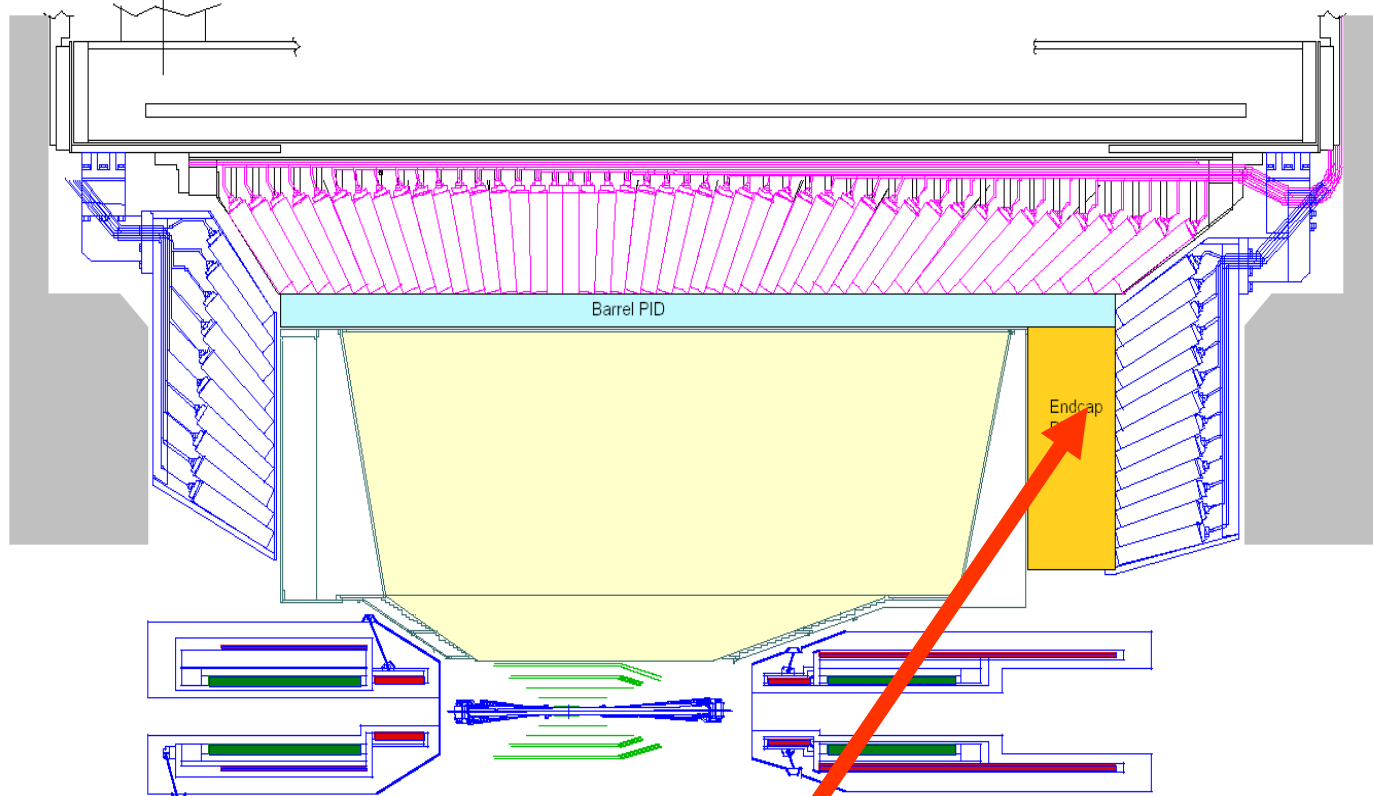


LHCb PID upgrade: TORCH



Expected performance with Photonis
Planacon MCP PMTs

Belle II PID system



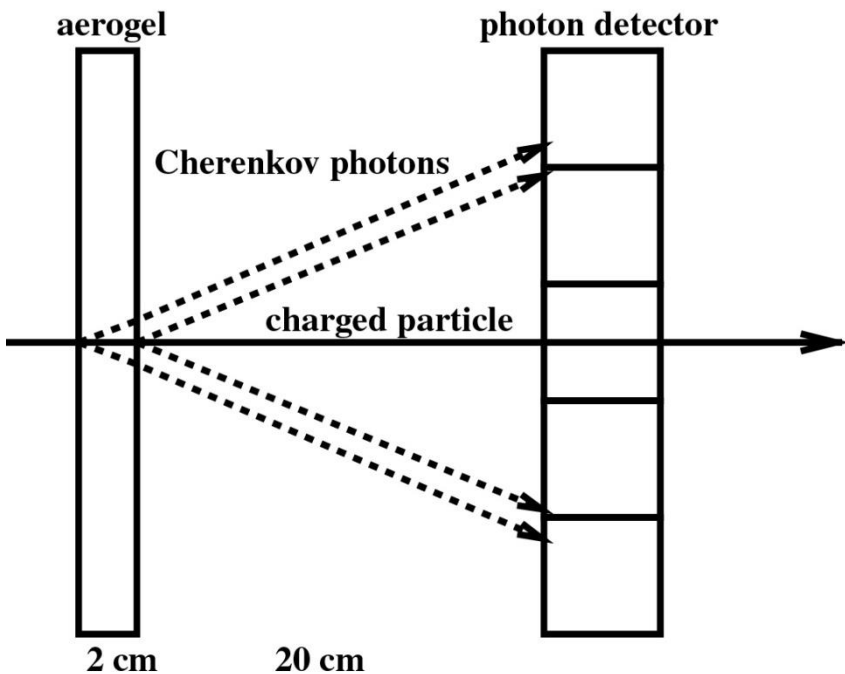
Two new particle ID devices, both RICHes:

Barrel: Time-of-propagation counter (TOP) counter

Endcap: proximity focusing RICH

Endcap: Proximity focusing RICH

K/ π separation at 4 GeV/c:
 $\theta_c(\pi) \sim 308$ mrad ($n = 1.05$)
 $\theta_c(\pi) - \theta_c(K) \sim 23$ mrad



For single photons: $\delta\theta_c(\text{meas.}) = \sigma_0 \sim 14$ mrad,
typical value for a 20mm thick radiator and
6mm PMT pad size

Per track:

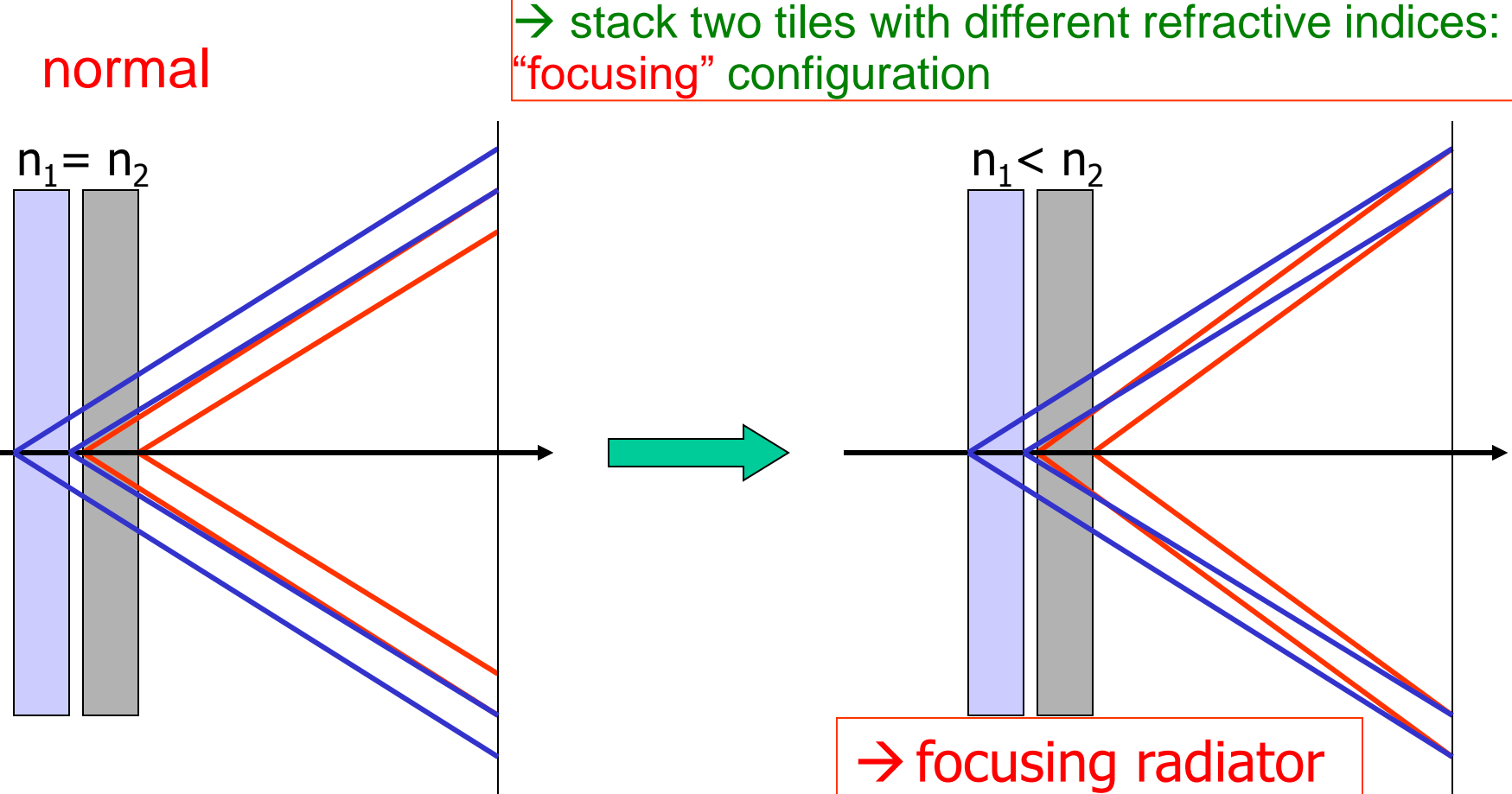
$$\sigma_{\text{track}} = \frac{\sigma_0}{\sqrt{N_{pe}}}$$

Separation: $[\theta_c(\pi) - \theta_c(K)] / \sigma_{\text{track}}$

→ 5 σ separation with $N_{pe} \sim 10$

Radiator with multiple refractive indices

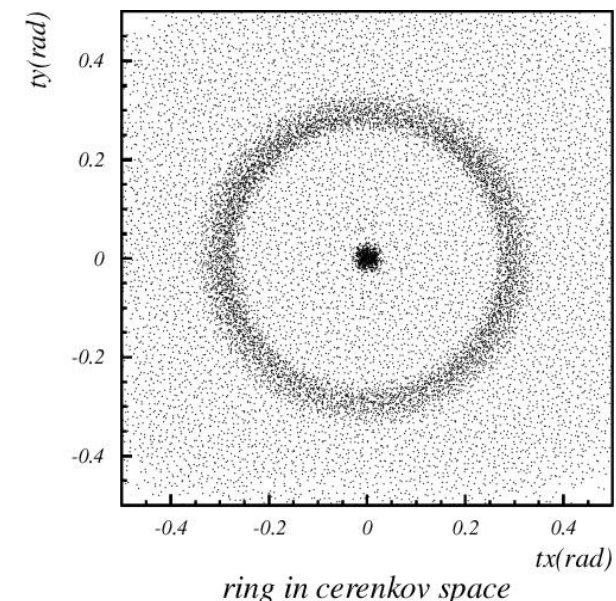
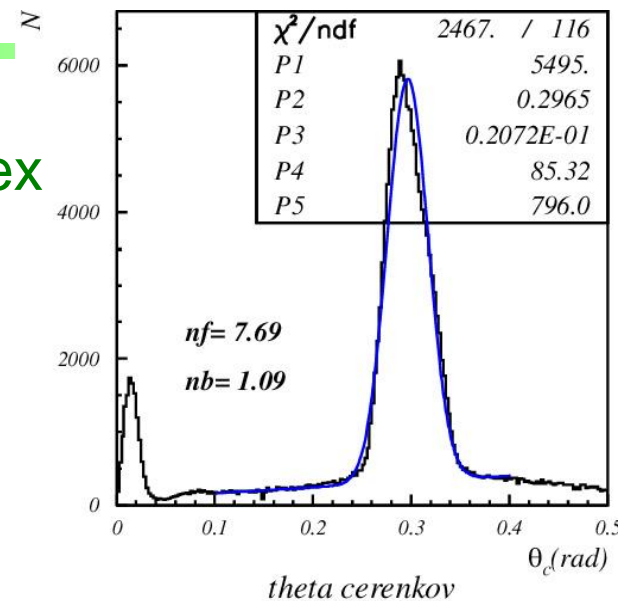
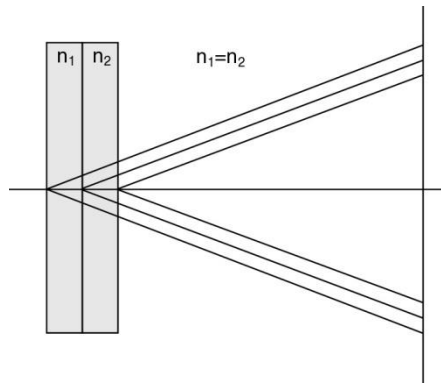
How to increase the number of photons without degrading the resolution?



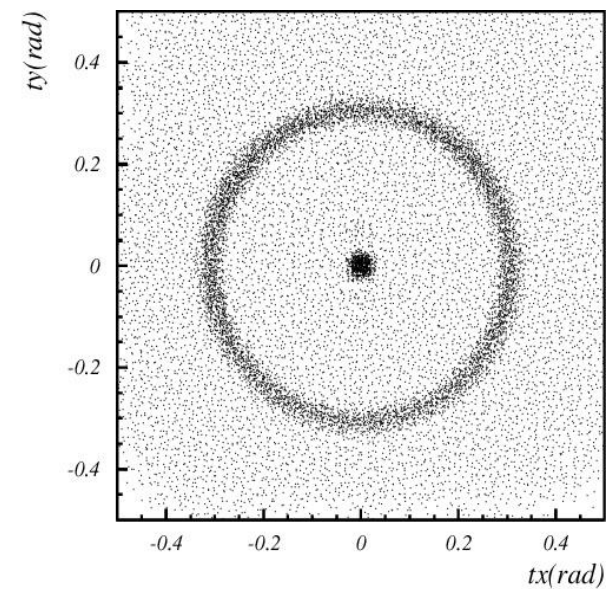
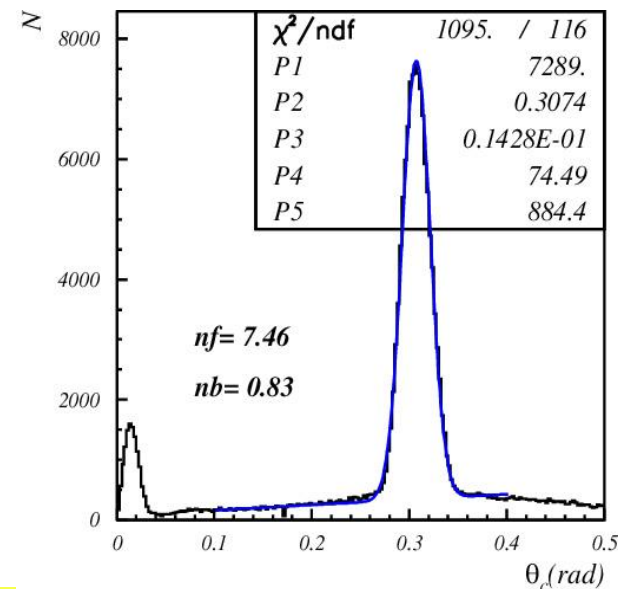
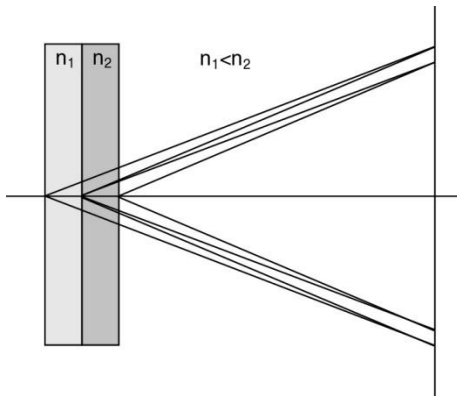
Such a configuration is only possible with aerogel (a form of Si_xO_y) – material with a tunable refractive index between 1.01 and 1.13.

Focusing configuration – data

4cm aerogel single index



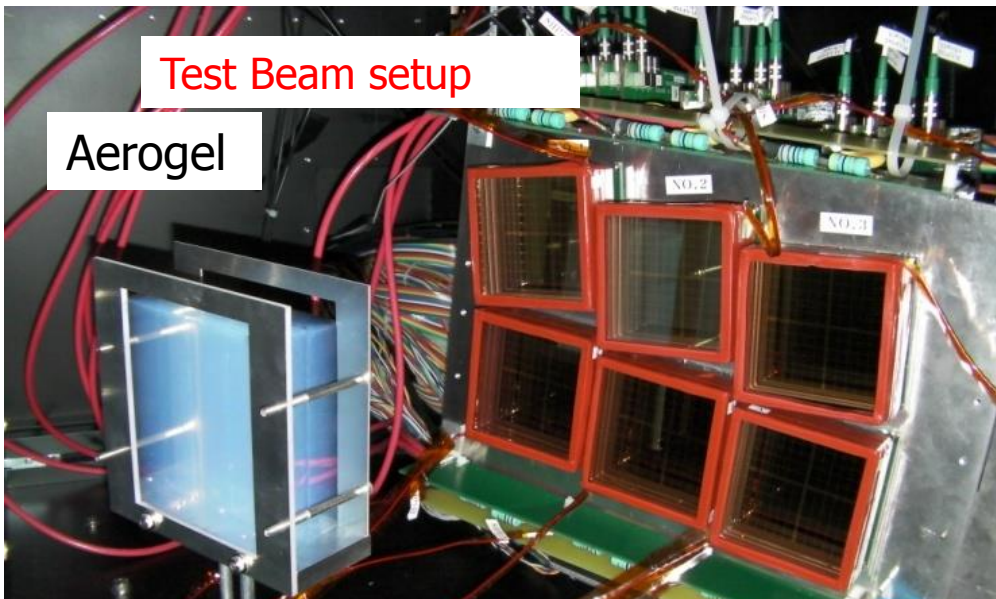
2+2cm aerogel



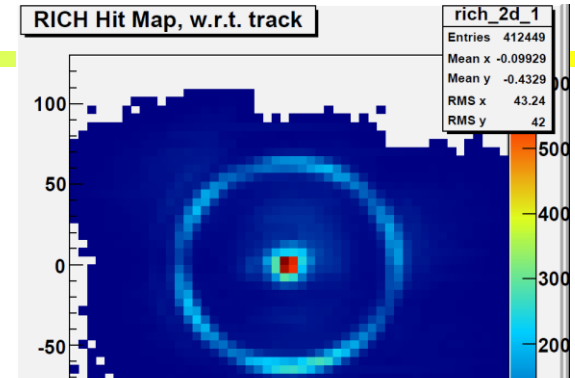
Aerogel RICH photon detectors

Need:
Operation in 1.5 T magnetic field
Pad size ~5-6mm

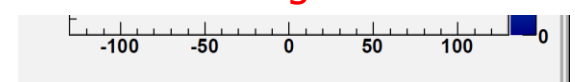
Baseline option: large active area HAPD
of the proximity focusing type



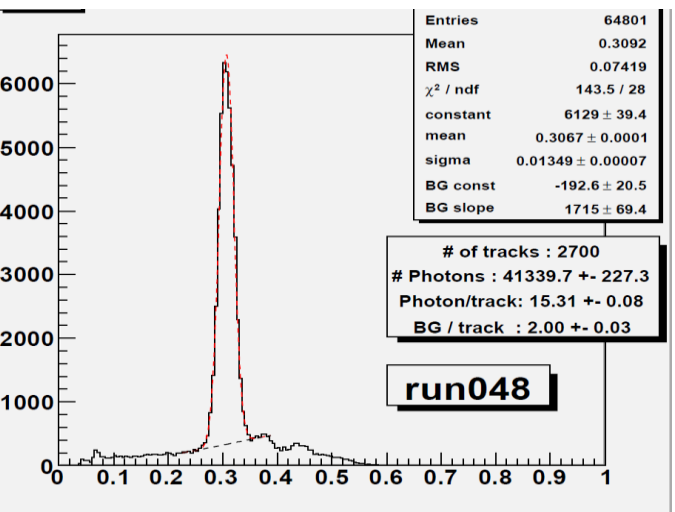
Hamamatsu HAPD
Q.E. ~33% (recent good ones)



Clear Cherenkov image observed



Cherenkov angle distribution



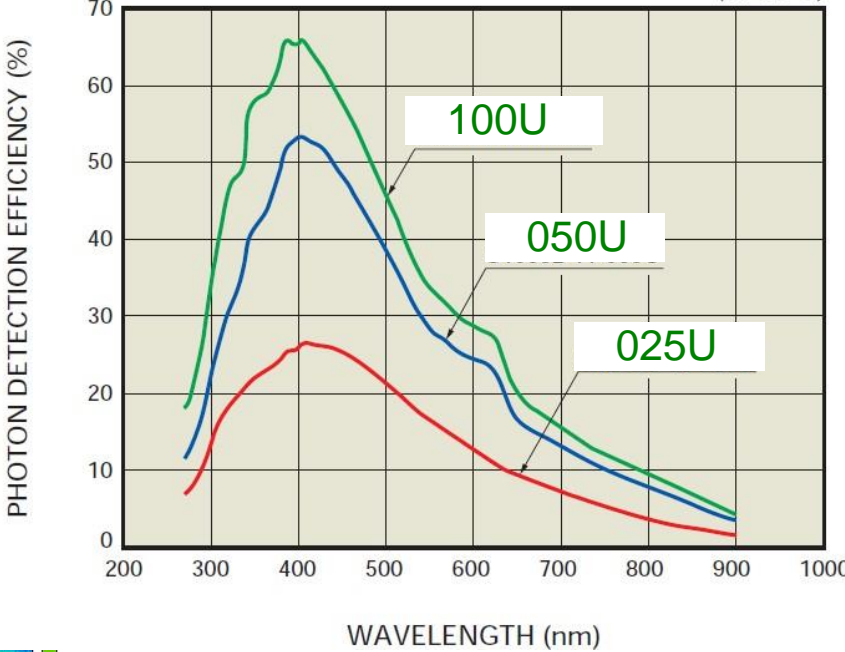
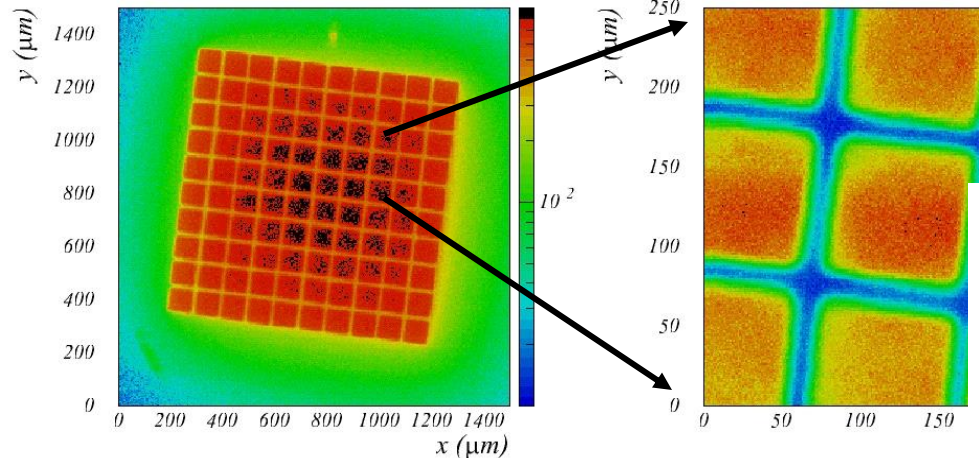
6.6 σ p/K at 4GeV/c !

→ NIM A595 (2008) 180

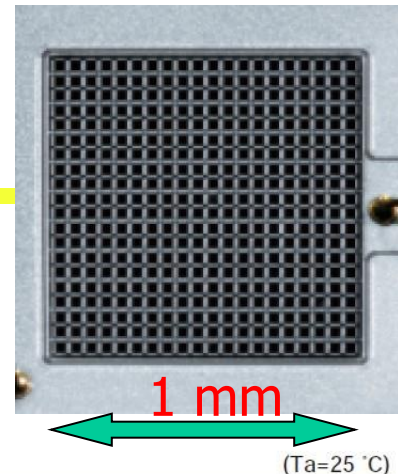
SiPMs as photon detectors?

SiPM is an array of APDs operating in Geiger mode. Characteristics:

- low operation voltage $\sim 10\text{-}100$ V
- gain $\sim 10^6$
- peak PDE up to 65%(@400nm)
$$\text{PDE} = \text{QE} \times \varepsilon_{\text{geiger}} \times \varepsilon_{\text{geo}}$$
 (up to 5x PMT!)
- ε_{geo} – dead space between the cells
- time resolution ~ 100 ps
- works in high magnetic field
- dark counts \sim few 100 kHz/mm²
- radiation damage (p,n)



Never before tested in a RICH where we have to detect single photons. ← Dark counts have single photon pulse heights (rate 0.1-1 MHz)

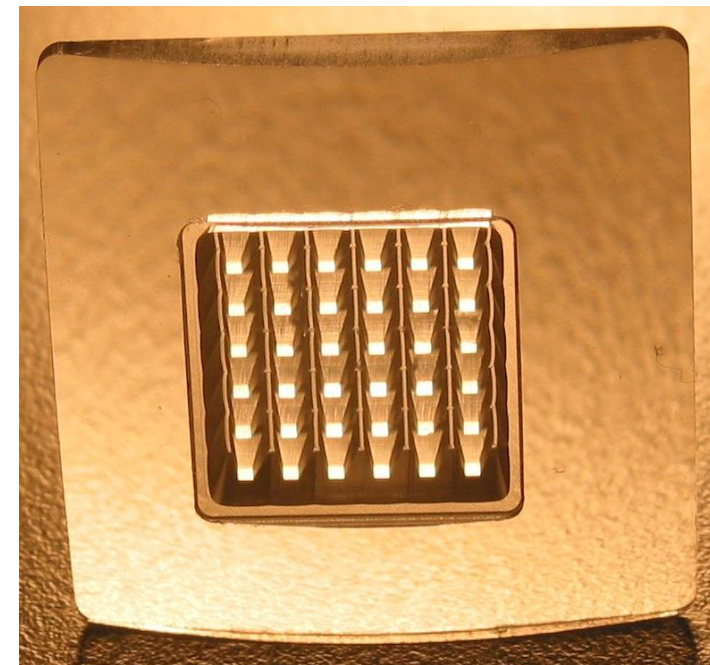
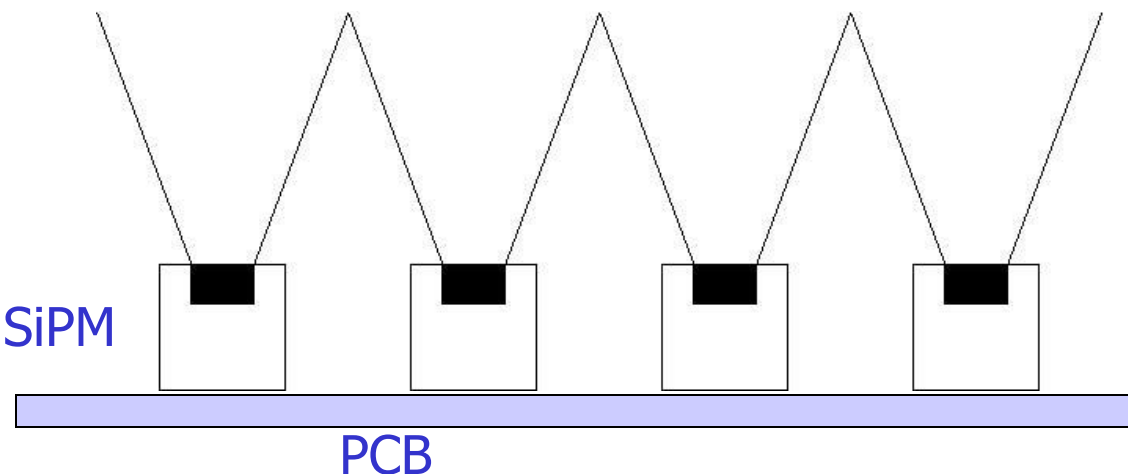


Can such a detector work?

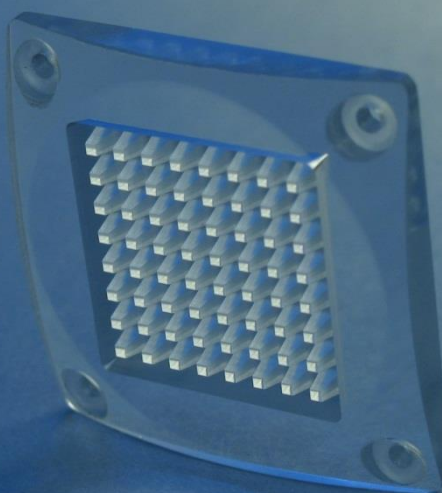
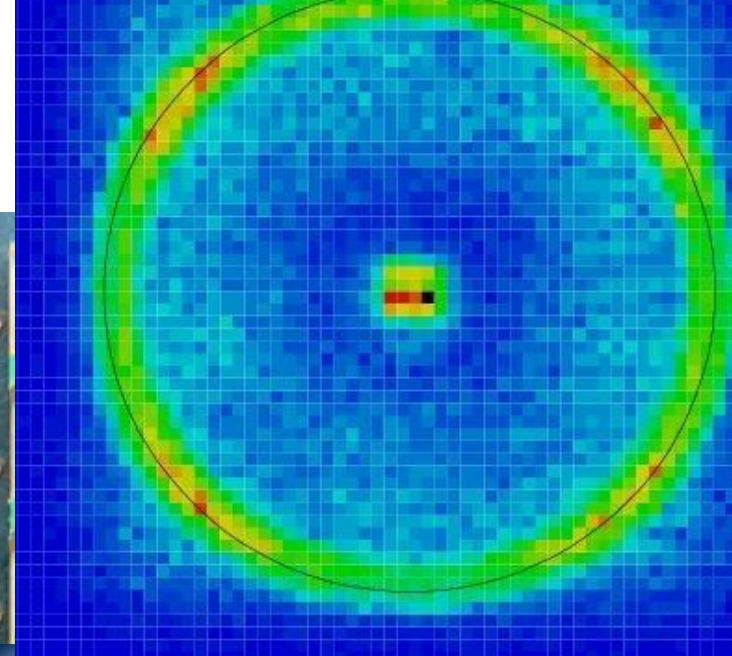
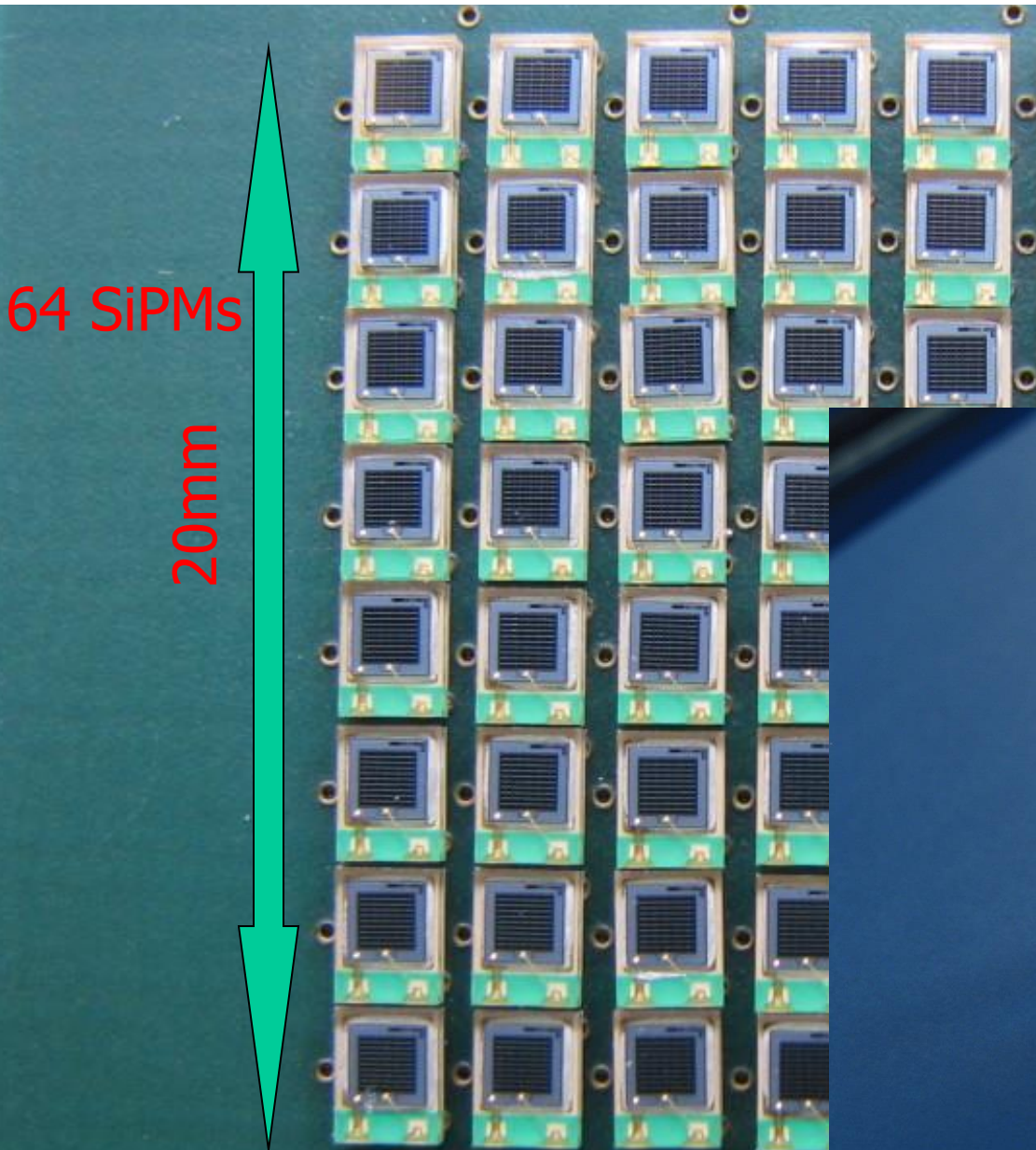
Improve the signal to noise ratio:

- Reduce the noise by a narrow (<10ns) time window
- Increase the number of signal hits per single sensor by using light collectors and by adjusting the pad size to the ring thickness

E.g. light collector with reflective walls
or plastic light guide

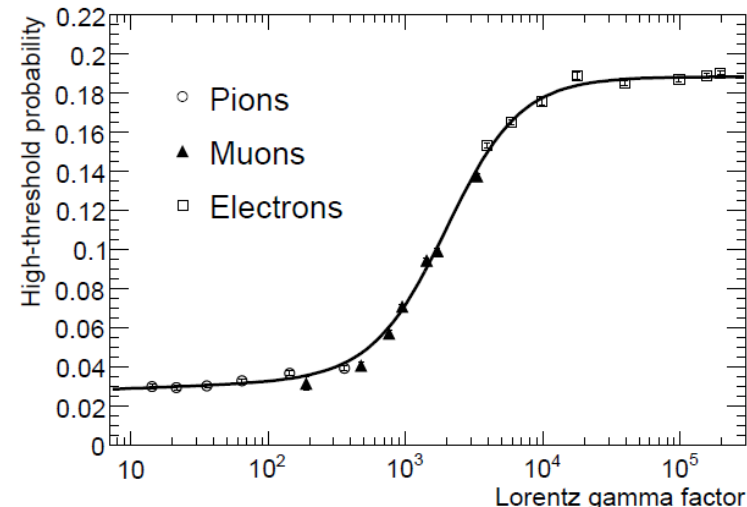
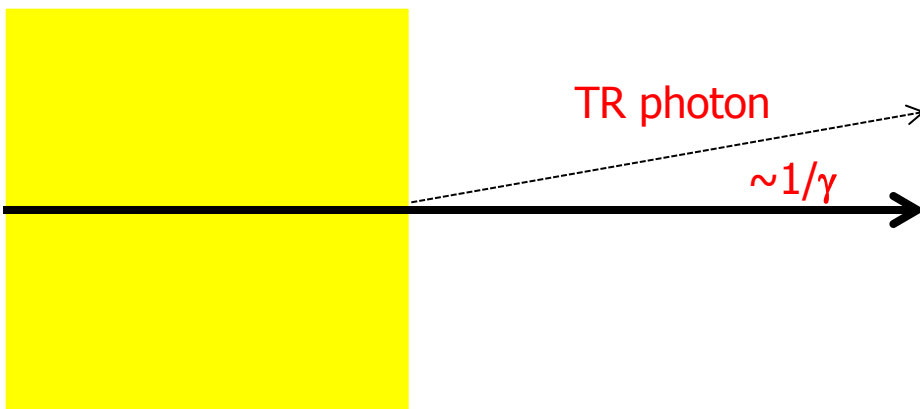


Photon detector with SiPMs and light guides



Transition radiation

E.M. radiation emitted by a charged particle at the boundary of two media with different refractive indices



Emission rate depends on γ (Lorentz factor): becomes important at $\gamma \sim 1000$

- Electrons at 0.5 GeV
- Pions above 140 GeV

Emission probability per boundary $\sim \alpha = 1/137$

Emission angle $\sim 1/\gamma$

Typical photon energy: ~ 10 keV → X rays

Transition radiation - detection

Emission probability per boundary $\sim \alpha = 1/137$

→ Need many boundaries

- Stacks of thin foils or
- Porous materials – foam with many boundaries of individual ‘bubbles’

Typical photon energy: ~ 10 keV → X rays

→ Need a wire chamber with a high Z gas (Xe) in the gas mixture

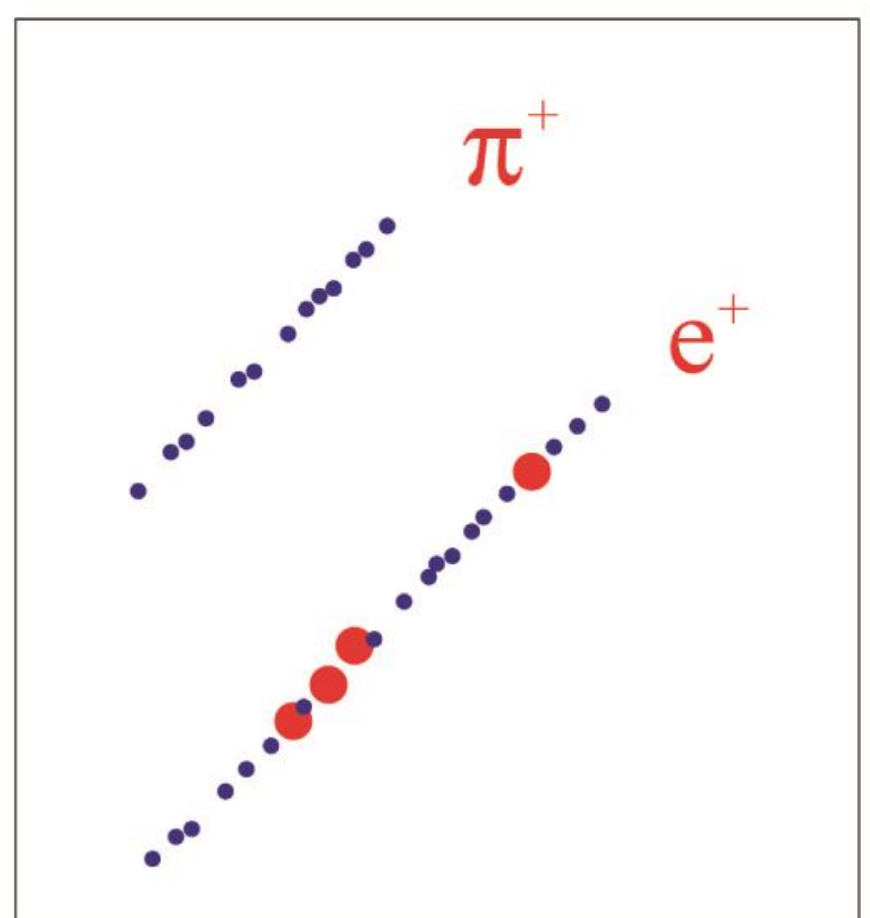
Emission angle $\sim 1/\gamma$

→ Hits from TR photons along the charged particle direction

- Separation of X ray hits (high energy deposit on one place) against ionisation losses (spread out along the track)
- Two thresholds: lower for ionisation losses, higher for X ray detection

Transition radiation - detection

- Hits from TR photons along the charged particle direction
- Separation of X ray hits (high energy deposit on one place) against ionisation losses (spread out along the track)
- Two thresholds: lower for ionisation losses, higher for X ray detection

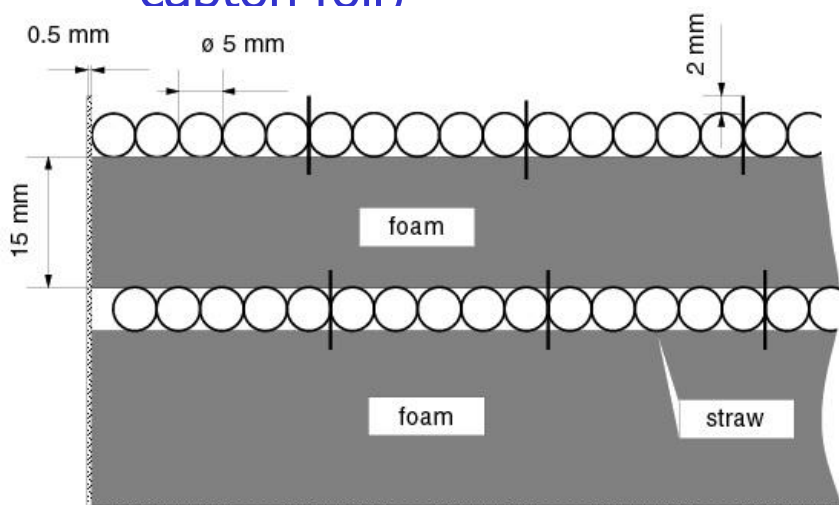


- Small circles: low threshold (ionisation)
- Big circles: high threshold (X ray detection)

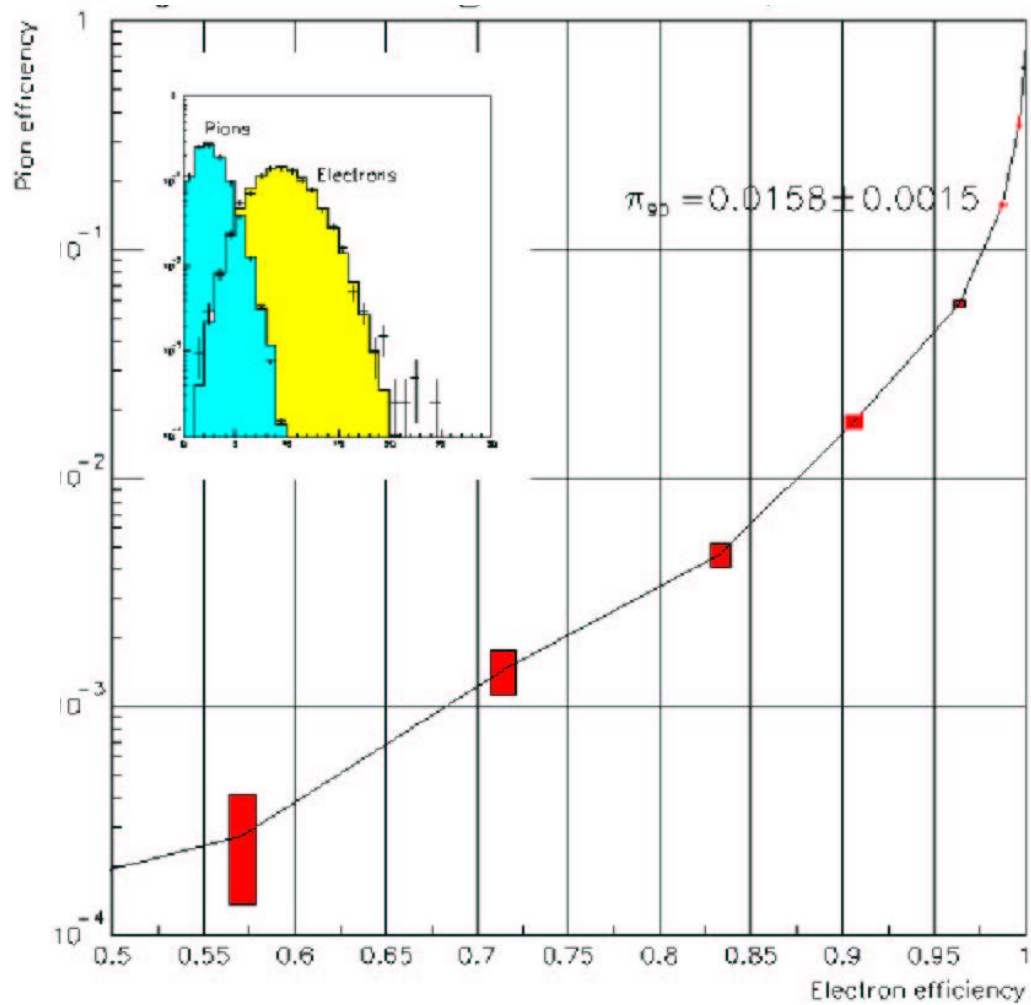
Transition radiation detectors

Example:

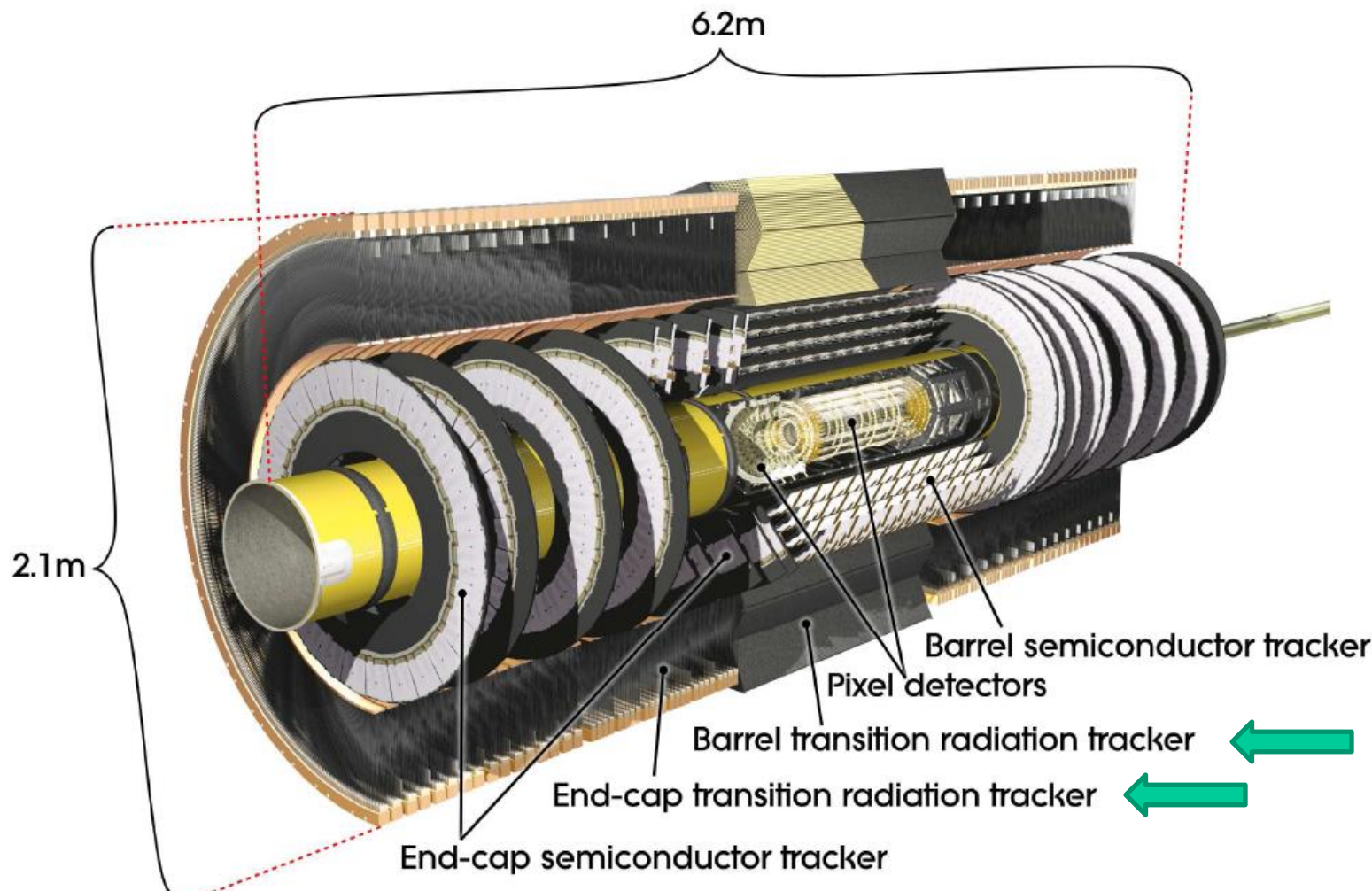
Radiator: organic foam
between the detector
tubes (straws made of
capton foil)

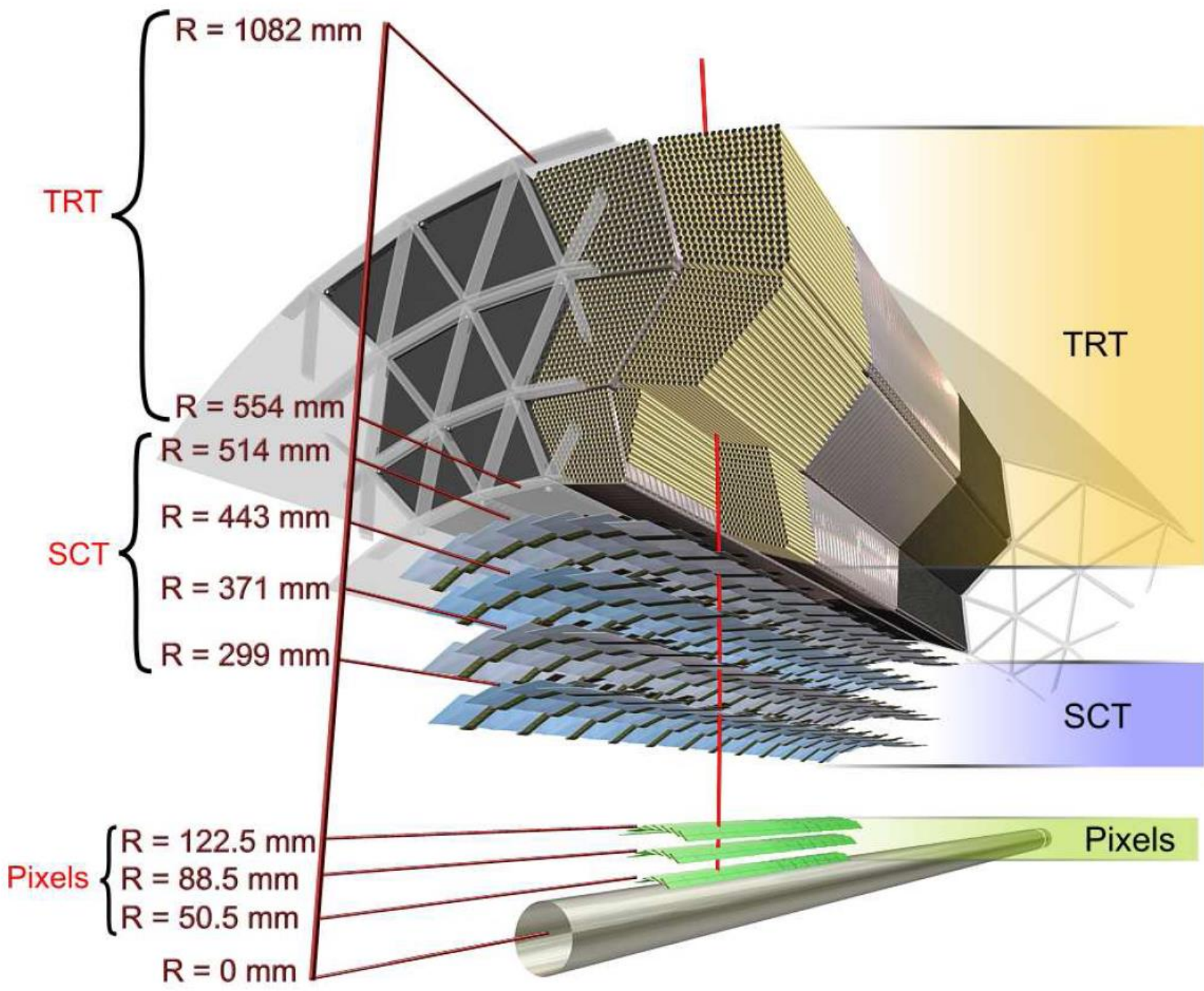


Performance: pion efficiency (fake prob.)
vs electron efficiency



Transition radiation detector in ATLAS: combination of a tracker and a transition radiation detector

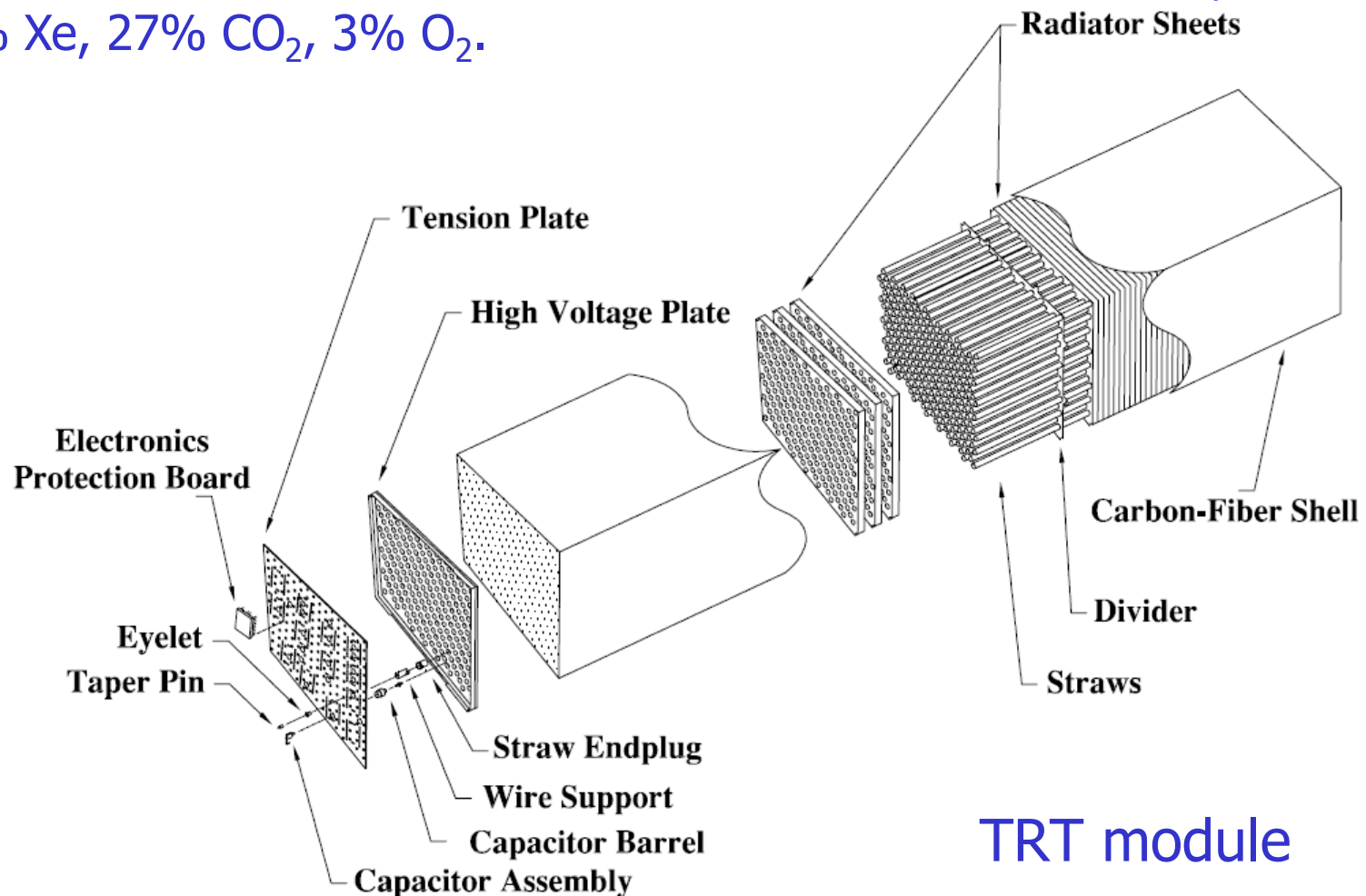




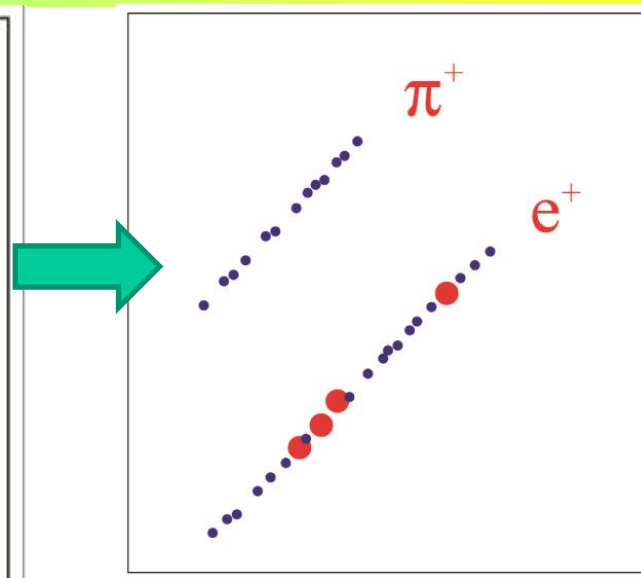
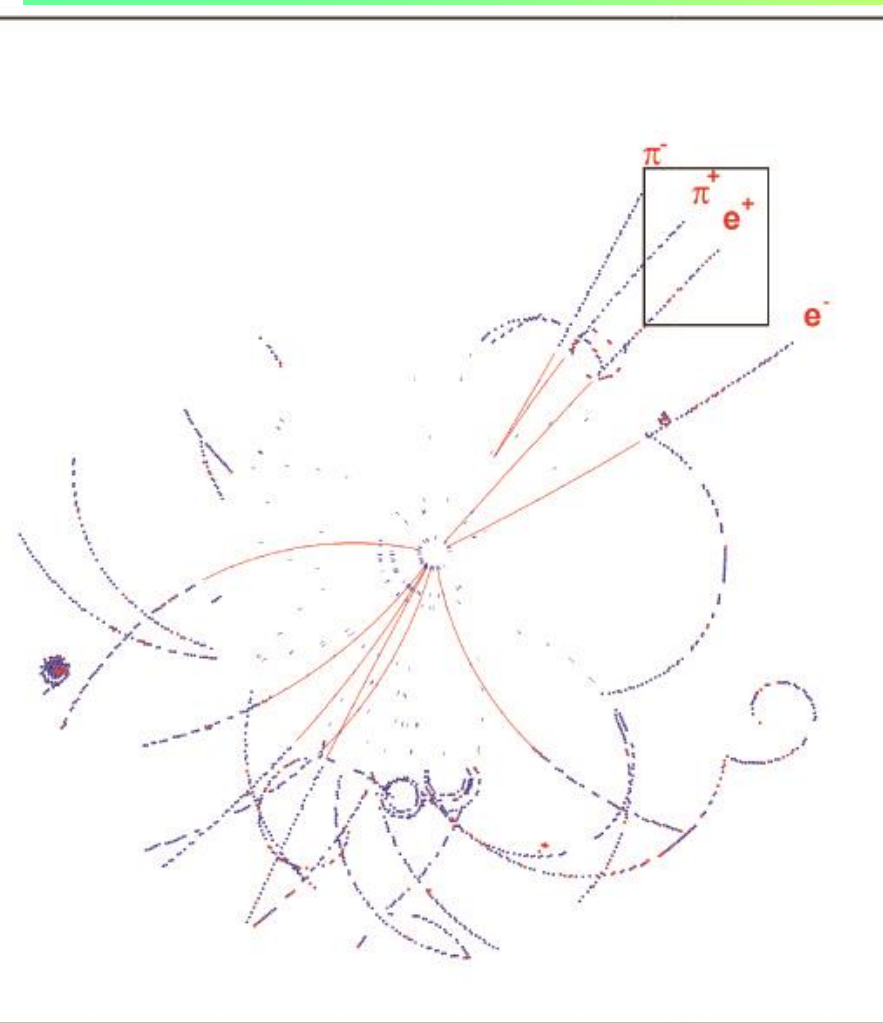
ATLAS TRT

Radiator: 3mm thick layers made of polypropylene-polyethylene fibers with ~19 micron diameter, density: 0.06 g/cm^3

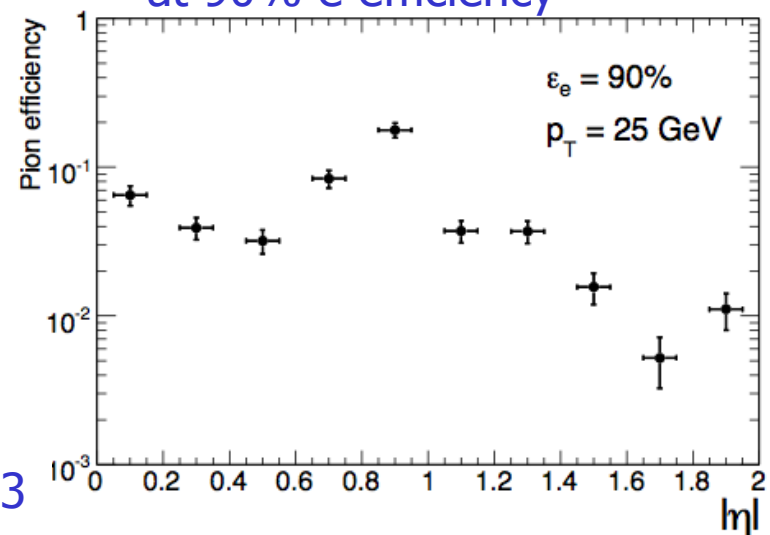
Straw tubes: 4mm diameter with 31 micron diameter anode wires,
gas: 70% Xe, 27% CO_2 , 3% O_2 .



TRT: pion-electron separation

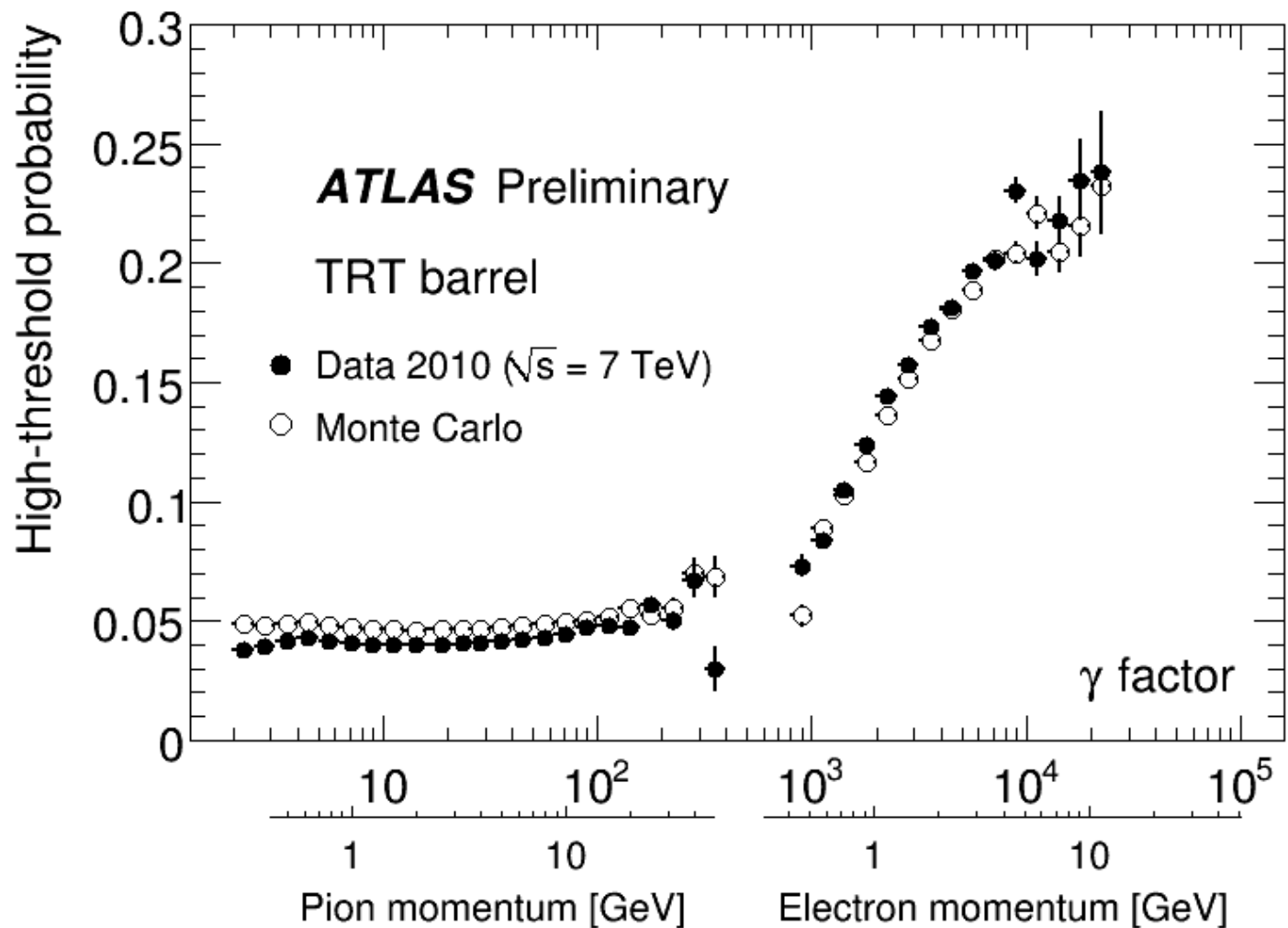


Expected π fake probability
at 90% e efficiency



TRT performance in 2010 data

e/pion separation: high threshold hit probability per straw



Muon and K_L detector at B factories

Separate muons from hadrons (pions and kaons): exploit the fact that muons interact only electromag., while hadrons interact strongly → need a few interaction lengths to stop hadrons (interaction lengths = about 10x radiation length in iron, 20x in CsI). A particle is identified as muon if it penetrates the material.



Detect K_L interaction (cluster): again need a few interaction lengths.

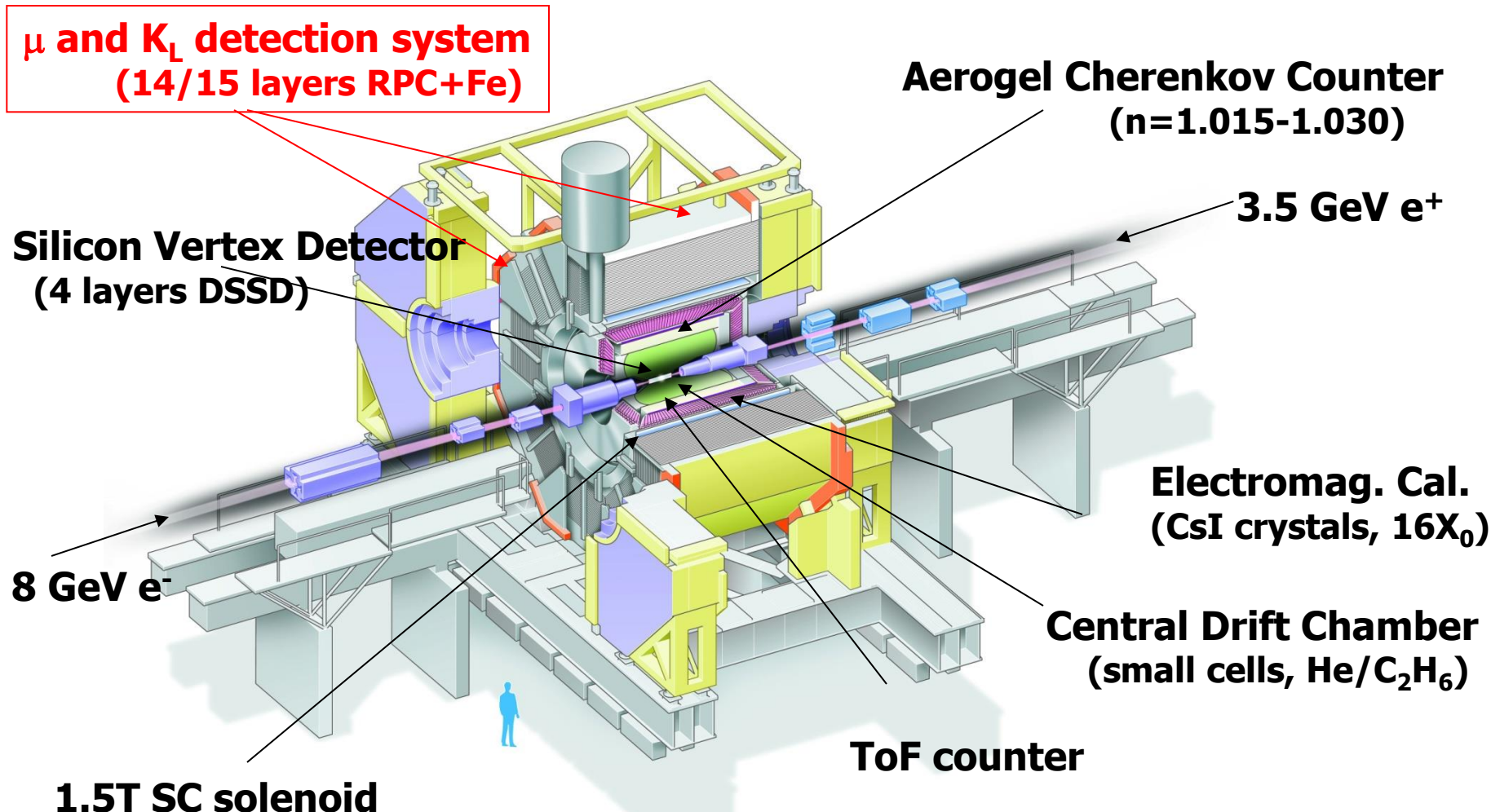
Some numbers: 0.8 interaction length (CsI) + 3.9 interaction lengths (iron)

Interaction length: iron 132 g/cm², CsI 167 g/cm²

$(dE/dx)_{min}$: iron 1.45 MeV/(g/cm²), CsI 1.24 MeV/(g/cm²)

→ $\Delta E_{min} = (0.36+0.11) \text{ GeV} = 0.47 \text{ GeV}$ → reliable identification of muons possible above ~600 MeV

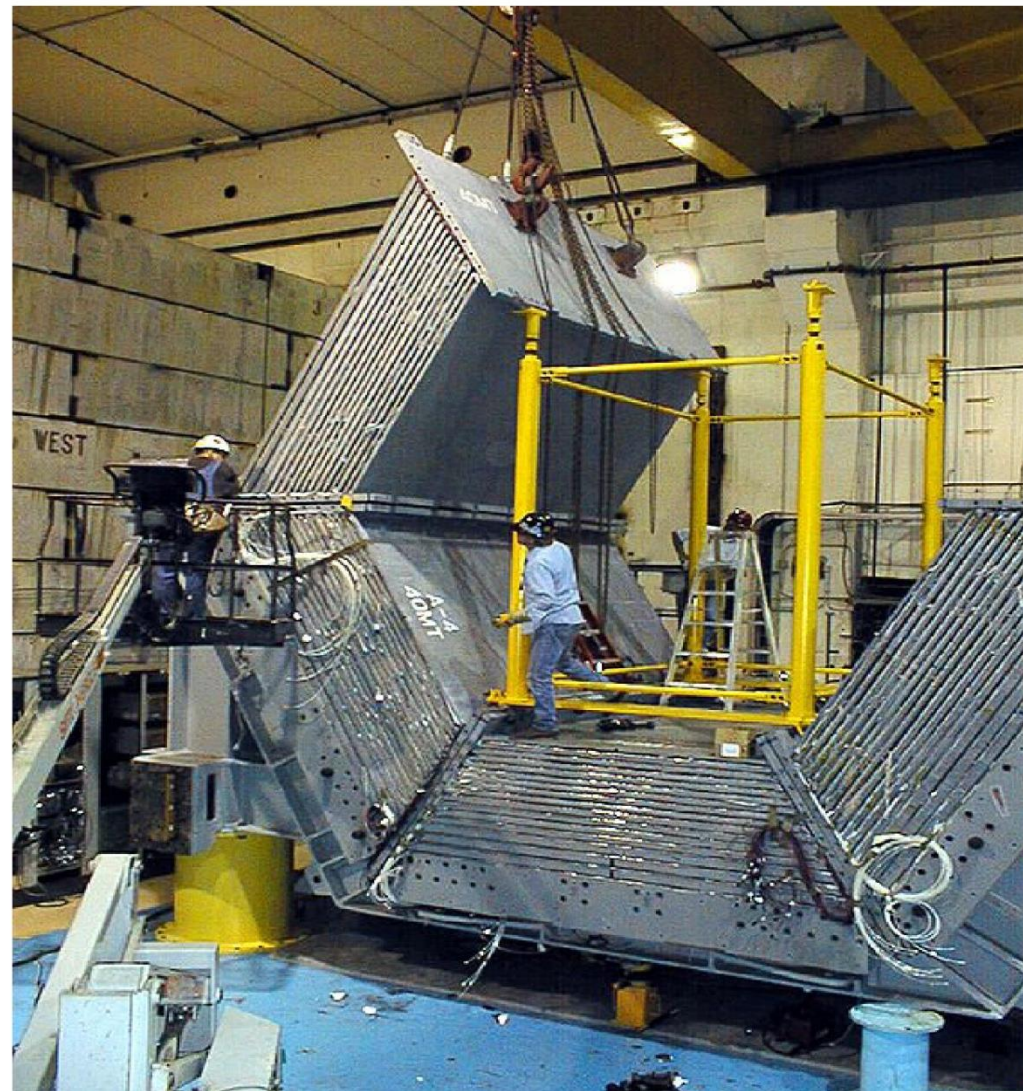
Example: Muon and K_L detection at Belle



Muon and K_L detector

Up to 21 layers of resistive-plate chambers (RPCs) between iron plates of flux return

Bakelite RPCs at BABAR
Glass RPCs at Belle
(better choice)



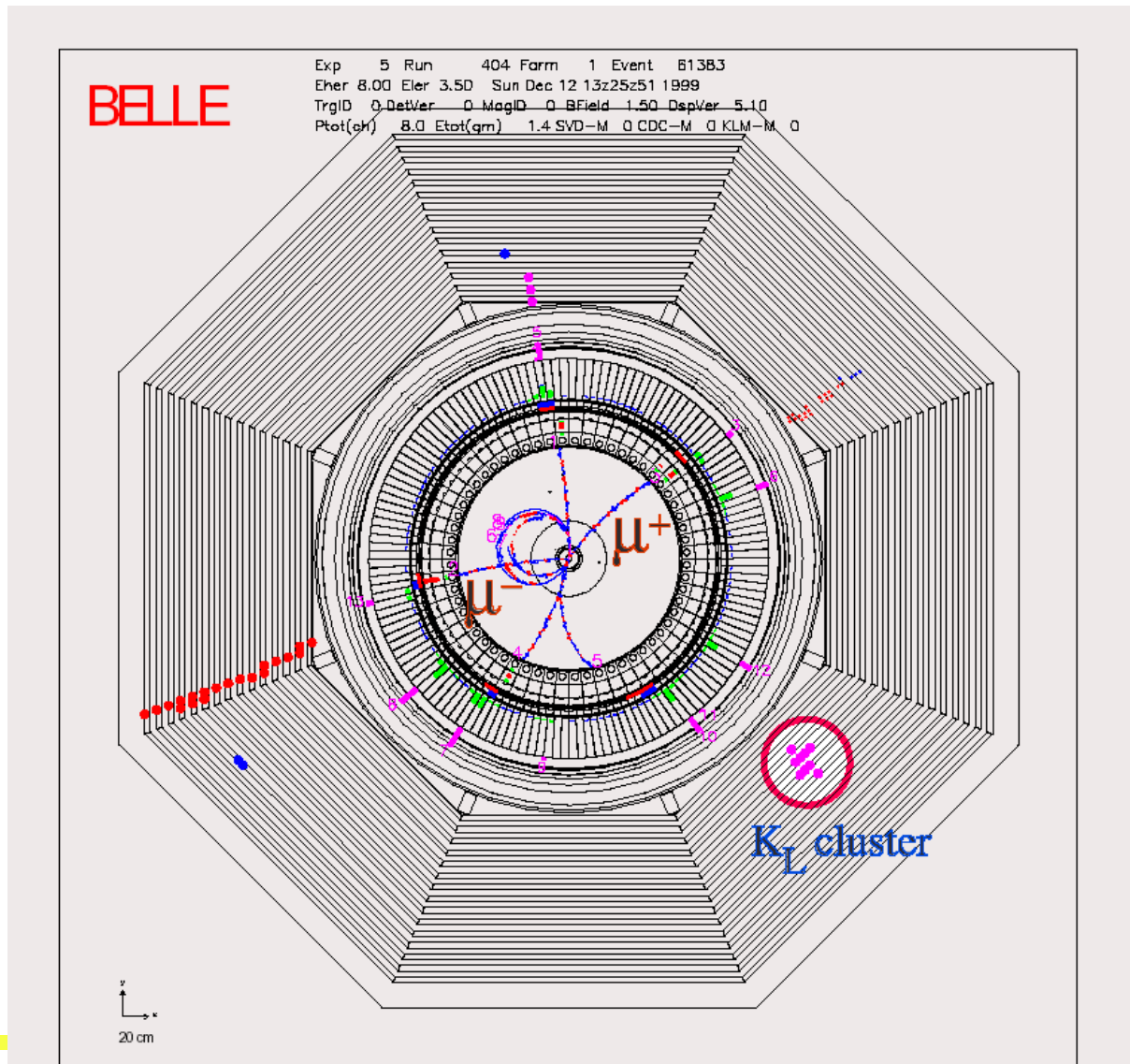
Muon and K_L detector

Example:

event with

- two muons and a
- K_L

**and a pion that
partly penetrated**



Muon and K_L detector performance

Muon identification: efficient for $p>800$ MeV/c

efficiency

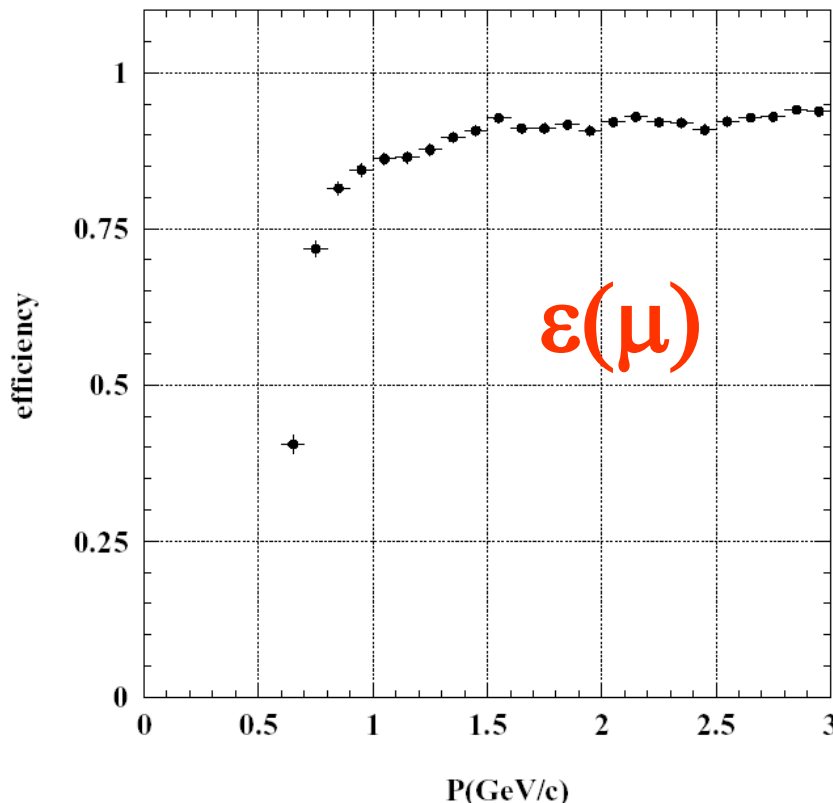


Fig. 109. Muon detection efficiency vs. momentum in KLM.

fake probability

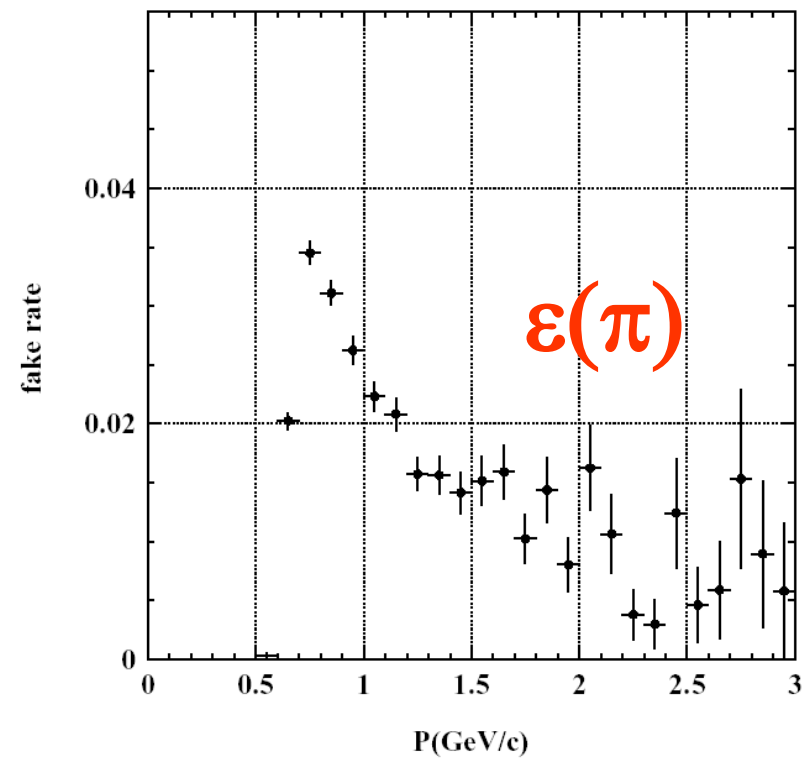


Fig. 110. Fake rate vs. momentum in KLM.

Muon and K_L detector performance

K_L detection: resolution in direction →

K_L detection: also with possible with electromagnetic calorimeter (0.8 interaction lengths)

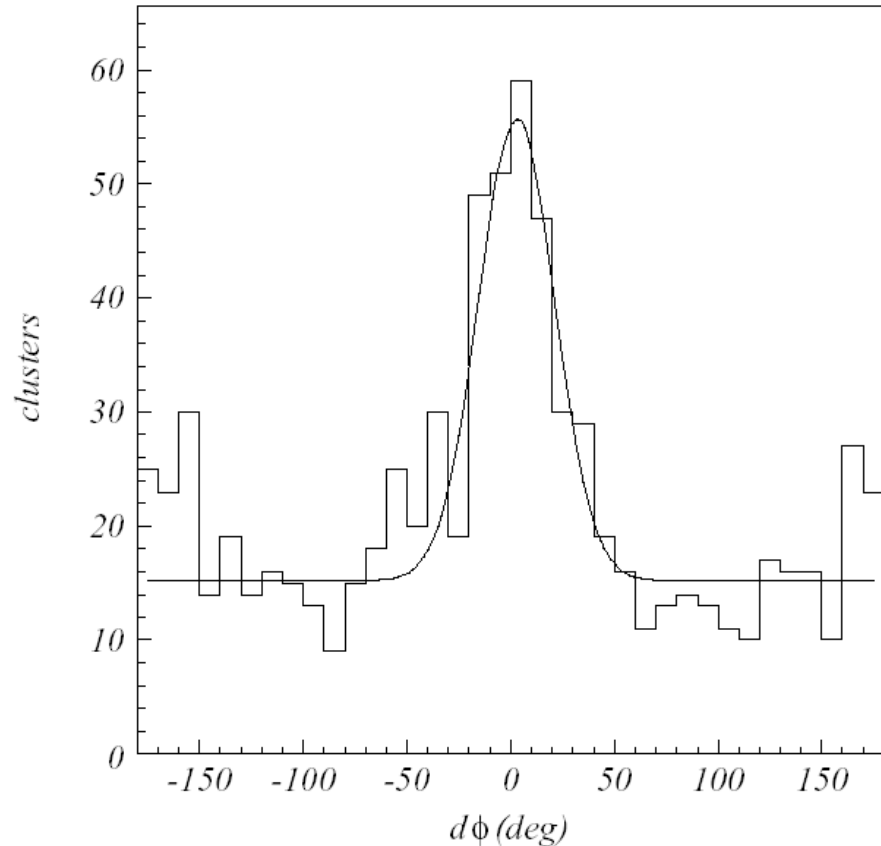
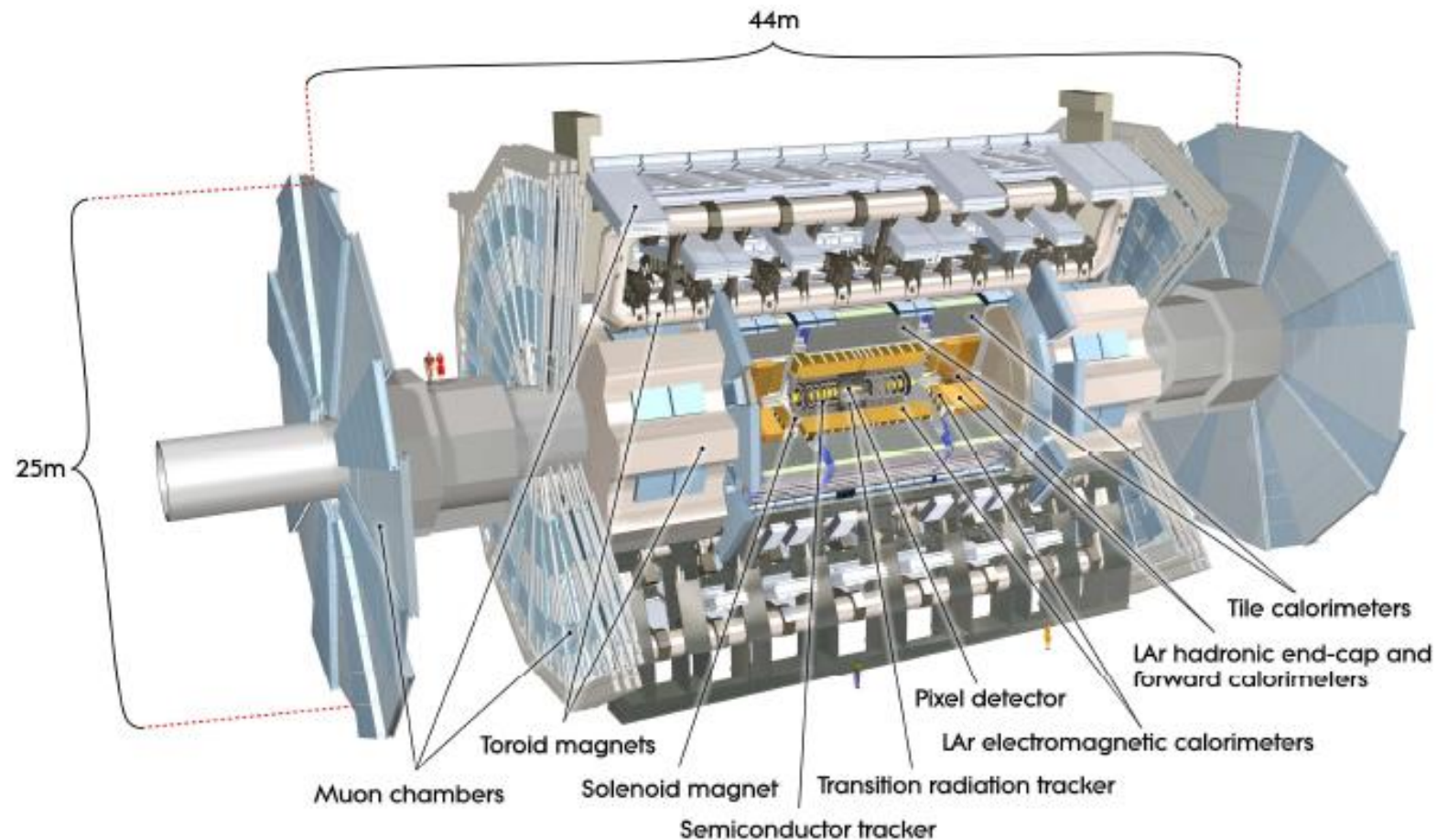


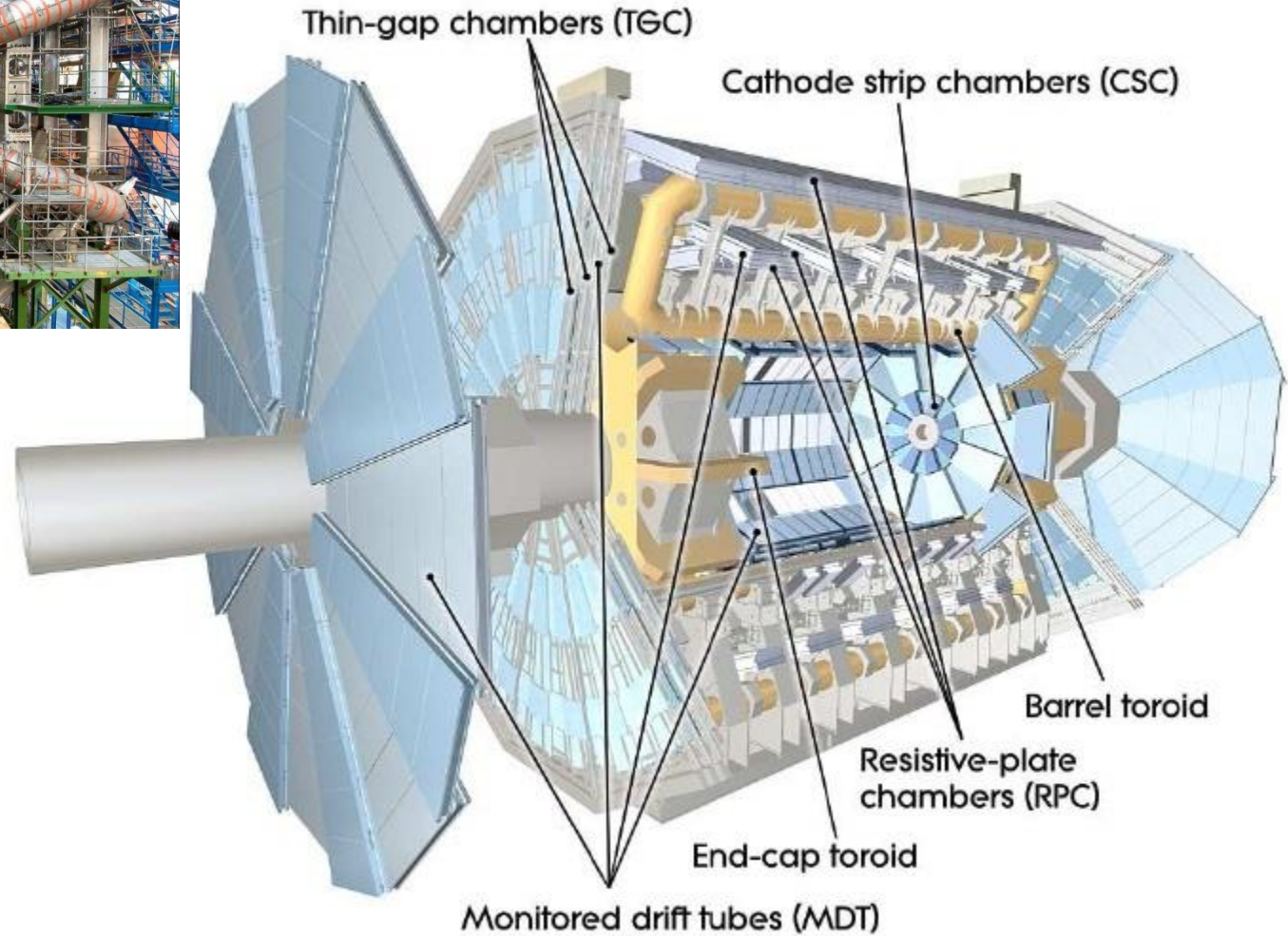
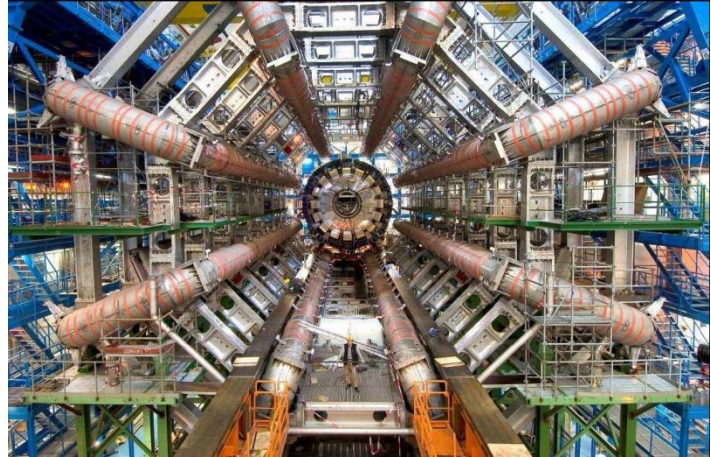
Fig. 107. Difference between the neutral cluster and the direction of missing momentum in KLM.

Identification of muons at LHC

- example ATLAS

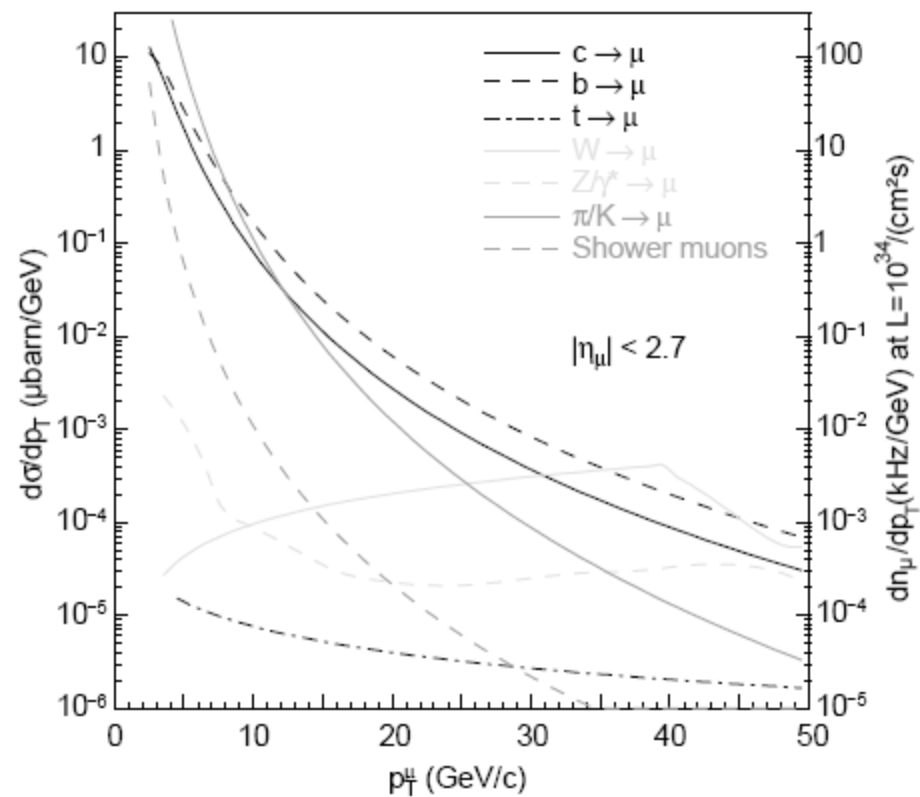
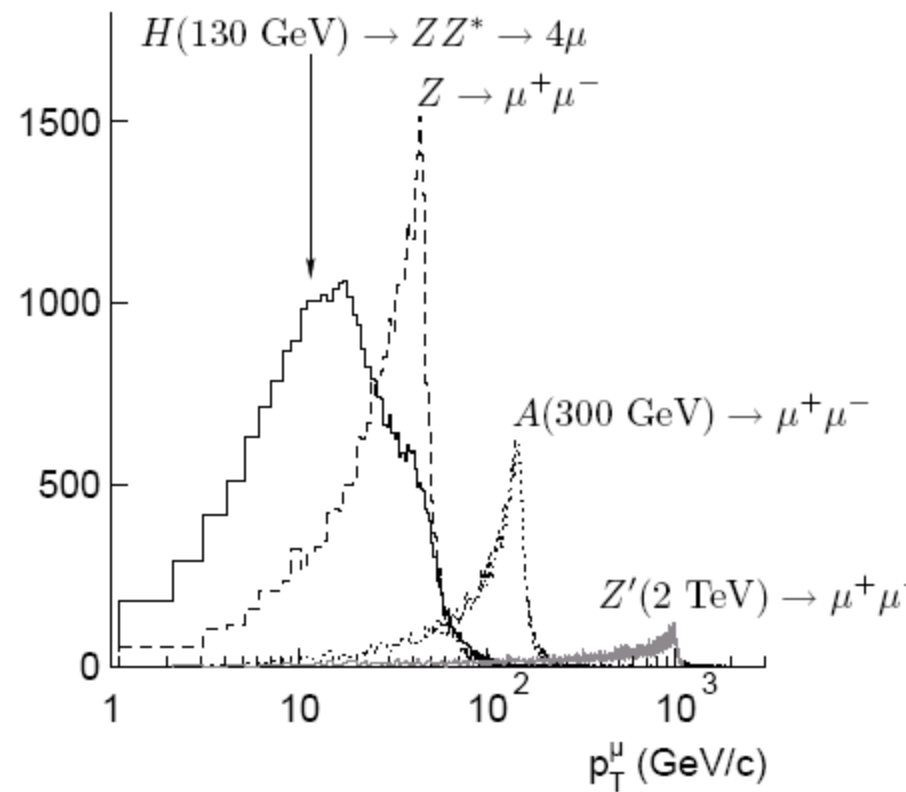


Identification of muons in ATLAS



- Identify muons
- Measure their momentum

Muon spectrum



Muon identification in ATLAS

Material in front of the muon system

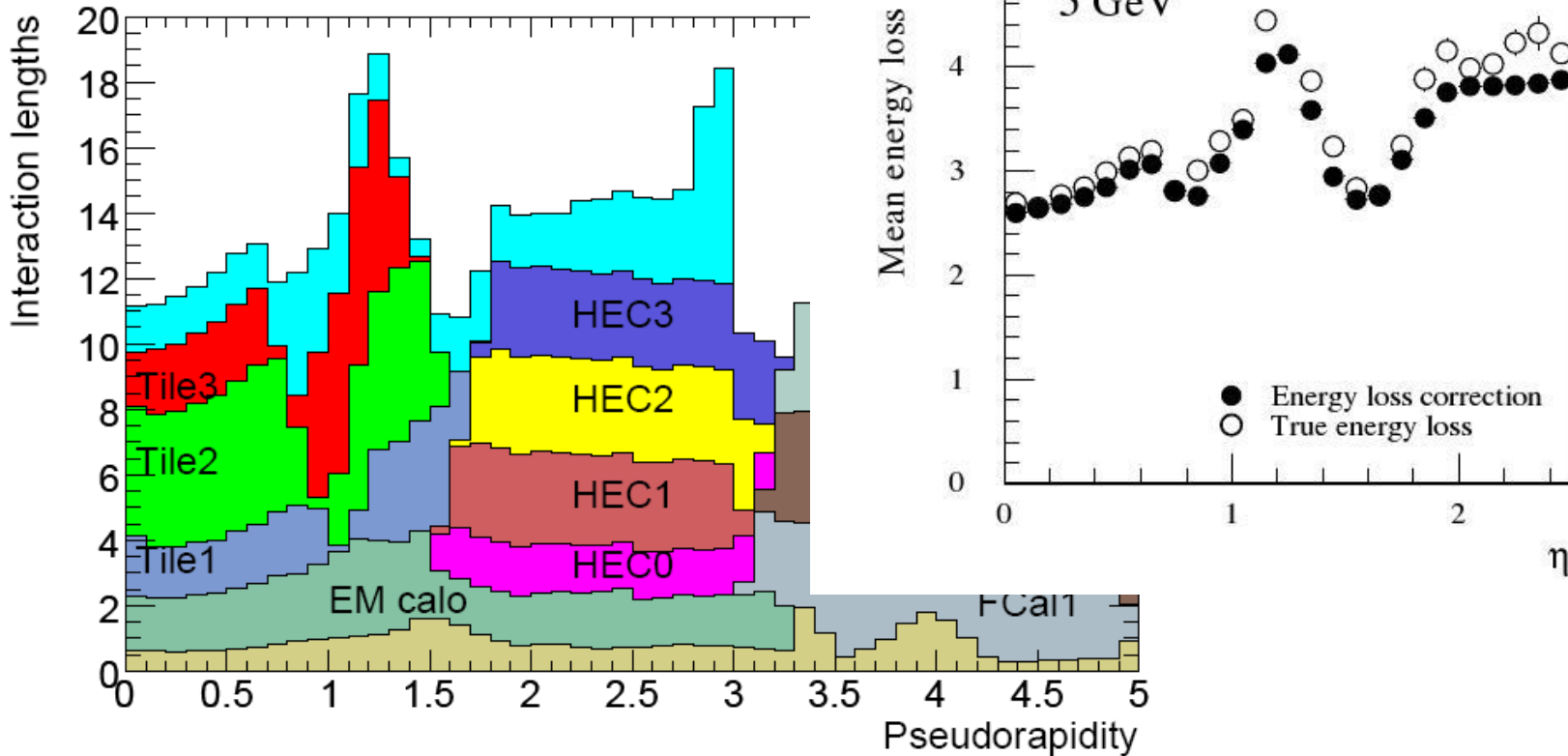


Figure 5.2: Cumulative amount of material, in units of interaction length, as a function of $|\eta|$, in front of the electromagnetic calorimeters, in the electromagnetic calorimeters themselves, in each hadronic layer, and the total amount at the end of the active calorimetry. Also shown for completeness is the total amount of material in front of the first active layer of the muon spectrometer (up to $|\eta| < 3.0$).

Muon identification efficiency

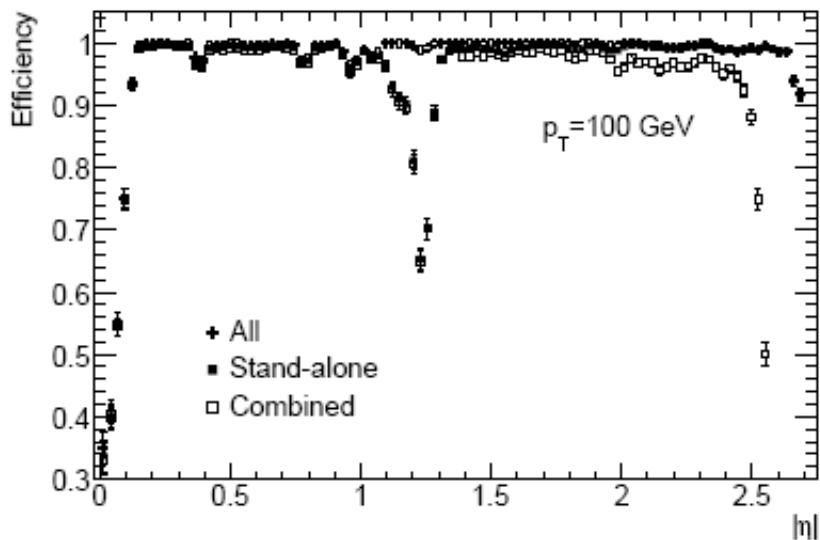


Figure 10.37: Efficiency for reconstructing muons with $p_T = 100 \text{ GeV}$ as a function of $|\eta|$. The results are shown for stand-alone reconstruction, combined reconstruction and for the combination of these with the segment tags discussed in the text.

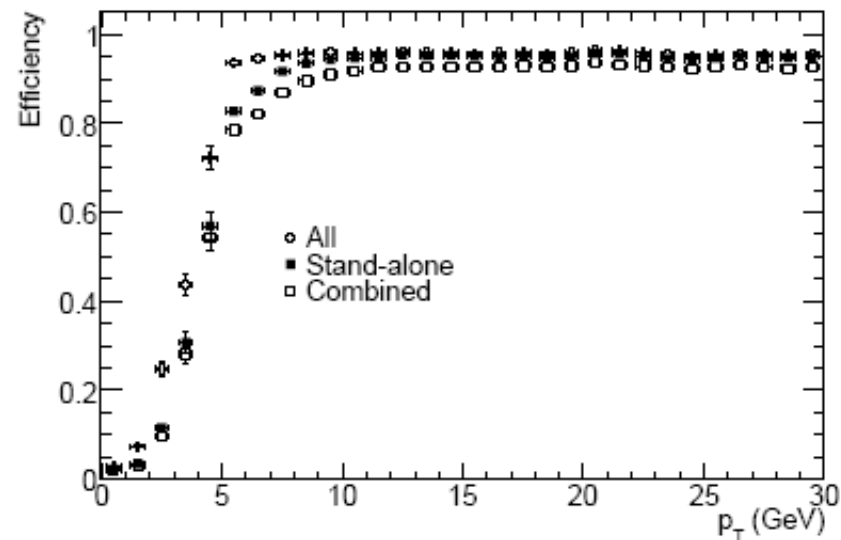


Figure 10.38: Efficiency for reconstructing muons as a function of p_T . The results are shown for stand-alone reconstruction, combined reconstruction and for the combination of these with the segment tags discussed in the text.

Muon fake probability

Sources of fakes:

- Hadrons: punch through negligible, >10 interaction lengths of material in front of the muon system (remain: muons from pion and kaon decays)
- Electromagnetic showers triggered by energetic muons traversing the calorimeters and support structures lead to low-momentum electron and positron tracks, an irreducible source of fake stand-alone muons. Most of them can be rejected by a cut on their transverse momentum ($pT > 5$ GeV reduces the fake rate to a few percent per triggered event); can be almost entirely rejected by requiring a match of the muon-spectrometer track with an inner-detector track.
- Fake stand-alone muons from the background of thermal neutrons and low energy γ -rays in the muon spectrometer ("cavern background"). Again: $pT > 5$ GeV reduces this below 2% per triggered event at $10^{33} \text{ cm}^{-2} \text{ s}^{-1}$. Can be reduced by almost an order of magnitude by requiring a match of the muon-spectrometer track with an inner-detector track.

Identification in astro-physics/astroparticle physics - 1

- Study composition of cosmic rays in balloon or satellite flights
- Identify (very) high energy cosmic rays and photons with detectors on the ground

Short flight small area detectors (Balloons)

Examples of Balloon-flown RICH detectors

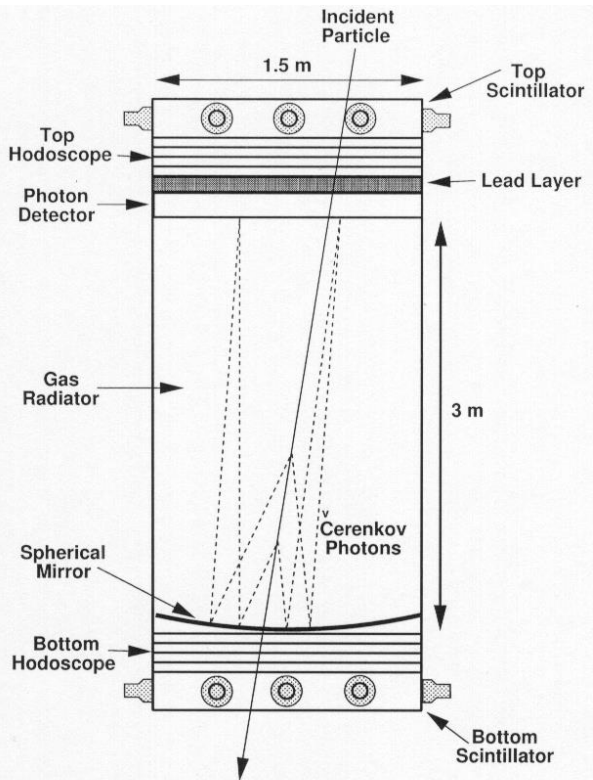
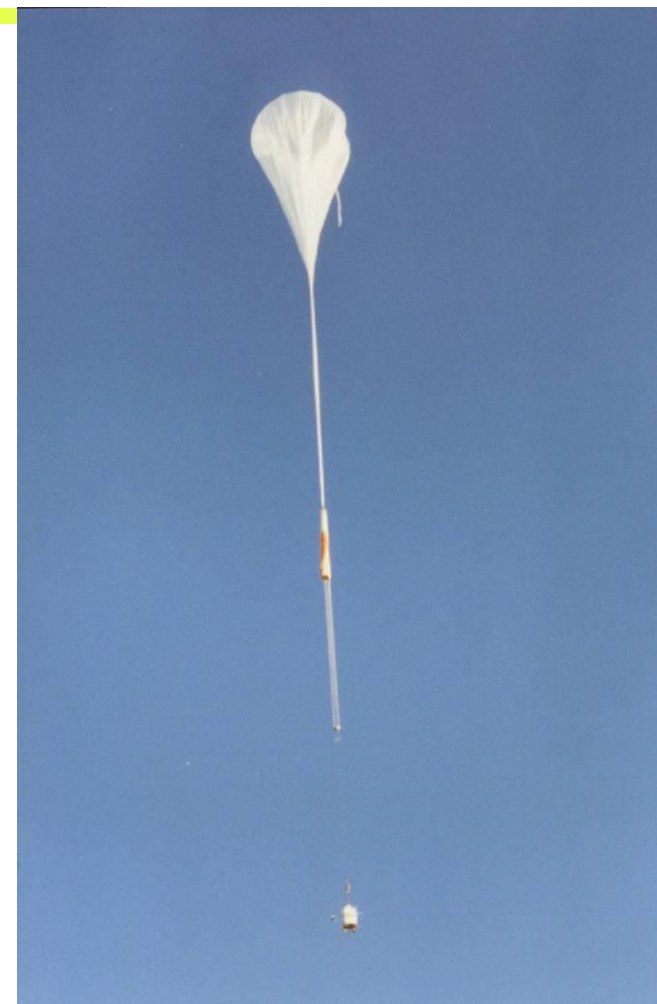
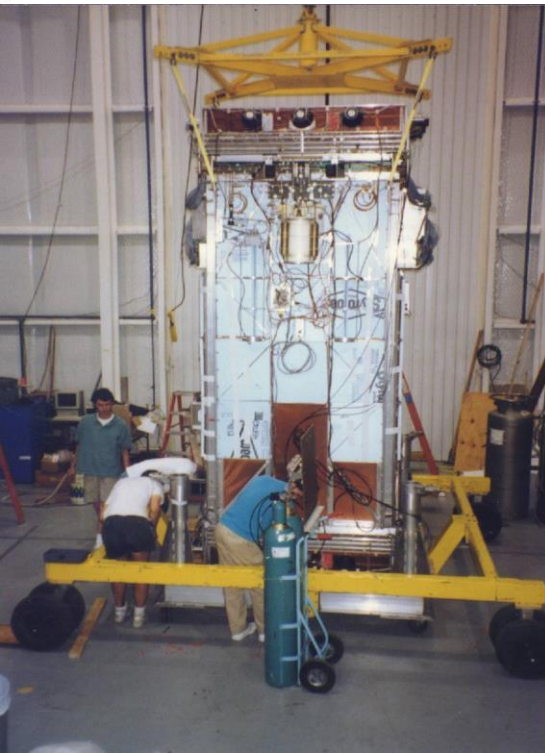


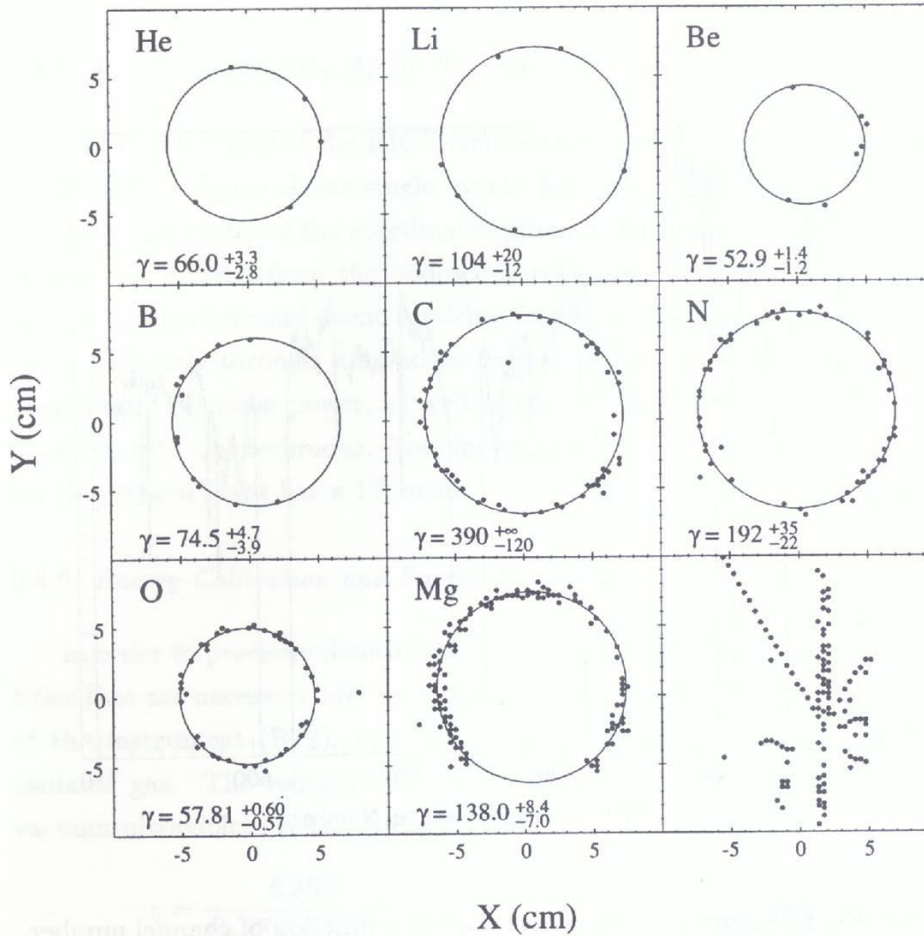
Fig. 1. Schematic cross-section of the instrument



3-metre N₂ radiator, TMAE/CH₄: $\gamma_{\text{th}}=40$
p + He at high energy:

3-metre C₂F₆ radiator, TMAE/C₂H₆: $\gamma_{\text{th}}=25$

Peter Križan, Ljubljana



**Heavy nucleus rings from 1991 flight –
Note that carbon here has total energy
 $\sim 12*390 \text{ GeV} = 4.6\text{TeV}$**

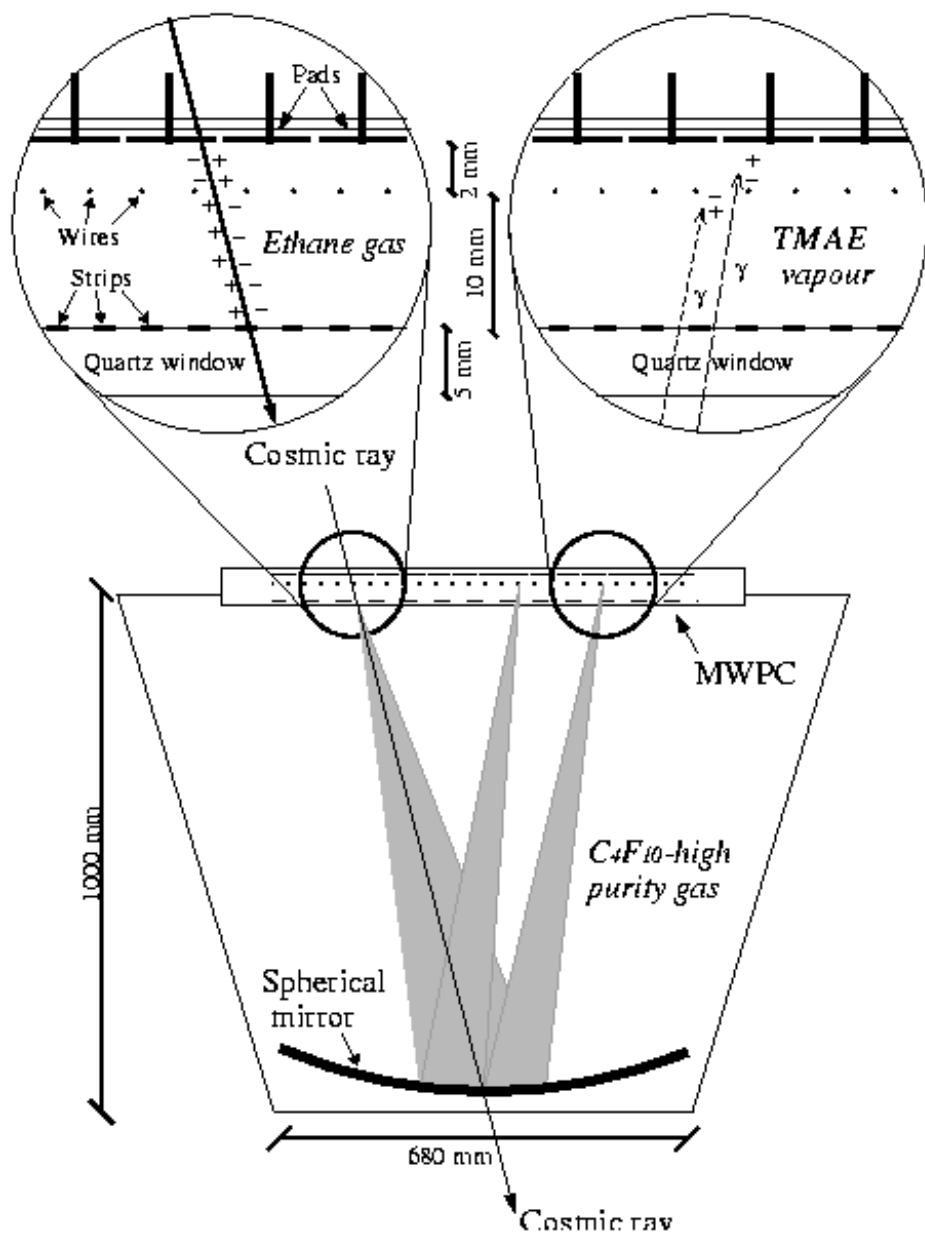


Figure 1.4: Schematic view of the CAPRICE98 RICH detector.

Summary

Particle identification is an essential part of several experiments, and has contributed substantially to our present understanding of elementary particles and their interactions, and will continue to have an important impact in searches for new physics.

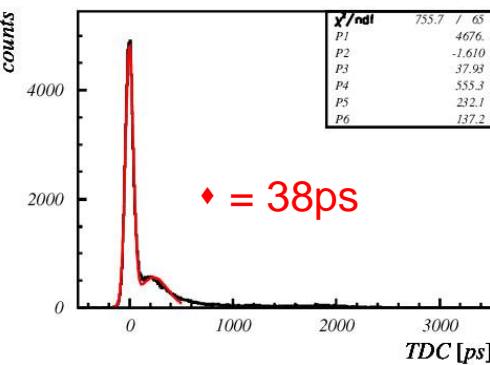
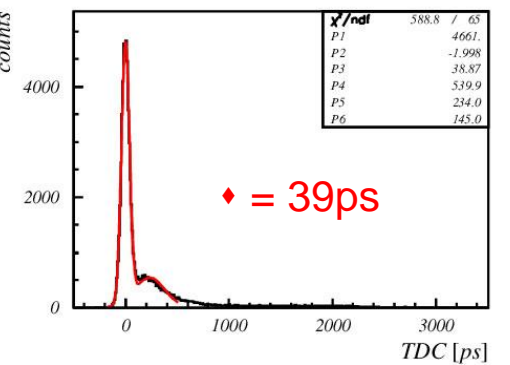
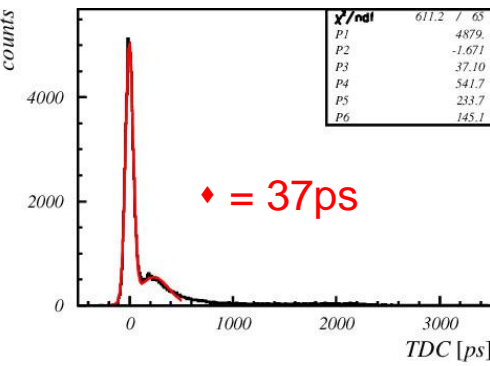
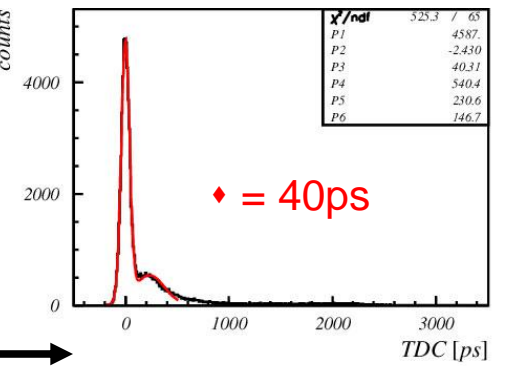
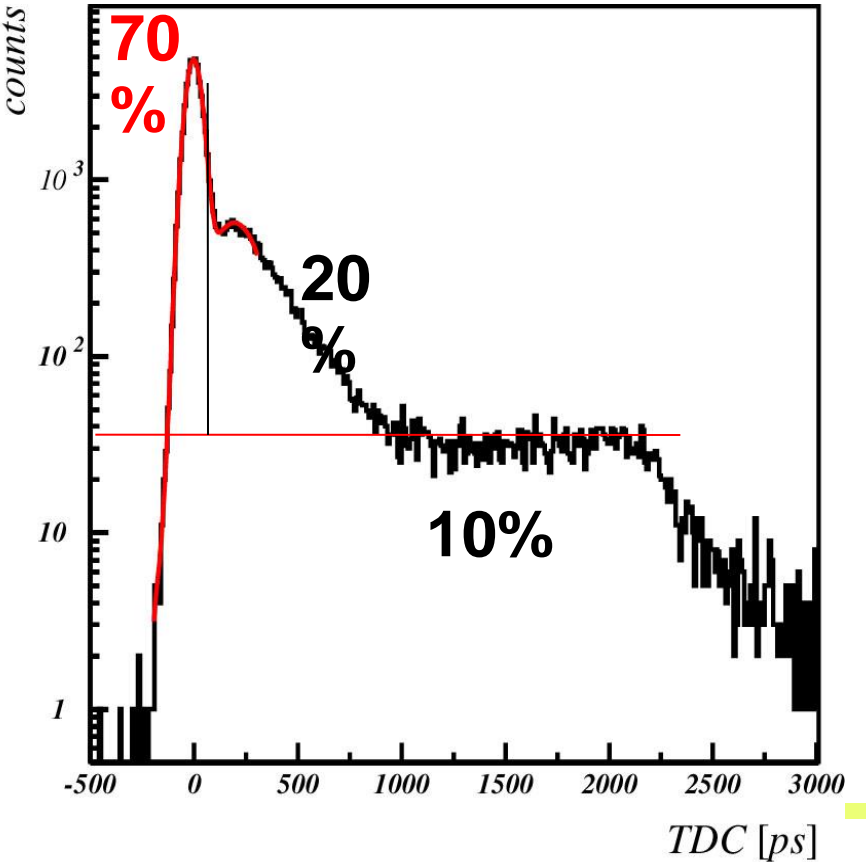
A large variety of techniques has been developed for different kinematic regions and different particles, based on Cherenkov radiation, TOF, dE/dx and TR.

New concepts and detectors are being studied → this is a very active area of detector R+D.

Back-up slides

Corrected TDC

Corrected TDC distributions
for all pads



Response:

- prompt signal ~ 70%
- short delay ~ 20%
- ~ 10% uniform distribution

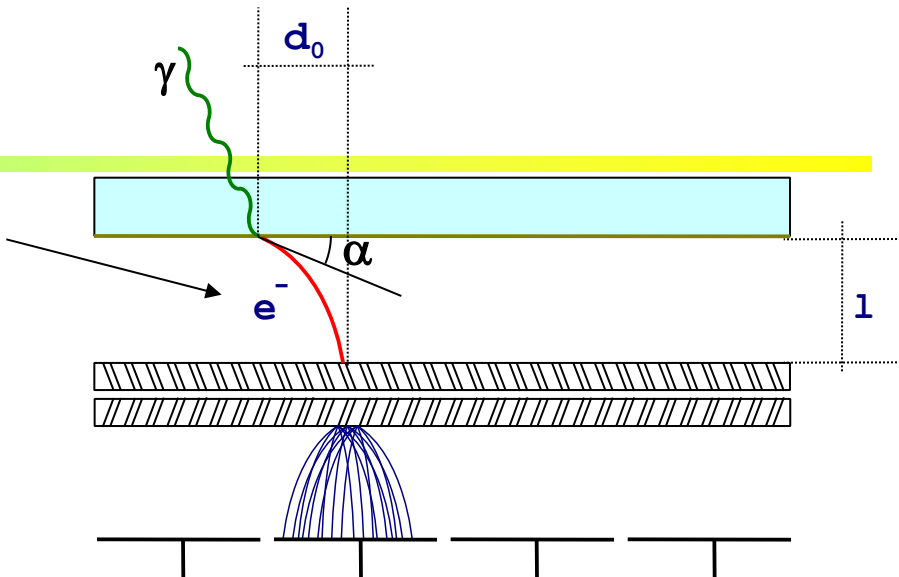
Photon electron detection: modeling

Parameters used:

- $U = 200 \text{ V}$
- $l = 6 \text{ mm}$
- $E_0 = 1 \text{ eV}$
- $m_e = 511 \text{ keV}/c^2$
- $e_0 = 1.6 \cdot 10^{-19} \text{ As}$

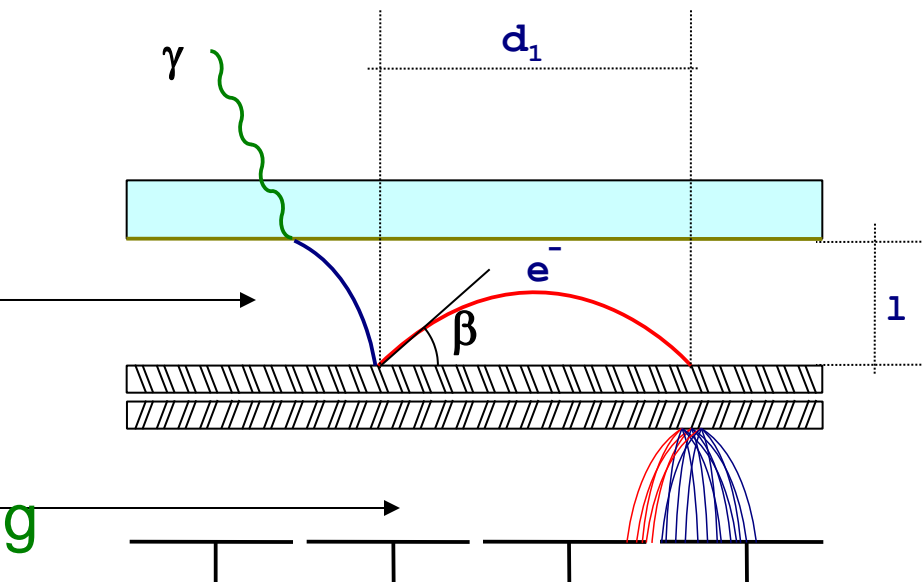
Photo-electron:

- $d_{0,\max} \sim 0.8 \text{ mm}$
- $t_0 \sim 1.4 \text{ ns}$
- $\Delta t_0 \sim 100 \text{ ps}$



Backscattering:

- $d_{1,\max} \sim 12 \text{ mm}$
- $t_{1,\max} \sim 2.8 \text{ ns}$

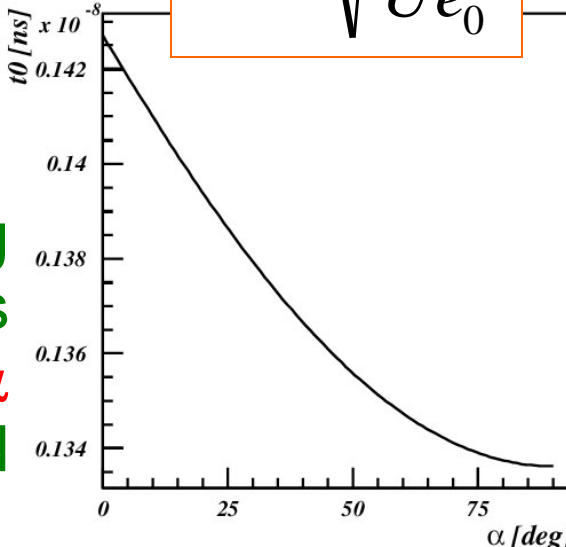


Charge sharing

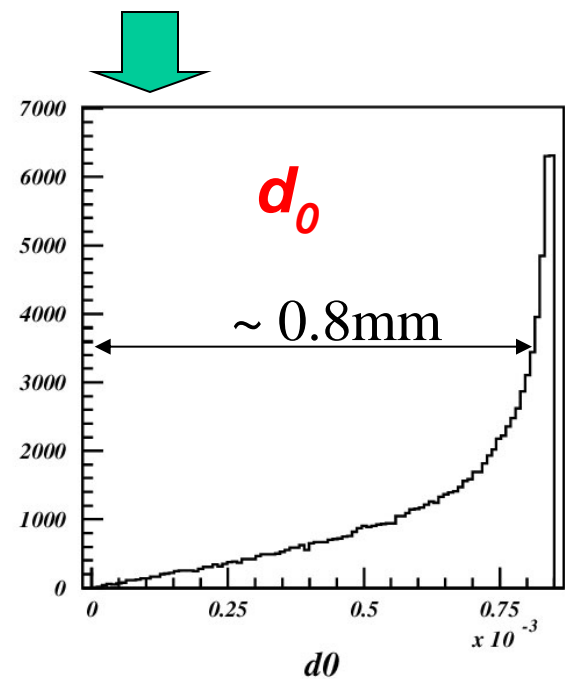
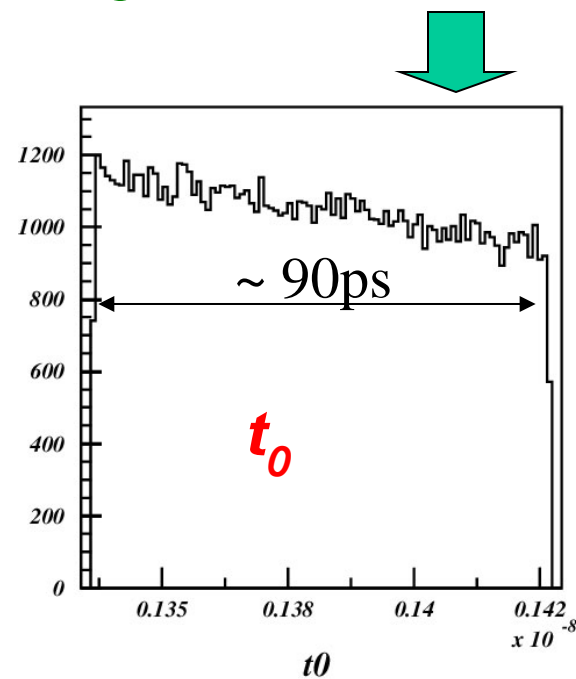
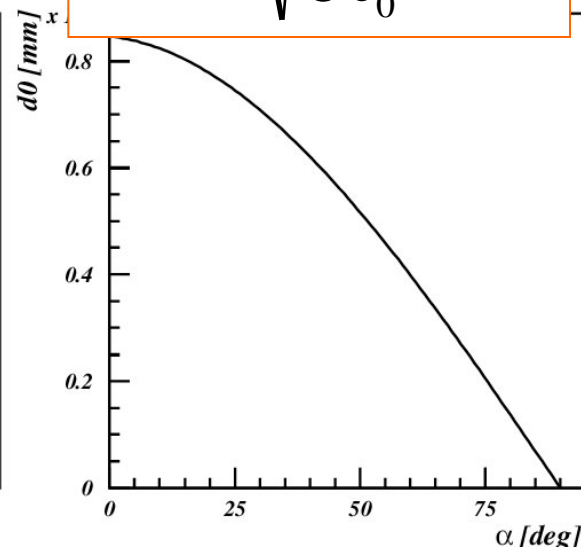
Photo-electron: simple estimates

Distributions assuming
that photo-electron is
emitted at angle α
uniformly over the solid
angle

$$t_0 \approx l \sqrt{\frac{2m_e}{Ue_0}}$$



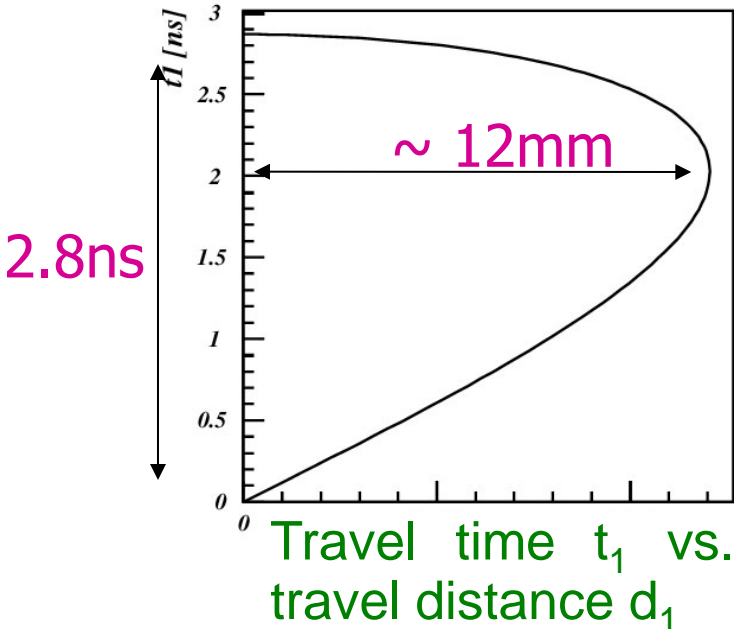
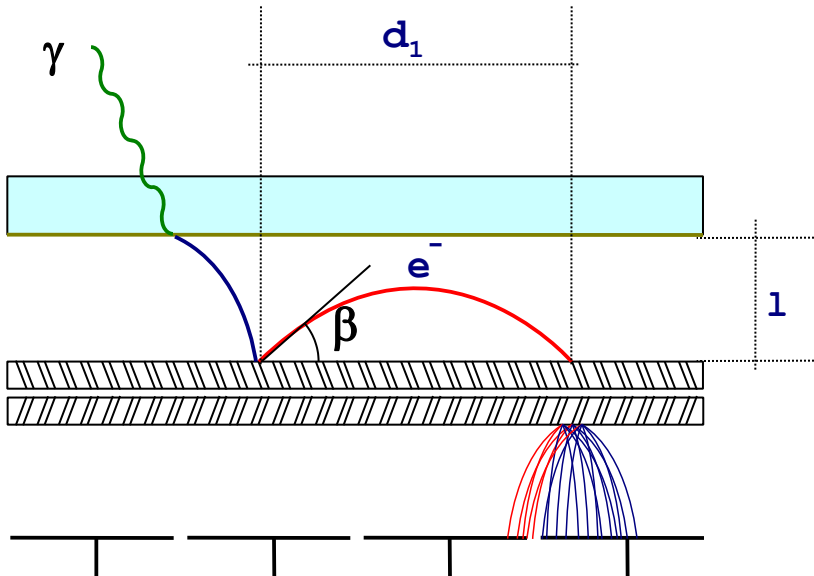
$$d_0 \approx 2l \sqrt{\frac{E_0}{Ue_0}} \cos \alpha$$



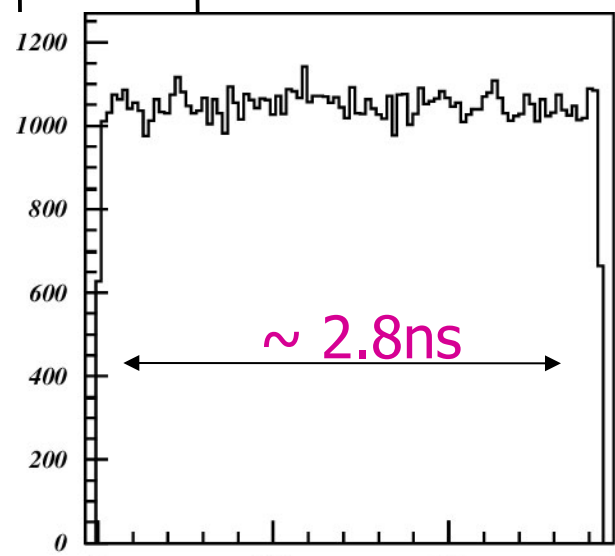
Maximum variation of
photo-electron travel
time.

$$\Delta t_0 \approx t_0 \sqrt{\frac{E_0}{Ue_0}} \approx \frac{l}{Ue_0} \sqrt{2m_e E_0}$$

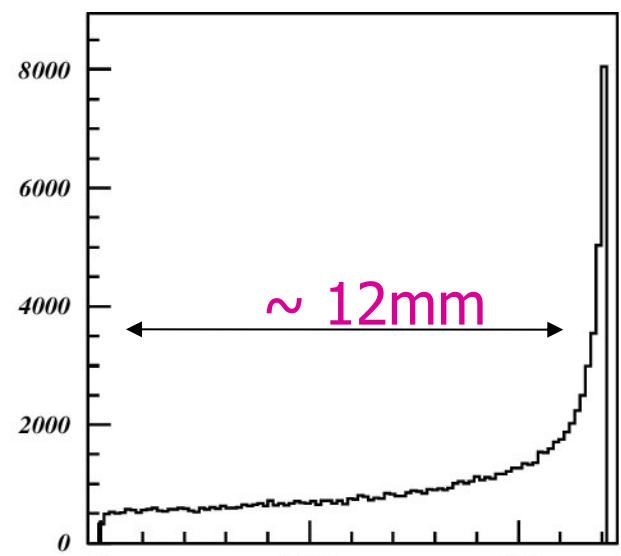
Elastic back-scattering



Distributions assuming that back-scattering by angle β is uniform over the solid angle



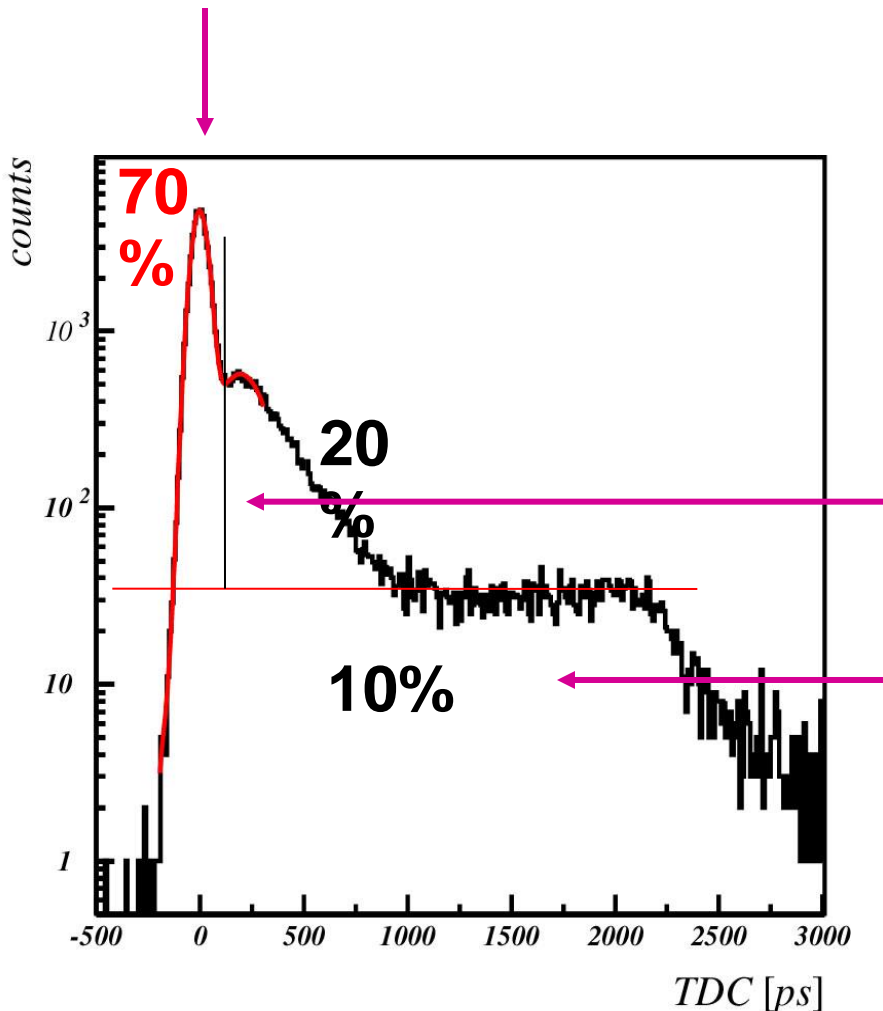
$$t_1 \approx 2t_0 \sin \beta$$



$$d_1 \approx 2l \sin 2\beta$$

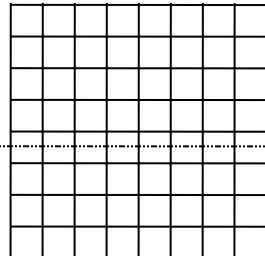
Understanding time-of-arrival distribution

Normal photo-electrons

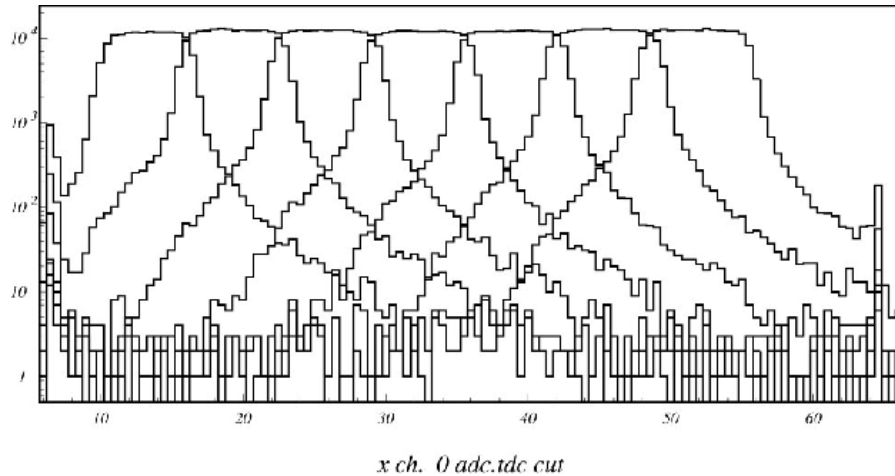


Inelastically scattered
photo-electrons?

Elastically scattered
photo-electrons

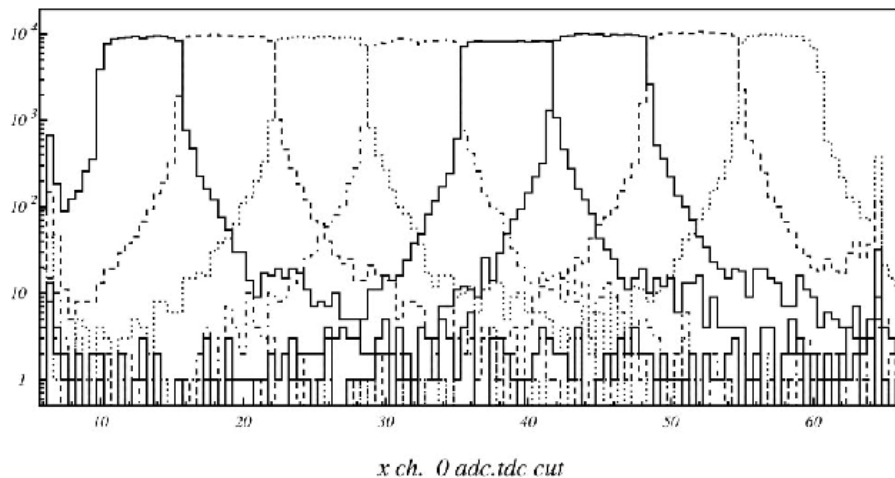


MCP PMT: sensitivity



Number of detected hits on individual channels as a function of light spot position.

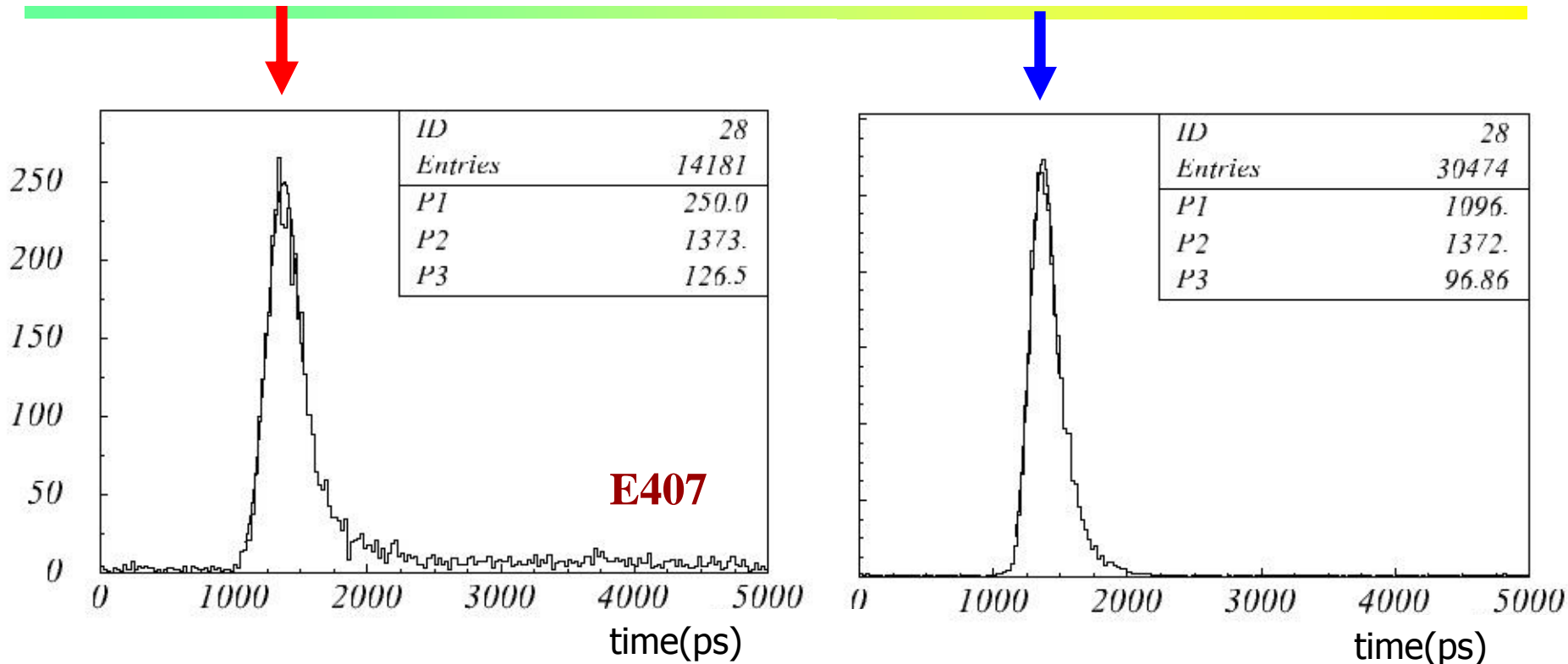
$B = 0 \text{ T}$,
 $\text{HV} = 2400 \text{ V}$



$B = 1.5 \text{ T}$,
 $\text{HV} = 2500 \text{ V}$

In the presence of magnetic field, charge sharing and cross talk due to long range photoelectron back-scattering are considerably reduced.

Time resolution: blue vs red



	E407	S137	H100C	H050C	H025C
σ_{red} (ps)	127	182	145	212	154
σ_{blue} (ps)	97	151	136	358	135

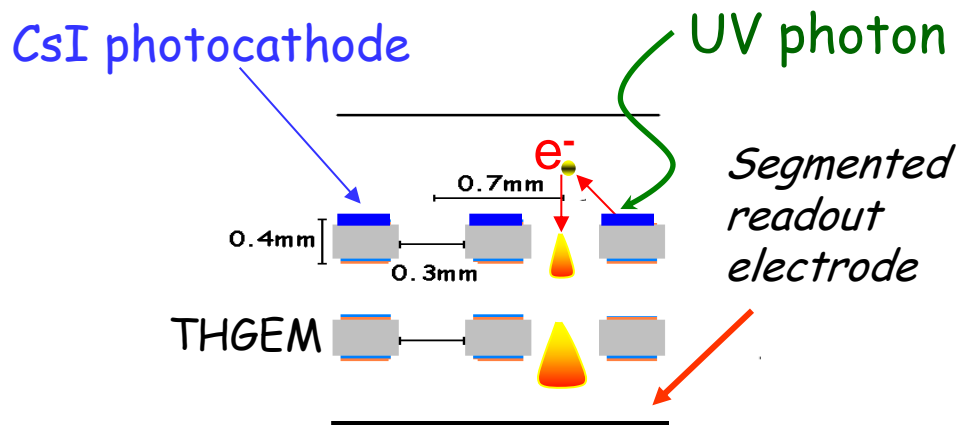
• $\sigma \approx 100$ ps

• $\sigma_{\text{red}} > \sigma_{\text{blue}}$

Wire chamber based photon detectors: recent developments

Instead of MWPC:

- Use multiple GEM with semitransparent or reflective photocathode → PHENIX RICH
- Use chambers with multiple thick GEM (THGEM) with transm. or refl. photocathode (considered for the COMPASS RICH)



Ion damage of the photocathode: ions can be blocked

TRT performance

at 90% electron efficiency

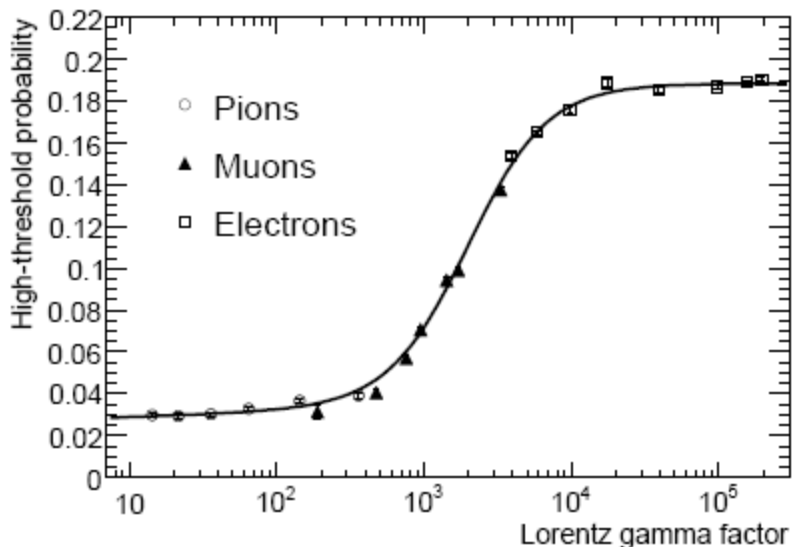


Figure 10.25: Average probability of a high-threshold hit in the barrel TRT as a function of the Lorentz γ -factor for electrons (open squares), muons (full triangles) and pions (open circles) in the energy range 2–350 GeV, as measured in the combined test-beam.

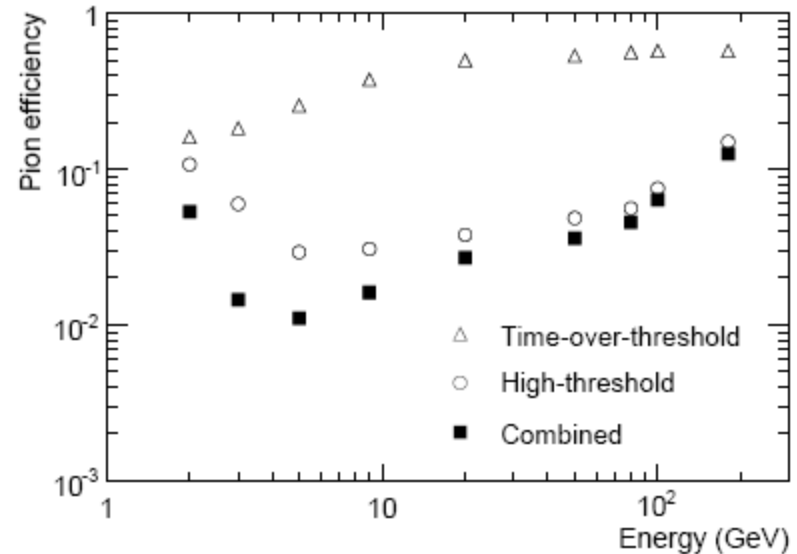
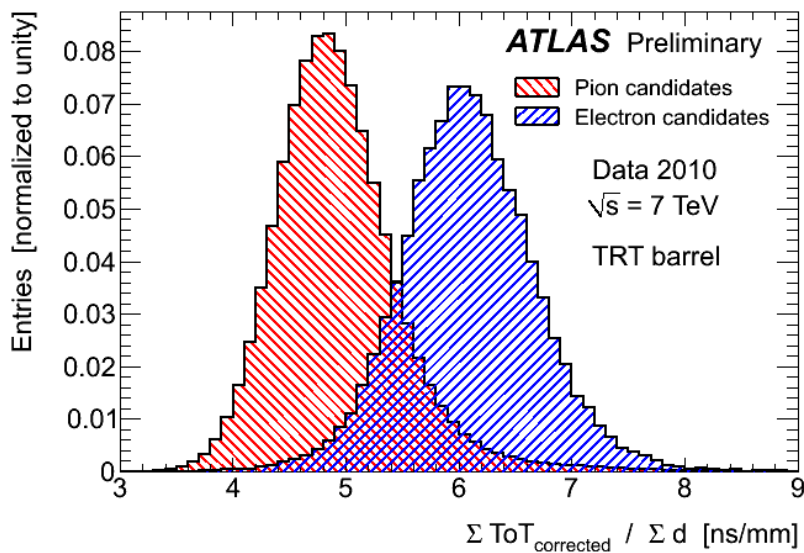
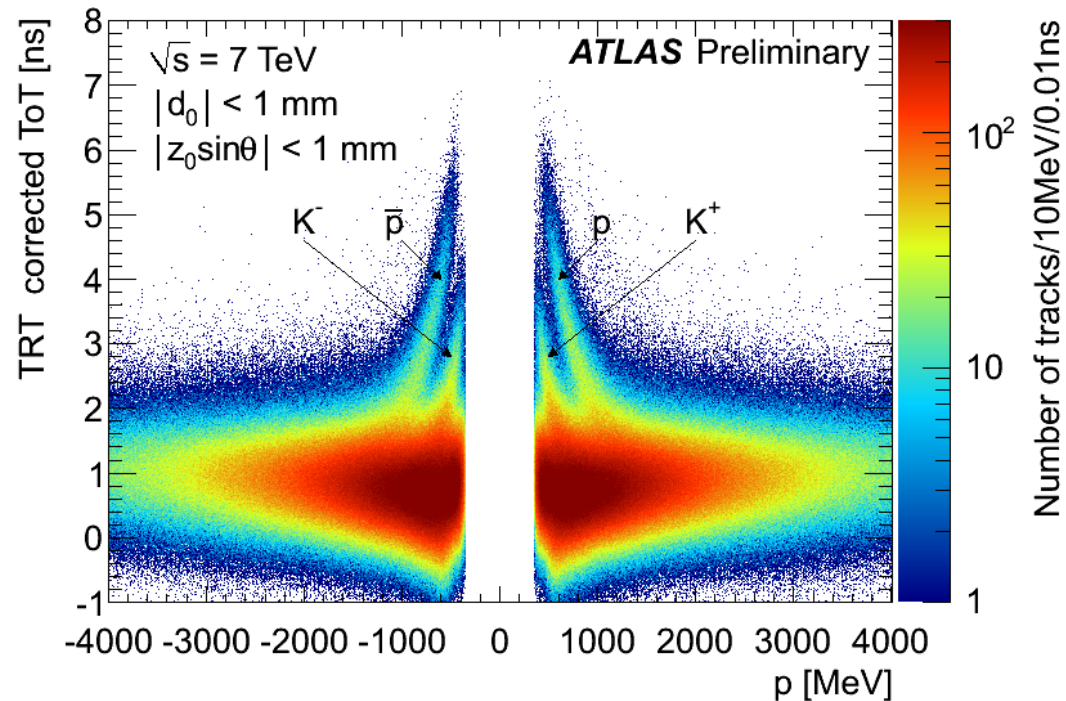


Figure 10.26: Pion efficiency shown as a function of the pion energy for 90% electron efficiency, using high-threshold hits (open circles), time-over-threshold (open triangles) and their combination (full squares), as measured in the combined test-beam.

TRT performance in 2010 data 2

dE/dx performance:
time-over-threshold

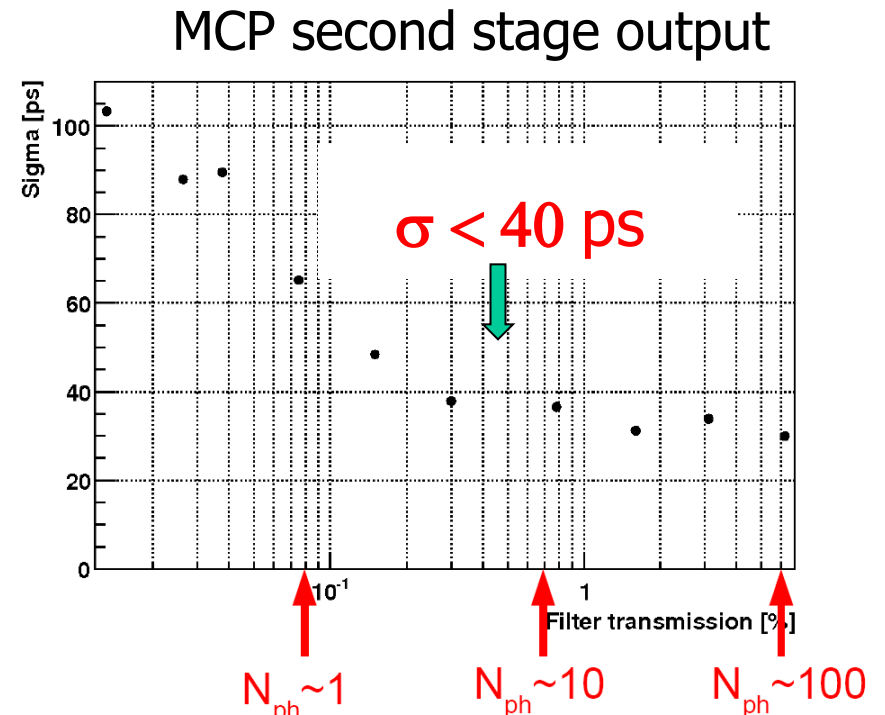
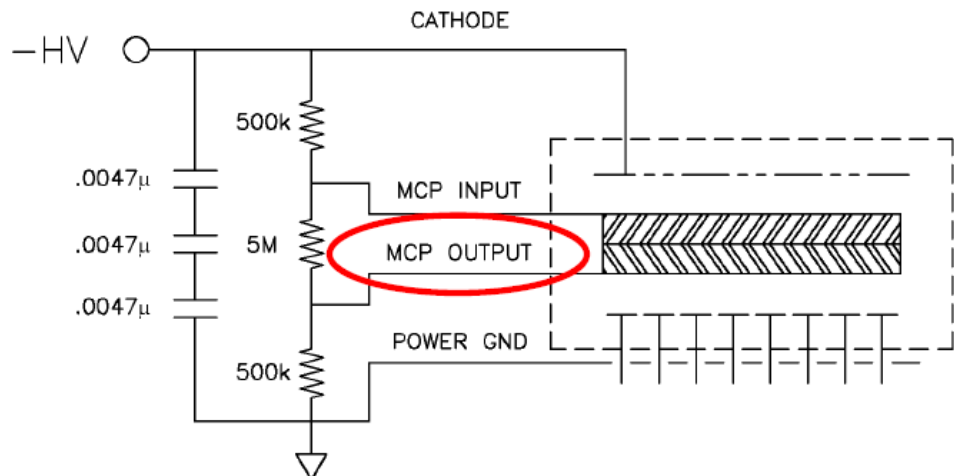


Additional e/pion separation in
time-over-threshold

Timing with a signal from the second MCP stage

If a charged particle passes the PMT window, ~ 10 Cherenkov photons are detected in the MCP PMT; they are distributed over several anode channels.

Idea: read timing for the whole device from a single channel (second MCP stage), while 64 anode channels are used for position measurement

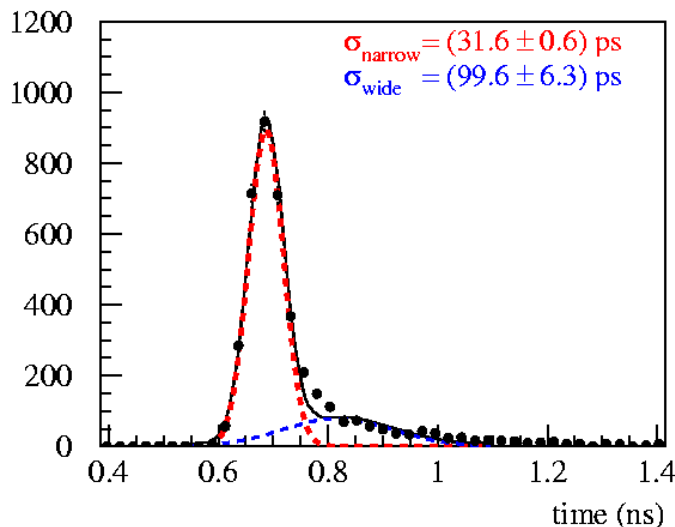


Timing resolution as a function of light intensity

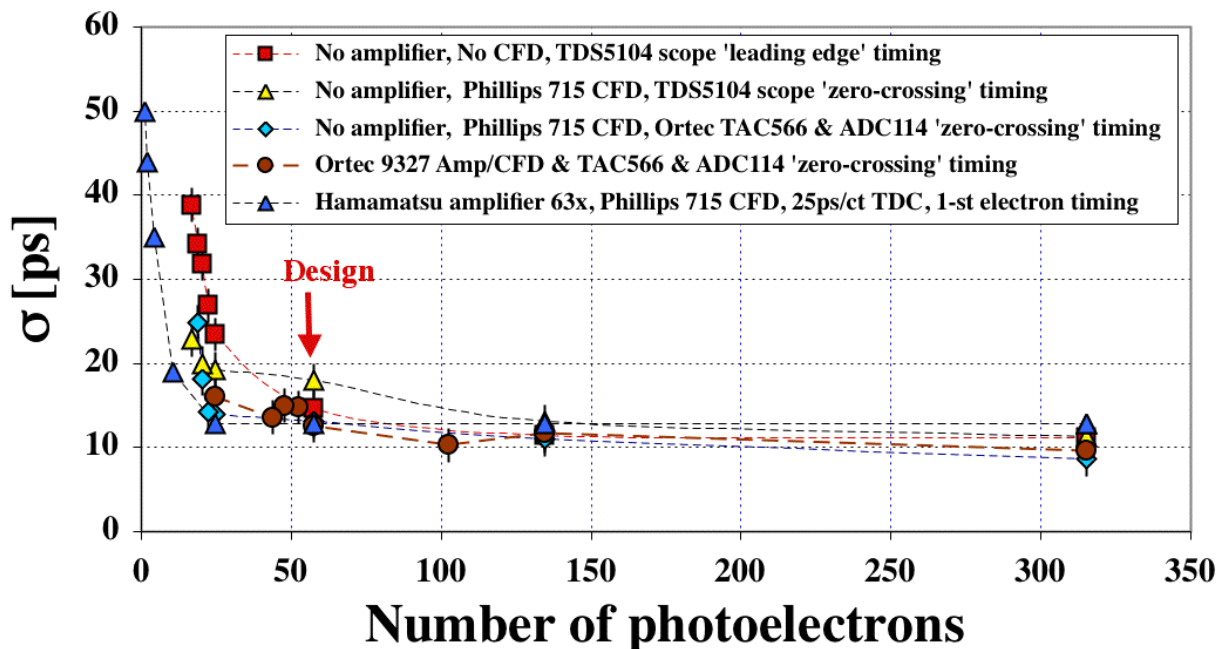
TOF counter with Burle/Photonis MCP-PMT

J. Va'vra, VCI2007

σ_{TTS} - single photo-electrons:



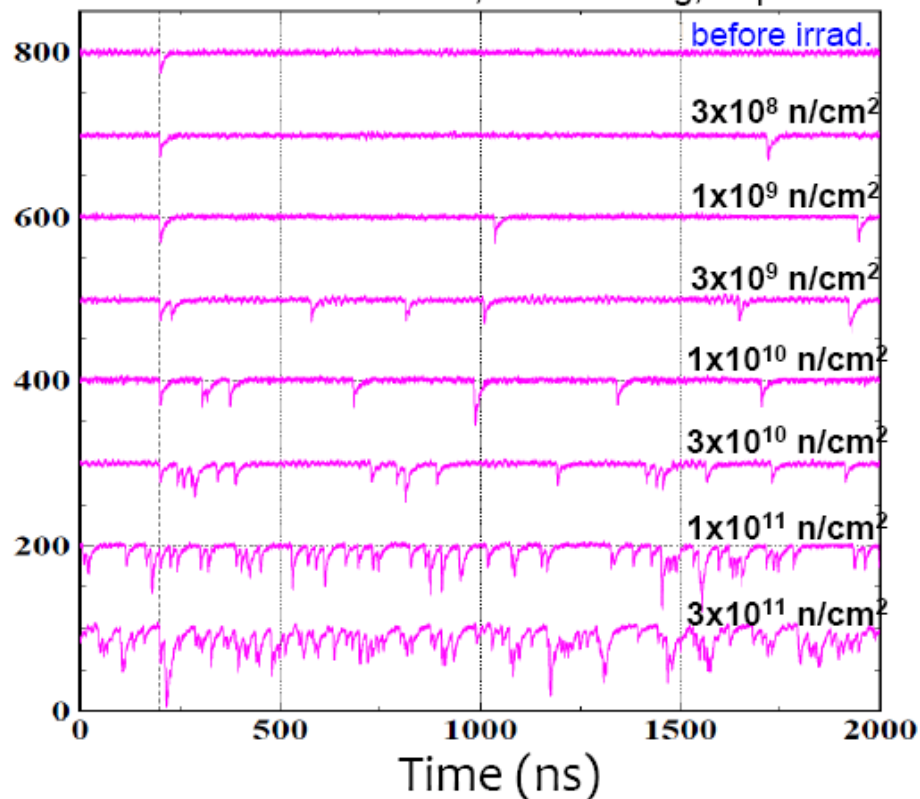
Timing resolution $\sigma = f(\text{Npe})$:



- **TOF counter: Burle/Photonis MCP-PMT with a 1cm thick quartz radiator**
- **Present best results with the laser diode:**
 - $\sigma \sim 12$ ps for $\text{Npe} \sim 50-60$, which is expected from 1cm of the radiator.
 - $\sigma_{\text{TTS}} \sim 32$ ps for $\text{Npe} \sim 1$.
 - **Upper limit on the MCP-PMT contribution:** $\sigma_{\text{MCP-PMT}} < 6.5$ ps.
 - **TAC/ADC contribution to timing:** $\sigma_{\text{TAC_ADC}} < 3.2$ ps.
 - **Total electronics contribution:** $\sigma_{\text{Total_electronics}} \sim 7.2$ ps.

Radiation damage

I.Nakamura, JPS meeting, Sep. 2008



Expected fluence at 50/ab at
Belle II: $2\text{-}20 \ 10^{11} \text{ n cm}^{-2}$
→ Worst than the lowest line

- Very hard to use present SiPMs as single photon detectors in Belle II because of radiation damage by neutrons
- Also: could only be used with a sofisticated electronics – wave-form sampling